Characterization of two components of the chloroplastic Tic complex

Dissertation der Fakultät für Biologie

der

Ludwig-Maximilians-Universität München

vorgelegt von

Johan Philipp Benz

aus Bremen

München

2009

Erstgutachter: Prof. Dr. J. Soll
Zweitgutachter: Prof. Dr. U.C. Vothknecht

Tag der mündlichen Prüfung: 22.06.2009

LITTERIS ET FLORIBUS

Summary

Translocation of nuclear-encoded preproteins across the inner envelope of chloroplasts is catalyzed by the multi-subunit Tic translocon. This machinery can be considered a bottleneck in the pathway of preproteins from the cytosol into the chloroplast. It is therefore perfectly situated to receive signals from inside of the organelle and implement regulatory control over the import process. Seven components have been identified as Tic subunits so far, two of which have been implicated in channel function: Tic110, the central protein of the translocon, and Tic20, a putative alternative channel protein. Another component, Tic62, is part of the so called "redox regulon" of the complex and was proposed to act as a redox sensor, in part because of its specific interaction with the photosynthetic protein ferredoxin-NADP(H) oxidoreductase (FNR) and its redox-dependent shuttling behavior between envelope and stroma. In the present work, the localization, structure, function, and regulation of Tic62 was analyzed in detail. In particular its association with FNR and the physiological role of a third, thylakoid-bound pool of Tic62 were investigated. Structural analyses reveal that Tic62 binds to FNR in a novel binding mode for flavoproteins with major contribution of hydrophobic interactions. At the thylakoids, both proteins form high molecular weight complexes that are dynamically regulated by light- and redox- signals, but clearly not involved in photosynthetic electron transfer. In absence of Tic62, membrane binding and stability of FNR is found to be drastically reduced. Moreover, loss of Tic62 affects the redox state of the stromal thioredoxin pool, which is likely due to an impaired allocation of FNR between the stroma and thylakoid compartments. It is concluded that Tic62 represents a major FNR interaction partner not only at the envelope and in the stroma, but also at the thylakoid membranes of higher plants. Association with Tic62 stabilizes FNR and is involved in its dynamic and light-dependent membrane binding and correct regulation of the stromal redox poise.

In the second part of the work, two efficient expression systems for the putative alternative channel protein Tic20 were established, allowing the heterologous production of protein for further analysis. The purified protein was used to obtain first biochemical and structural data. Moreover, since Tic20 and Tic110 have been suggested to possibly act in concert in the import of precursors, the basic preconditions for this hypothesis were investigated. The results however indicate that (I) both genes are not co-regulated throughout the plant and (II) Tic20 and Tic110 form separate complexes in the inner envelope membrane, inconsistent with a co-operative function in translocation.

Zusammenfassung

Der Transport von im Zellkern kodierten Vorstufenproteinen über die innere Hüllmembran wird von dem aus mehreren Untereinheiten bestehenden Tic-Komplex katalysiert. Diese Maschinerie kann als Nadelöhr auf dem Weg von Vorstufenproteinen aus dem Zytosol in den Chloroplasten verstanden werden. Sie ist daher perfekt platziert, um Signale aus dem Inneren des Organells zu empfangen und eine regulatorische Kontrolle auf den Translokationsprozess auszuüben. Bislang wurden sieben Komponenten als Tic Untereinheiten identifiziert, wovon zwei mit einer Funktion als Kanal in Verbindung gebracht wurden: Tic110, das zentrale Protein des Translokationsapparates, und Tic20, ein möglicherweise alternatives Kanalprotein. Eine weitere Komponente, Tic62, ist Teil des sogenannten „Redox-Regulons" des Komplexes und wurde vorgeschlagen als Redox-Sensor zu wirken, zum Einen da es spezifisch mit dem photosynthetischen Protein Ferredoxin-NADP(H) Oxidoreduktase (FNR) interagiert und zum Anderen da die Verteilung des Proteins zwischen der Hüllmembran und dem Stroma Redox-abhängig veränderbar ist.

In der vorliegenden Arbeit wurde eine genaue Untersuchung der Lokalisierung, Struktur, Funktion und Regulation von Tic62 vorgenommen. Insbesondere wurden seine Verbindung mit der FNR und die physiologische Funktion von Tic62 an den Thylakoiden untersucht, welches ein drittes Tic62-enthaltendes Kompartiment darstellt. Strukturanalysen zeigen, dass Tic62 in einer für Flavoproteine neuartigen Art und Weise und unter hauptsächlicher Beteiligung von hydrophoben Wechselwirkungen an die FNR bindet. An den Thylakoiden bilden beide Proteine hochmolekulare Komplexe aus, die durch Licht- und Redoxsignale reguliert, aber eindeutig nicht am photosynthetischen Elektronentransport beteiligt sind. Wie beobachtet werden kann, ist die Anbindung an Membranen sowie die Stabilität der FNR in Abwesenheit von Tic62 nachhaltig vermindert. Darüber hinaus beeinflusst ein Verlust von Tic62 Protein den Reduktionsstatus des stromalen Thioredoxin, was höchstwahrscheinlich auf eine gestörte Verteilung von FNR zwischen Stroma und den Thylakoiden zurückzuführen ist. Es kann gefolgert werden, dass Tic62 in höheren Pflanzen einen Hauptinteraktionspartner der FNR darstellt, und zwar nicht nur an der Hüllmembran oder im Stroma, sondern darüber hinaus auch an den Thylakoiden. Die spezifische Bindung an Tic62 führt zur Stabilisierung der FNR und ist eingebunden in die dynamische und Licht-abhängige Membrananbindung des Enzyms sowie in die korrekte Regulierung des stromalen Redox-Gleichgewichts.

In einem zweiten Teil dieser Arbeit wurden zwei effiziente Expressionssysteme für das möglicherweise alternative Kanalprotein Tic20 etabliert, was die heterologe Herstellung

dieses Proteins für weitere Analysen möglich macht. Das aufgereinigte Protein wurde verwendet, um erste biochemische und strukturelle Daten aufzunehmen. Da vorgeschlagen wurde, dass Tic20 während der Translokation von Vorstufenproteinen direkt mit Tic110 zusammenarbeiten könnte, wurden zudem die grundlegenden Voraussetzungen für diese Hypothese untersucht. Die Ergebnisse dieser Untersuchung deuten jedoch darauf hin, dass erstens die entsprechenden Gene der beiden Proteine nicht überall in der Pflanze co-reguliert sind, und zweitens, dass Tic20 und Tic110 voneinander unabhängige Komplexe in der inneren Hüllmembran ausbilden, was eine co-operative Funktion während der Translokation unwahrscheinlich macht.

Table of contents

Abbreviations

Φ_{PSII}	quantum yield of PSII
2D	two dimensional
At	*Arabidopsis thaliana*
AGI	*Arabidopsis* Genome Initiative
AP	alkaline phosphatase
ATPase	CF_OCF_1 ATP synthase (complex)
AUC	analytical ultracentrifugation
β-ME	β-mercaptoethanol
BN-PAGE	blue-native polyacrylamide gel electrophoresis
Brij-35	polyoxy-ethylene (23) alkyl-ether or polyoxyethyleneglycol dodecyl ether
CaM	calmodulin
CD	circular dichroism
CEF	cyclic electron flow
CHAPS	3-[(3-cholamidopropyl)dimethylammonio]-1-propanesulfonate
Chl	chlorophyll
Clp	caseinolytic protease
CS	contact site(s)
Ct	carboxy terminus
$Cytb_6f$	cytochrome b_6f (complex)
Cyt c	cytochrome c
Da	Dalton
DDM	*n*-dodecyl-*β*-D-maltoside
DeMa	*n*-decyl-*β*-maltoside
DoPG	dodecyl-phospho-*rac*-glycerol
DTT	dithiothreitol
ECL	enhanced chemiluminescence
E. coli	*Escherichia coli*
EM	electron microscopy
FAD	flavin adenine dinucleotide
FBPase	fructose-1,6-bisphosphatase
Fd	ferredoxin
FNR	ferredoxin-NADP(H) oxidoreductase
FTR	ferredoxin-thioredoxin reductase
F_o	minimal chlorophyll fluorescence (in the dark)
F_m	max. chlorophyll fluorescence (in the light)
F_v	variable chlorophyll fluorescence
F_s	steady-state chlorophyll fluorescence
F_v/F_m	max. quantum yield of PSII
GL	growth-light
GOI	gene of interest
GUS	β-glucuronidase
His	histidine
HL	high-light
HMW	high molecular weight
IE	inner envelope
IEF	isoelectric focusing
IMS	intermembrane space
k, K	kilo, times 1000
Kan	kanamycin

LB	left border (of T-DNA)
Le	*Lycopersicon esculentum*
LEF	linear electron flow
Mal	maleimide
Mega9	nonanoyl-*N*-methylglucamide
Met	methionine
MDH	malate dehydrogenase
MS	mass spectrometry
NAD	nicotinamide adenine dinucleotide
$NADP^+$	nicotinamide adenine dinucleotide phosphate, oxidized form
NADPH	nicotinamide adenine dinucleotide phosphate, reduced form
NDH	NAD(P)H dehydrogenase
N-LS	*n*-lauroylsarcosine
NP-40	Nonidet P-40
NPQ	non-photochemical quenching
Nt	amino terminus
NTR	NADPH-thioredoxin reductase
OE/OEM	outer envelope / outer envelope membrane
OEC	oxygen evolving complex (of PSII)
PAGE	polyacrylamide gel electrophoresis
PEG	polyethylene glycol
PGK	phosphoglycerate kinase
Pp	*Physcomitrella patens*
PQ	plastoquinone
Pro	proline
Ps	*Pisum sativum*
PSI, PSII	photosystem I, II
qP, 1-*qP*	photochemical quenching, excitation pressure of PSII
rpm	revolutions per minute
RT	room temperature
RuBisCO	ribulose-1,5-bisphosphate carboxylase/oxygenase
SD	standard deviation
SDR	short-chain dehydrogenase/reductase
SDS	sodium dodecyl sulphate
Ser	serine
SPP	stromal processing peptidase
SSU	ribulose-1,5-bisphosphate carboxylase/oxygenase, small subunit
Tic	translocon at the inner envelope of chloroplasts
TEM	transmission electron microscopy
TM	transmembrane (domain)
Toc	translocon at the outer envelope of chloroplasts
TP	transit peptide
TPR	tetratricopeptide repeat
Trx	thioredoxin
TX-100	Triton X-100
WT	wild-type
w/v	weight per volume
v/v	volume per volume
x g	times the force of gravity

Introduction

1 General mechanism of preprotein import into chloroplasts

Plastids need to permanently communicate with the surrounding cell, to be able to fulfill their functions correctly (*e.g.* for photosynthesis, nitrite and sulphate assimilation, fatty acid biosynthesis, etc.). This requires a substantial traffic of substances like nutrients, metabolites and proteins into and out of the organelle, which have to be funneled across the two envelope membranes surrounding all plastid types (Figure 1). Among these transport processes, the translocation of proteins is of particular significance. Due to the loss of >90% of their genetic information to the host nucleus during evolution, plastids have become almost completely dependent on the surrounding cell. Of ~ 3000 proteins present in chloroplasts, typically only 50-250 (dependent on the species) are encoded for on the plastome (for review see *e.g.* Gould *et al.*, 2008). The majority of proteins has therefore to be imported posttranslationally from the cytoplasm, which is generally performed via two translocation machineries present in the outer (OE) and inner envelope (IE) membrane, called Toc (translocon at the outer envelope of chloroplasts) and Tic (translocon at the inner envelope of chloroplasts), respectively (for further review see Benz *et al.*, 2007; Inaba and Schnell, 2008; Jarvis, 2008 and references therein). Preproteins using the so-called "general import pathway" are translated with an N-terminal extension called transit peptide, which allows targeting of the precursor to the organelle and specific recognition by the Toc receptor proteins on the surface (the GTPases Toc34 and Toc159; Kessler *et al.*, 1994; Perry and Keegstra, 1994; Hirsch *et al.*, 1994; Seedorf *et al.*, 1995). Cytosolic chaperones like Hsp90 and Hsp70, the latter forming a "guidance complex" with 14-3-3 proteins, support the targeting step by keeping the preproteins in an unfolded conformation, which is required for import (Ko *et al.*, 1992; May and Soll, 2000; Qbadou *et al.*, 2006). Subsequently, translocation through the channel proteins Toc75 and Tic110 can occur (Figure 2; Perry and Keegstra, 1994; Ma *et al.*, 1996; Lübeck *et al.*, 1996; Heins *et al.*, 2002; Hinnah *et al.*, 2002). It is generally accepted that preprotein import occurs simultaneously through the OE and IE in distinct electron microscope (EM)-visible patches where the two envelopes come in close physical proximity, called contact sites (CS; Figure 1; Schnell *et al.*, 1990; Schnell *et al.*, 1994; Perry and Keegstra, 1994). Toc and Tic complexes are believed to interact in these areas to enable a more direct translocation of preproteins from the cytosol into the chloroplast stroma. An intermembrane space (IMS) complex composed of two Toc subunits (Toc64 and the J-domain protein Toc12), one Tic component (Tic22) and an isHsp70 is thought to be involved in this step (Becker *et al.*, 2004).

The transit peptide is then cleaved off by the stromal processing peptidase (SPP), resulting in the mature form of the protein (Richter and Lamppa, 1998). The entire process is superficially reminiscent of that mediated by the protein translocases TOM and TIM located in the inner and outer membrane of mitochondria (Neupert and Herrmann, 2007), but plastids have developed their own ways to solve the main three tasks of protein translocation: (a) the formation of a preprotein-specific pore in the membrane (the channel); (b) exerting the necessary driving force (the motor); (c) installing components which allow regulation of the translocation efficiency dependent on developmental or environmental conditions (the regulon). The composition and function of the Tic channel as well as the regulon will be introduced in the following.
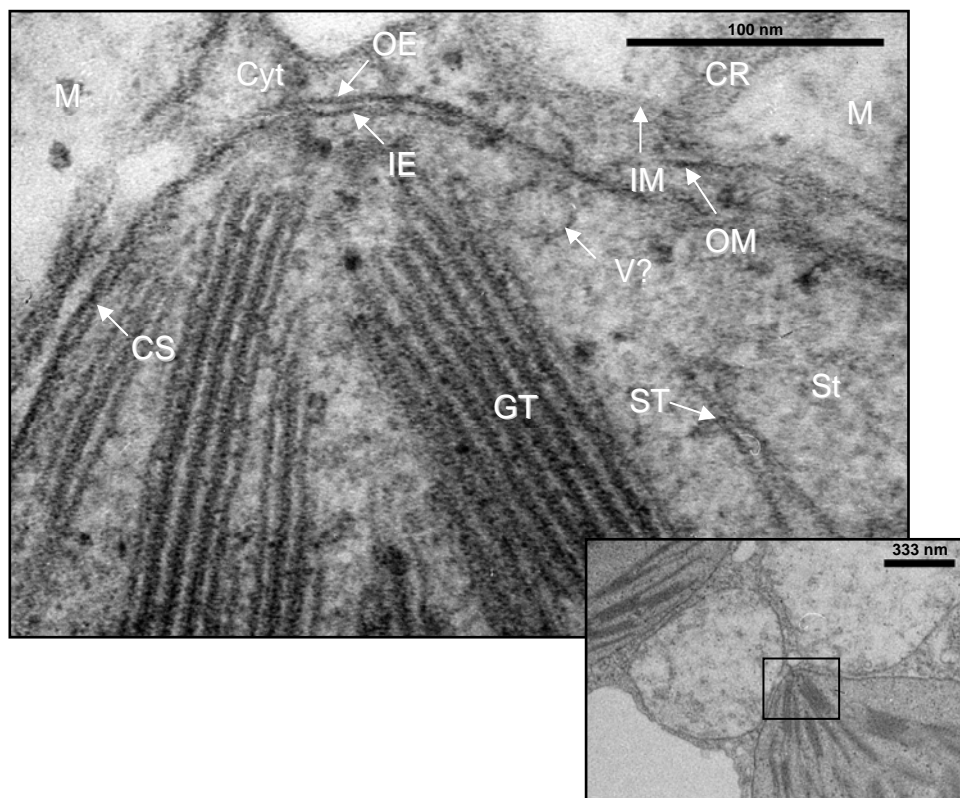
Figure 1: Transmission electron microscopy picture of the chloroplast envelopes. Highly magnified view of the outer area of a chloroplast displaying contact sites between the OE and IE membranes. Overview picture (small): 7,000 x magnification; scale bar: 0.33 μm; the area visible in the main picture is indicated by a box. Main picture: 85,000 x magnification; scale bar: 0.1 μm. CS, contact site; CR, cristae; Cyt, cytosol; GT, grana thylakoids; IE, chloroplast inner envelope; IM, inner mitochondrial membrane; M, mitochondrion/matrix; OE, chloroplast outer envelope; OM, outer mitochondrial membrane; ST, stroma thylakoids (stroma lamellae); V?, vesicular structure possibly budding from the IE.

2 The Tic complex

Based on biochemical and genetic evidence, seven proteins have been implicated with preprotein import at the IE membrane of chloroplasts so far: Tic110, Tic62, Tic55, Tic40, Tic32, Tic22, and Tic20 (Figure 2). For each of those, either a direct contact with imported precursor or a close interaction with one of the established Tic core proteins (usually Tic110) has been demonstrated. Last but not least, the chaperone Hsp93/ClpC (<u>c</u>aseino<u>l</u>ytic <u>p</u>rotease <u>C</u>) constitutes a central component of the Tic motor complex.
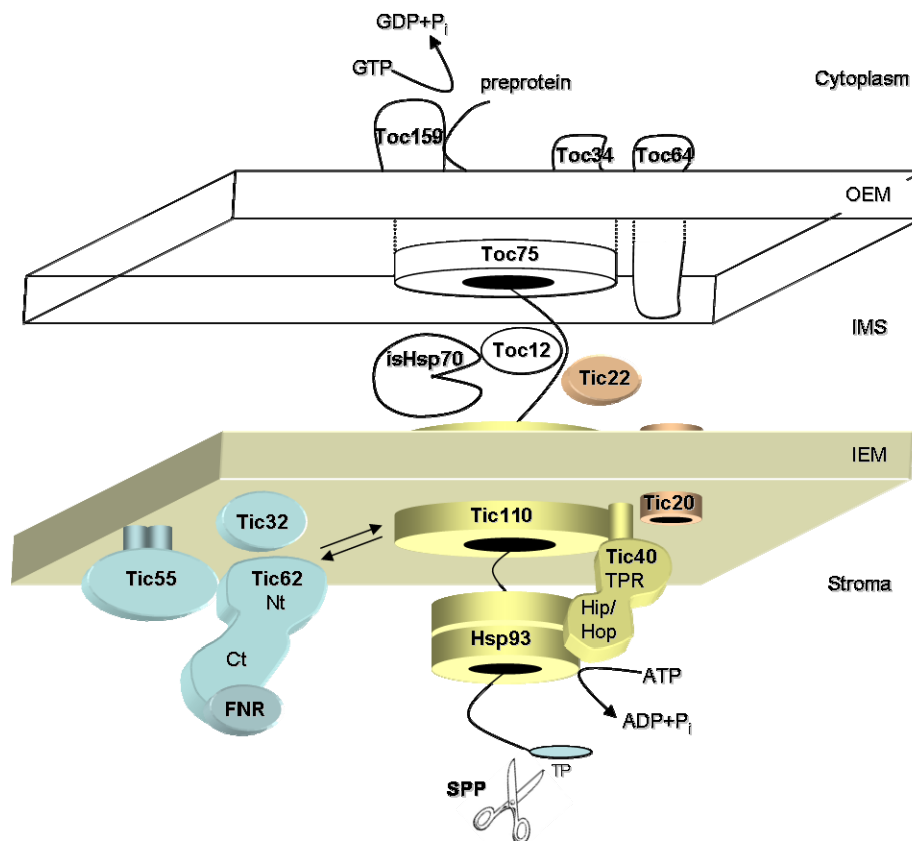
Figure 2: Schematic illustration of the Toc and Tic chloroplast import machineries with focus on the components involved in preprotein translocation at the IE membrane (modified from Benz *et al.*, 2009). Individual Tic components are colored and labeled with their respective names. Some key functional domains are additionally indicated (Tic40 and Tic62); Toc components are named but not colored. The predicted TM domains of Tic40 and Tic55 are shown as small columns protruding into the IE membrane. Components of the channel/motor complex are depicted in yellow (Tic110, Tic40, and Hsp93), redox-regulatory subunits in blue (Tic62 with associated FNR, Tic55, and Tic32), the proposed alternative import channel Tic20 and the IMS component Tic22 in red. Shown is a cytoplasmatically translated preprotein with an N-terminal transit peptide (TP) during its translocation through the Toc and Tic complexes. Stable binding at and translocation through the Toc complex requires GTP-hydrolysis. Tic22 may be involved in the stabilization of the Toc/Tic/preprotein supercomplex. In this model, Tic110 forms the channel protein and also acts in the recruitment of Hsp93 in concert with the co-chaperone Tic40. The TPR domain of Tic40 is thought to mediate the interaction with Tic110, whereas the Sti1-like Hip/Hop domain was shown to enhance the ATPase activity of the chaperone Hsp93. The motor activity of this AAA+ ATPase probably accounts for most of the ATP requirement of the import reaction. The Stromal Processing Peptidase (SPP) is thought to act very early after the preprotein emerges from the Tic channel. The association of the redox-sensing regulatory subunits Tic62 (with FNR bound to the Ct) and Tic32 seems to be dynamic (double arrows). It is not known whether this is also true for the Rieske-protein Tic55, but a similar behavior is assumed in this model.

2.1 The Tic channel

Tic110 is undoubtedly the central protein of the translocon. It is not only the largest, most abundant and best studied of all Tic proteins, but also probably the only component involved in translocation steps happening on both sides of the IE membrane. This includes the assembly of Toc-Tic "supercomplexes" (Schnell and Blobel, 1993; Akita *et al.*, 1997; Nielsen *et al.*, 1997), preprotein recognition (Inaba *et al.*, 2003), translocation, and folding steps of successfully imported precursor proteins in the stroma (Kessler and Blobel, 1996; Heins *et al.*, 2002). Two transmembrane (TM)-helices at the extreme N-terminus (Nt) anchor the protein in the membrane. The position and function of the long hydrophilic C-terminal tail on the other hand has been discussed controversially (Lübeck *et al.*, 1996; Jackson *et al.*, 1998; Heins *et al.*, 2002; Inaba *et al.*, 2003; Inaba *et al.*, 2005; Balsera *et al.*, 2009). Part of it clearly faces the stroma, where it functions as a scaffold for the organization of stromal processes occurring during import, including the recruitment of chaperones to the import apparatus as well as providing a transit peptide docking site (Jackson *et al.*, 1998; Inaba *et al.*, 2003; Inaba *et al.*, 2005). Moreover, full-length protein as well as the Tic110 C-terminus (Ct) was shown to insert into liposomes and form a cation-selective and transit peptide-sensitive ion channel (Heins *et al.*, 2002; Balsera *et al.*, 2009), probably mediated by four amphipathic α-helices that were identified around the proposed transit peptide binding site (Inaba *et al.*, 2003; Balsera *et al.*, 2009).

Another putative channel protein is Tic20. Structural predictions place Tic20 within the large group of small hydrophobic proteins with four TM-domains, including *e.g.* the TIM channel proteins Tim17 and Tim23. Distant sequence similarity also exists between Tic20 and two prokaryotic branched-chain amino acid transporters (Reumann and Keegstra, 1999). No data have been published demonstrating channel activity yet, but since Tic20 has prokaryotic ancestors, it was speculated that it could have been one of the very early constituents of an evolving protein import translocon (for review see Reumann *et al.*, 2005). In contrast to this, Tic110 only has homologs in the genomes of Plantae (Gross and Bhattacharya, 2009).

Tic20 and Tic110 also display some similar features. When expression was silenced by antisense or completely abolished using a T-DNA knockout, both mutants exhibit severe phenotypes in *Arabidopsis thaliana* (Chen *et al.*, 2002; Inaba *et al.*, 2005; Teng *et al.*, 2006). Tic110 was shown to be essential for chloroplast biogenesis and embryo development and displays a rare semi-dominant phenotype, since plants with a heterozygous knockout are already clearly affected (Inaba *et al.*, 2005). Antisense plants of the *Pisum sativum* (pea) ortholog and main *Arabidopsis* isoform of Tic20, AtTic20-I, likewise exhibit pronounced

chloroplast defects, and *attic20-I* knockouts were albino even in the youngest parts of the seedling (Chen *et al*., 2002; Teng *et al*., 2006). The presence of at least one other Tic20 isoform (AtTic20-IV) may prevent *attic20-I* plants from lethality. Two more isoforms have been detected in *Arabidopsis* (AtTic20-II and AtTic20-V), which however do not possess a predicted transit peptide (Reumann *et al*., 2005). Furthermore, chloroplasts from *attic20-I* antisense plants as well as from heterozygous *attic110* were demonstrated to be defective in preprotein import across the IE membrane (Chen *et al*., 2002; Inaba *et al*., 2005). More recently, an additional study demonstrated that a highly divergent member of the Tic20 protein family in *Toxoplasma gondii* (TgTic20) is important for protein import also into apicoplasts (non-photosynthetic secondary plastids). Based on these similarities, the hypothesis has been put forward that Tic20 and Tic110 could dynamically associate to cooperate in channel formation (Inaba *et al*., 2003). The only biochemical indication for this suggestion is co-elution of a minor fraction of Tic110 (~ 5%) with Tic20 (and Tic22) in a Toc-Tic supercomplex (Kouranov *et al*., 1998). However, no co-elution was detected in the absence of the Toc complex, making a direct or permanent interaction unlikely.

In summary, both Tic20 and Tic110 are clearly important for plant viability and preprotein translocation, but only for Tic110 electrophysiological and biochemical data demonstrate channel activity as well as involvement in the import motor complex. Similar data for Tic20 are still missing, and thus further investigations will be necessary to clarify these points.

2.2 The redox regulon

As outlined above, a great amount of protein traffic has to take place at the envelope membranes of chloroplasts, which has to be tightly regulated to ensure that the supply correlates to the demand of the organelle at any given time. Translocation across the envelope is surely a *bottleneck* in the path of transported proteins from the cytosol to their final destination in the chloroplast. The Tic and Toc translocons are therefore perfectly situated to impose a regulatory control over incoming preproteins. Additionally, since the demand of the chloroplast is "sensed" *inside* the organelle, the IE membrane is closest to the origin of the signal, and thus regulation at the Tic complex could be one of the fastest ways to react and adapt the chloroplast protein content accordingly. Up to now, the "regulon" of the Tic complex comprises three proteins: Tic62, Tic32 and Tic55. The former two proteins belong to the (extended) family of SDRs (<u>s</u>hort-chain <u>d</u>ehydrogenases/<u>r</u>eductases) and have been demonstrated to possess dehydrogenase activity *in vitro* (Küchler *et al*., 2002; Chigri *et al*., 2006; Stengel *et al*., 2008). The redox properties of Tic55, on the other hand, have not been

5

investigated in detail yet. Sequence analysis revealed the presence of a Rieske-type [2Fe-2S] cluster and a mononuclear iron-binding site (Caliebe *et al.*, 1997). Database research classifies Tic55 as a member of the CAO/PAO (chlorophyll *a* oxygenase/phaeophorbide *a* oxygenase)-like oxygenases, which act *e.g.* in chlorophyll (Chl) biogenesis or oxygen dependent degradation pathways. Rieske proteins generally play important roles in electron transfer, *e.g.* in the cytochromes present in the respiratory chain of mitochondria or in the thylakoids of chloroplasts, but whether Tic55 acts as an oxygenase *in vitro* or *in vivo* has not been studied so far.

3 Regulation of the Tic complex

At least three types of regulatory signals are known to convene at the Tic complex: (I) a calcium/calmodulin-mediated signal which is associated with Tic32 (Chigri *et al.*, 2006), (II) a thioredoxin (Trx)-mediated signal, acting at Tic110 and possibly the Rieske protein Tic55 (Bartsch *et al.*, 2008; Balsera *et al.*, 2009), and (III) the stromal $NADP^+$/NADPH ratio sensed via Tic62 and Tic32, giving information about the metabolic state of the chloroplast (Küchler *et al.*, 2002; Hörmann *et al.*, 2004; Figure 3).
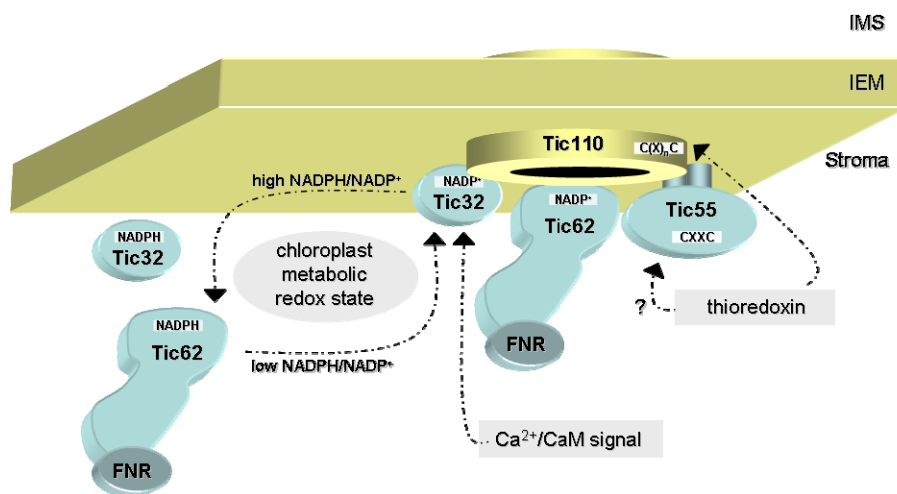
Figure 3: Schematic model of the proposed regulatory signals sensed by the Tic complex and their effect on the involved subunits (modified from Benz *et al.*, 2009). Three signals are thought to convene at the Tic complex: (I) information about the chloroplast metabolic redox state, represented by the stromal $NADP^+$/NADPH ratio and sensed by the two dehydrogenases Tic62 and Tic32, (II) a calcium signal, mediated by a still unknown plastidic calmodulin (CaM) or CaM-like protein binding to Tic32, and (III) a second redox-related signal, in which a stromal thioredoxin might interact with a conserved cysteine pair (CXXC) of the Rieske-protein Tic55 and/or the channel protein Tic110. The redox-state of the $NADP^+$/NADPH pool was demonstrated to affect the association of Tic62 and Tic32 with the Tic complex. Both components dissociate from the complex at high NADPH concentrations. Tic62 was shown to reversibly shuttle between the stroma the IE membrane dependent on the $NADP^+$/NADPH ratio. For Tic32, a similar relocalization as for Tic62 is assumed in this model.

3.1 Thioredoxin-mediated regulation

Trxs are small, ubiquitous proteins, that play crucial roles in the regulation of many cellular processes, since they are able to activate (or deactivate) their target enzymes by the reversible reduction of inter- or intramolecular disulfide bonds, often arranged in a conserved CXXC motif (Figure 4 A; for review see *e.g.* Buchanan and Balmer, 2005; Hisabori *et al.*, 2007; Schürmann and Buchanan, 2008; Montrichard *et al.*, 2009). In chloroplasts, Trxs are known to be involved in the regulation of *e.g.* the Calvin-Benson cycle, the oxidative pentose phosphate cycle, starch metabolism, fatty acid biosynthesis and also nitrogen and sulphur metabolism (for review see Buchanan and Balmer, 2005; Lindahl and Kieselbach, 2009). Trx are themselves reduced by ferredoxin (Fd) and Fd-Trx-reductase (FTR) in chloroplasts and by NADPH via a flavin enzyme, NADPH-Trx-reductase (NTR), in the other cell compartments (Figure 4 B).
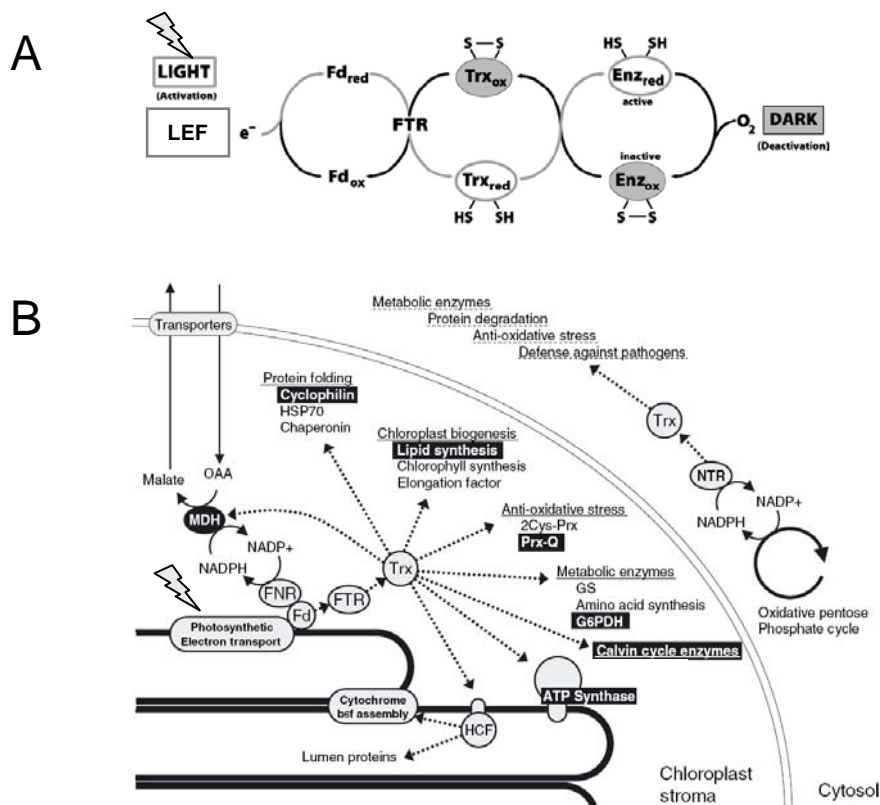
Figure 4: Thioredoxin function in the plant. (**A**) (modified from Buchanan and Balmer, 2005) Role of the Fd/Trx system in chloroplasts showing the classical role of Trxs as an 'eye' in the sensing of light. This information is then conveyed to target enzymes (Enz) for activation (at day) or deactivation (at night). Irradiation is indicated by a lightning bolt. The electron flow by thiol-disulfide exchange is indicated by arrows (grey: reducing; black: oxidizing). LEF, linear electron flow (photosynthetic). (**B**) (adapted from Hisabori *et al.*, 2007) Schematic Trx network in chloroplasts and in the cytosol. The figure depicts some of the Trx-dependent regulatory pathways in the chloroplast (established: white letters; others: implied by proteomics data). Trxs themselves can be reduced either in the stroma by electrons derived from the photosynthetic electron chain via Fd and the Fd-Trx-Reductase (FTR) or by NADPH in the cytosol via the NADPH-Trx-Reductase (NTR). Dotted arrows show the flow of electrons.

Two recent studies provide evidence for a Trx-mediated regulation at the level of the Tic complex (Figure 3; Bartsch *et al.*, 2008; Balsera *et al.*, 2009): Tic55 was identified as a target of stromal Trxs in barley chloroplasts (Bartsch *et al.*, 2008), and another study demonstrated that also the Tic channel protein Tic110 possesses at least one redox-active disulfide bridge that can be reversibly reduced (Balsera *et al.*, 2009).

3.2 Redox regulation

Redox regulation is long known to play a prominent role in the chloroplast metabolism, and obviously also affects protein import. Two preproteins, FNRII and the non-photosynthetic FdIII of maize, for instance, were demonstrated to be differentially imported in the light compared to the dark (Hirohashi *et al.*, 2001). Diurnal changes at the thylakoids or, more generally, the stromal redox system (*e.g.* the $NADP^+$/NADPH pool) thus seem to have an impact on the import characteristics of the organelle. It is therefore not surprising to find proteins with redox-active domains as Tic constituents (see above). Investigation of the Tic complex under changing redox conditions revealed a high degree of dynamics: addition of NADPH *e.g.* leads to dissociation of the two dehydrogenases Tic32 and Tic62 from the complex, indicating that the metabolic state of the organelle might have a profound influence on Tic composition (Chigri *et al.*, 2006).

4 Tic62 and FNR

4.1 The redox-sensor protein Tic62

Tic62 has been characterized as a redox-sensor of the Tic complex based on its dehydrogenase domain and its specific interaction with FNR, a key photosynthetic enzyme (Küchler *et al.*, 2002). It is made up of two very different modules of about equal size (Figure 5): the Nt contains the NADP(H) binding site as well as a hydrophobic patch, which is supposed to mediate the membrane attachment of the protein (Balsera *et al.*, 2007). The Tic62 Ct contains several Pro/Ser-rich repeats (their number varying dependent on the species), which mediate the interaction with FNR. Association with this oxido-reductase seems to be an evolutionary young trait of Tic62. This notion derives from an extensive database analysis looking for homologs of Tic62 in other organisms (Balsera *et al.*, 2007). It was found that the N-terminal half of the protein, comprising the dehydrogenase domain, is highly conserved in all oxyphototrophs, and homologs can be found even in green sulphur bacteria. In contrast, the Ct, containing the FNR binding repeats, is present only in flowering plants, and therefore

seems to have been added only recently in evolution. The (full-length) Tic62 protein could thus represent one of the youngest Tic constituents.
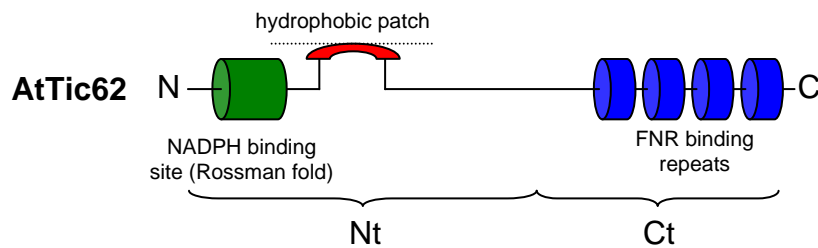
Figure 5: Schematic representation of the functional domains of Tic62 (modified from Benz *et al.*, 2009). Tic62 belongs to the extended family of SDRs and can be divided into two distinct modules. The N-terminus (Nt) contains the dehydrogenase domain (green) and might mediate membrane binding via a hydrophobic patch on the surface of the protein (red), while the C-terminus (Ct) features a series of Pro/Ser-rich repeats (blue) which allow specific binding of FNR. The dotted line indicates a membrane surface.

Further studies with Tic62 revealed that this protein is shuttling between the chloroplast membranes and the stroma dependent on the stromal $NADP^+$/NADPH ratio (Stengel *et al.*, 2008; Figure 3). Oxidized conditions lead to fast membrane binding and subsequent integration into the Tic complex. Reduced conditions on the other hand cause solubilization into the stroma. These results demonstrate that Tic62 is able to react very sensitively to redox changes in the chloroplast and to adjust its localization accordingly, in line with its proposed role as a redox-sensor protein in the chloroplast (Küchler *et al.*, 2002; Stengel *et al.*, 2008). How exactly changes in the redox-state of the chloroplast affect the translocation is not known yet, but it has been speculated that the dynamic Tic composition could influence the import characteristics of a certain subset of preproteins, which might also act in redox-dependent pathways (Stengel *et al.*, 2008).

The reason for the specific association of Tic62 with FNR is one of many intriguing questions, which are still unanswered. Since flavin-containing proteins have already been described to be present in redox chains in chloroplast envelope membranes (Jäger-Vottero *et al.*, 1997), one possibility is a recruitment of FNR from the stroma or even thylakoids to the Tic complex by Tic62 in order to become part of the hypothetical electron transfer chain mentioned above.

4.2 The role of FNR in photosynthesis and metabolism

By the help of its FAD-cofactor, FNR catalyzes the (reversible) electron transfer between Fd and NADP(H) (Figure 6; for review see Carrillo and Ceccarelli, 2003). This reaction is best known as the last step of the photosynthetic electron chain in chloroplasts, which basically converts light-energy into utilizable chemical energy (Figure 7).
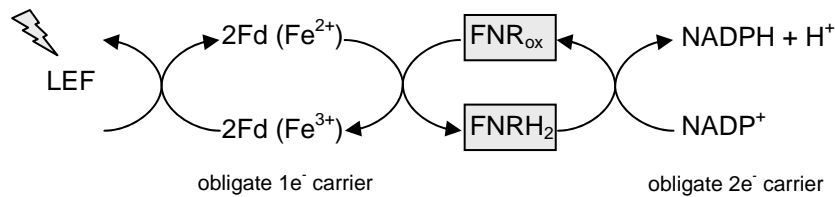
Figure 6: FNR catalytic mechanism. The (freely reversible) oxido-reduction of FNR and its most common substrates NADP(H) and Fd is shown. One of the striking features of FNR is its ability to mediate the electron (e^-) transfer between obligate 1 e^- and 2 e^- carriers, which is a direct consequence of the biochemical properties of its prosthetic group FAD. The reduction status of the iron (Fe) in the [2Fe-2S] center of Fd is indicated. Irradiation is indicated by a lightning bolt and the electron flow is by arrows. LEF, linear electron flow (photosynthetic).

Several protein complexes present in the thylakoids participate in this process: photosystem II (PSII), the plastoquinone (PQ) pool, the cytochrome b_6f complex (Cytb$_6$f) and PSI (for review see Dekker and Boekema, 2005; Jensen *et al.*, 2007). The transported electrons are ultimately derived from H_2O in the thylakoid lumen, which is split by the oxygen-evolving complex (OEC) of PSII into molecular oxygen (O_2, which is released), protons and electrons. These are then transported in a light-driven process by the so-called linear electron flow through the photosynthetic complexes to be finally used by FNR for the production of NADPH, the general reducing equivalents of the organelle for the reductive metabolism. The $CF_O CF_1$-ATP synthase (ATPase) in parallel makes use of the concomitant acidification of the thylakoid lumen and converts the energy that is saved in the electrochemical proton gradient into the production of ATP (for review see Richter *et al.*, 2005).

However, FNRs have also been isolated from a variety of other tissues and organisms with both phototrophic and heterotrophic metabolisms (Ceccarelli *et al.*, 2004). In contrast to photosynthetic organisms, the reaction is driven towards Fd or flavodoxin reduction in non-photosynthetic tissue and bacteria, or heterotrophic eukaryotes. In *Arabidopsis*, this fact is reflected by a set of tissue-specific FNR isoforms in leaves (LFNR1 and LFNR2) and roots (RFNR1 and RFNR2), allowing an efficient electron flux of the NADP(H)-FNR-Fd cascade to the respective metabolism in both photosynthetic and non-photosynthetic cells (Hanke *et al.*, 2005).

Besides its role in the linear electron flow, FNR has also been implicated in cyclic electron flow (Guedeney *et al.*, 1996; Quiles and Cuello, 1998; Quiles *et al.*, 2000; Breyton *et al.*, 2006). At least two routes exist, which "re-cycle" electrons around PSI, thereby leading to an enhanced production of ATP without accumulation of NADPH (Figure 7; for review see Rumeau *et al.*, 2007).
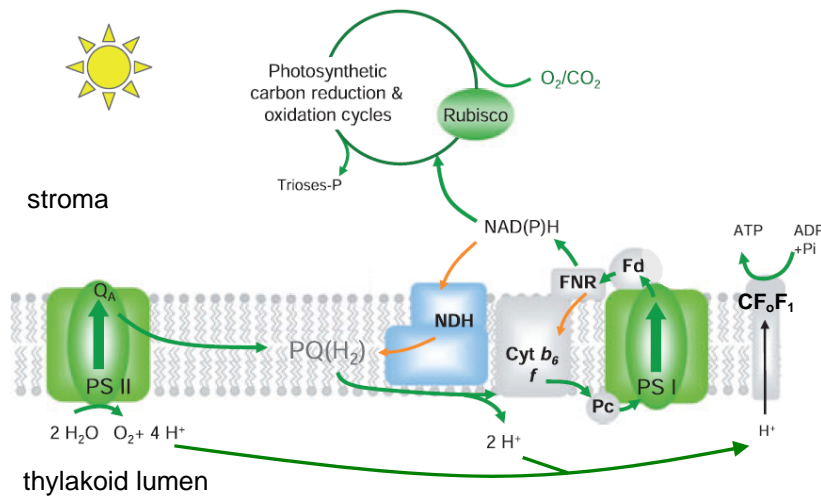
Figure 7: Electron transfer reactions during oxygenic photosynthesis (modified from Rumeau *et al.*, 2007) Two electron transfer routes exist in the thylakoids: The light-driven linear electron flow (LEF) starts with the H_2O-splitting activity at PSII and transfers the electrons to $NADP^+$ via the plastoquinone (PQ) pool, $Cytb_6f$, PSI, Fd and FNR (green arrows). The reduction equivalents can then be used for the reductive metabolism in the stroma. The cyclic electron flow (CEF) is centred around PSI (orange arrows). That way, electrons are re-inserted into the system via the NDH or the $Cytb_6f$ complexes, thereby further reducing the PQ pool and increasing the acidification of the thylakoid lumen. This results in the production of ATP without accumulation of NADPH. Besides LEF, FNR has been implicated with both CEF routes (see text for details). PSII, photosystem II; PSI, photosystem I; CF_0F_1, ATP synthase; NDH, NAD(P)H dehydrogenase complex; PTOX, plastid terminal oxidase; $Cytb_6f$, cytochrome b_6f complex; PQ, plastoquinone; Rubisco, ribulose-1,5-bisphosphate carboxylase/oxygenase.

In cyclic electron flow, FNR has been discussed to either be part of the diaphorase moiety of the NAD(P)H dehydrogenase (NDH) complex, which represents a plastid homolog of the respiratory NDH complex of bacteria and mitochondria, or to possibly re-insert electrons via association with the $Cytb_6f$ complex directly (Guedeney *et al.*, 1996; Quiles and Cuello, 1998; Zhang *et al.*, 2001; Okutani *et al.*, 2005). In addition to this, FNR was supposed to interact with several other thylakoidal proteins, such as the PsaE subunit of PSI, a still uncharacterized 10 kDa protein called connectein, or a subunit initially described as part of the OEC of PSII (*e.g.* Vallejos *et al.*, 1984; Shin *et al.*, 1985; Matthijs *et al.*, 1986; Chan *et al.*, 1987; Soncini and Vallejos, 1989; Andersen *et al.*, 1992). These reports could explain the observed anchoring of the hydrophilic FNR to the thylakoid membrane, but are nevertheless still disputed and many questions remain.

By generation of reduction equivalents, FNR also represents a link from light-driven photosynthesis to general metabolism. A number of different reactions depend on the reducing power of NADPH, ranging from carbon fixation (Calvin-Benson cycle) over nitrogen metabolism to lipid and Chl biosynthesis. Moreover, the stromal $NADP^+$/NADPH ratio has important regulatory and signaling functions in the chloroplast, as exemplified by the dynamic composition of the Tic complex in response to redox changes (Chigri *et al.*, 2006). The maintenance of the $NADP^+$/NADPH ratio is closely linked to other redox signaling systems in the chloroplast, as *e.g.* the Trx system. Interestingly, the electrons for the (re-) reduction of Trx come via Fd from the photosynthetic electron chain, and since this reaction is catalyzed by FTR, this protein is a competitor of FNR for reduced Fd.

Taken together, FNR is a crucial enzyme at the bifurcation of various redox-active pathways. Knowledge about its regulation by association with other proteins in the chloroplast is fundamental in understanding the general chloroplast metabolism. Its highly specific interaction with Tic62 was furthermore discussed as an important feature for the redox-regulation of preprotein import into the organelle, as it provides a link between photosynthetic electron transport and protein translocation. Interestingly, Peltier *et al*., 2004 found the *Arabidopsis* homolog of Tic62 to be associated with thylakoids by proteomic analysis, indicating a triple localization of Tic62 in the chloroplast, similar to FNR, and an even more extended shuttling of the protein within the chloroplast sub-compartments than experimentally explored so far. The novel function of Tic62 in the thylakoids mandated further studies examining how this localization might be involved in the respective redox sensing pathway.

[Passages of the text were taken out of previous publications of the author (Benz *et al*., 2007; Benz *et al*., 2009)]

5 Aim of this work

5.1 The Tic62/FNR complex

Successful translocation of nuclear-encoded chloroplast proteins across the IE membrane requires the well coordinated action of multiple proteinaceous components that comprise the Tic translocon. While the knowledge about the Tic motor complex is relatively detailed, much less is known about the components of the so-called redox-regulon: Tic62, Tic55 and Tic32. In particular the close interaction of Tic62 with the photosynthetic enzyme FNR as well as its multiple localization within the chloroplast holds the intriguing possibility of a function as a redox-sensor protein. Nevertheless, many aspects of these specific features of Tic62 remain elusive. A better understanding of the Tic62/FNR complex will provide essential insight into the redox network of the chloroplast and its connection to the import translocon. The major aim of the present work was therefore to elucidate the functional role of Tic62 with a focus on its interplay with FNR.

5.2 Heterologous expression of Tic20

Up to date, no experimental data have provided any direct indication for a channel activity of Tic20. The analysis of the protein is however hampered by its high hydrophobicity, and all attempts to heterologously express and purify the protein so far have failed. Especially the investigation of electrophysiological and biochemical properties depends highly on the availability of pure protein. Therefore, a second aim of this work was concerned with the establishment of an expression system that is capable of producing sufficient amounts of pure protein for these downstream applications. In addition, further experiments were aimed at the corroboration of a so far unsubstantiated functional cooperation of Tic20 and the main translocon channel protein Tic110.

Materials

1 Chemicals

All used chemicals were purchased in high purity from Sigma-Aldrich (Steinheim, Germany), Fluka (Buchs, CH), Roth (Karlsruhe, Germany), Roche (Penzberg, Germany), Merck (Darmstadt, Germany), AppliChem (Darmstadt, Germany), or Serva (Heidelberg, Germany). Radiolabeled amino acids ([^{35}S]Met) were obtained from DuPont-NEN (Dreieich, Germany).

2 Detergents

Detergents used in this work were from the following suppliers: *n*-dodecyl-*β*-D-maltoside (DDM), sodium dodecyl sulphate (SDS), and Triton X-100 (TX-100) were obtained from Roth, *n*-decyl-*β*-maltoside (DeMa) from Glycon (Luckenwalde, Germany), polyoxy-ethyleneglycol dodecyl ether (Brij-35) from Merck, digitonin and 3-[(3-cholamidopropyl) dimethylammonio]-1-propanesulfonate (CHAPS) from Calbiochem/Merck, dodecyl-phospho-*rac*-glycerol (DoPG) from Alexis (Läufelfingen, CH), *n*-lauroylsarcosine (N-LS) from Sigma and Nonidet P-40 (NP-40) from Fluka. Mega9 (nonanoyl-*N*-methylglucamide) was a kind gift from the lab of Prof. Dr. R.Wagner (Biophysics, University Osnabrück, Germany).

3 Enzymes

Restriction enzymes for cloning, RNA- and DNA-polymerases, and T4-DNA ligases were obtained from Roche (Penzberg, Germany), MBI Fermentas (St. Leon-Rot, Germany), New England Biolabs (Frankfurt a. M., Germany), Qiagen (Hilden, Germany), Eppendorf (Hamburg, Germany), Diagonal (Münster, Germany), GeneCraft (Köln, Germany) and Finnzymes (Espoo, Finnland). Reverse Transkriptase was from Promega (Madison, USA), RNase-free DNase I from Roche and RNase from Amersham Biosciences (Uppsala, Sweden). Cellulase R10 and Macerozyme R10 for digestion of the plant cell wall were from Yakult (Tokyo, Japan) and Serva (Heidelberg, Germany).

4 Kits

RNA from plants was isolated using the "Plant RNAeasy Kit" from Qiagen (Hilden, Germany). For high yield DNA purification, the "Plasmid Midi Kit" and for purification of DNA fragments from agarose gels the "Nucleospin Extract II Kit" from Macherey and Nagel (Düren, Germany) was used. *In vitro* translation was performed with the "Flexi Rabbit Reticulocyte Lysate System" from Promega (Madison, USA).

Initial experiments for *in vitro* protein synthesis were performed with the Rapid Translation System "RTS 100 & 500 *E. coli* HY Kit" from Roche.

5 Strains, vectors, clones and oligonucleotides

Cloning in *E. coli* was performed in the following strains: DH5α (Invitrogen, Karlsruhe, Germany), TOP10 (Invitrogen), and JM109 (New England Biolabs). Strains BL21 (DE3) and BL21 (DE3) RIL (both Novagen/Merck, Darmstadt, Germany) were used for heterologous expression of proteins.

Following vectors were used for cloning: pCR2.1 (Invitrogen), pET21d (Novagen/Merck), pCOLDII (Takara-Bio, Kyoto, Japan), pIVEX2.3 (Roche), and pSP65 (Promega). GUS-reporter gene vector pBI101 (Clontech, Mountain View, CA, USA) was a kind gift of Prof. Dr. N.M.Crawford (UCSD, CA, USA). The vectors pOL-GFP and pOL-RFP for transient transformation of *Arabidopsis* protoplasts were a kind gift of Prof. Dr. U.C.Vothknecht (Dept. Biologie I, Botany, LMU München; Mollier *et al.*, 2002).

Oligonucleotide primers used in this work were ordered in standard desalted quality from either Invitrogen or Operon (Köln, Germany)

6 Molecular weight markers and DNA standards

*Eco*RI and *Hind*III digested λ–Phage DNA (MBI Fermentas) was used as a molecular size marker for agarose-gel electrophoresis.

For SDS-PAGE the "MW-SDS-70L" and "MW-SDS-200" markers from Sigma-Aldrich (Steinheim, Germany) were used and for BN-PAGE the "HMW Native Marker Kit" from GE Healthcare (München, Germany)

7 Antibodies

The following primary antibodies were generated in this work: αTic20 (mature protein from *Pisum sativum*), αTic62 (C-terminus from *Arabidopsis thaliana*), and αFructose-1,6-bisphosphatase (αFBPase; full-length protein from *Arabidopsis thaliana*). Production and purification of the respective antigens is described in section 2.11 of Methods. All peptides/proteins were sent to BioGenes (Berlin, Germany) for immunization of rabbits.

Primary antibodies directed against Tic110, Tic62 (C-terminus from *Pisum sativum*), Tic55, Tic40, Tic32, Tic20 (N-terminal peptide from *Arabidopsis thaliana*), and LFNR1 (leaf isoform from *Arabidopsis thaliana*) were already available in the lab. Antisera recognizing Ndh-H, Cytf (PetA), and CF$_1$α/β (AtpA,B) were kind gifts of PD Dr. J.Meurer (Dept. Biologie I, Botany, LMU München) and that detecting PsaF was a kind gift of Prof. Dr. D.Leister (Dept. Biologie I, Botany, LMU München).

8 Plant material

All experiments were performed on *Arabidopsis thaliana* plants, ecotype Col-0 (Lehle Seeds; Round Rock, USA). The T-DNA insertion lines used for Tic62 (At3g18890) and LFNR1 (At5g66190) were: SAIL_124G04 (*tic62-1*), GABI_439H04 (*tic62-2*), SALK_085403 (*lfnr1-1*) and SALK_067668 (*lfnr1-2*) (Alonso *et al*., 2003; Rosso *et al*., 2003) and were purchased from NASC (University of Nottingham, GB) and GABI-Kat (MPI for Plant Breeding Research, Köln, Germany). Plants depleted for LFNR2 (At1g20020) by RNAi were line AGRIKOLA - N204598 (<u>A</u>rabidopsis <u>G</u>enomic <u>R</u>NA<u>i</u> <u>K</u>nock-<u>o</u>ut <u>L</u>ine <u>A</u>nalysis; Hilson *et al*., 2004) and were a kind gift of PD Dr. P.Mulo (University of Turku, Finland).

Peas (*Pisum sativum*) var. "Arvica" were ordered from Bayerische Futtersaatbau (Ismaning, Germany).

Methods

1 Molecular biological methods

1.1 General molecular biological methods

General molecular biological methods like growing conditions of bacteria, preparation of transformation-competent bacteria, DNA precipitation, determination of DNA concentration, and bacterial transformation were performed as described (Sambrook *et al.*, 1989) with slight modifications. Preparation of plasmid DNA, restrictions, ligations, and agarose gel electrophoresis were performed as described (Sambrook *et al.*, 1989) with modifications according to the manufacturer's recommendations.

1.2 Clones used in this work

Table 1: Plasmid DNA clones that were used in this work.
Additional information on the insert, cloning strategy, intended use and source (in case the clones were not generated by the author) are specified.

construct	AGI code	construct info	vector	restriction sites	use
pTic62*::*GUS	promoter of At3g18890	translational fusion: bp -1550 to +15	pBI101	*Sal*I - *Xba*I	GUS-reporter gene
pTic110*::*GUS	promoter of At1g06950	translational fusion: bp -1878 to +21	pBI101	*Xba*I - *Bam*HI	GUS-reporter gene
pTic20-I*::*GUS	promoter of At1g04940	translational fusion: bp -1754 to +21	pBI101	*Hind*III - *Spe*I	GUS-reporter gene
AtTic62-GFP	At3g18890	full-length	pOL-GFP	*Spe*I - *Sal*I	localization
AtTic62Nt-GFP	At3g18890	Met-1 to Val-333	pOL-GFP	*Spe*I - *Sal*I	localization
AtTic62Ct-GFP	At3g18890	Met-1 to Ser-66 (TP) and Pro-334 to His-641	pOL-GFP	*Spe*I - *Sal*I	localization
AtTic55-GFP	At2g24820	full-length	pOL-GFP	*Spe*I - *Sal*I	localization
AtLFNR1-RFP	At5g66190	full-length	pOL-RFP	*Nhe*I - *Sal*I	localization
AtLFNR2-RFP	At1g20020	full-length	pOL-RFP	*Nhe*I - *Sal*I	localization
PsTic62-IA3	Küchler *et al.*, 2002				expression in *E.coli*
LeTic62-fl	Stengel *et al.*, 2008				expression in *E.coli*
LeTic62-Nt	Stengel *et al.*, 2008				expression in *E.coli*
PsmFNR-L	-	Glu-53 to Tyr-360	pET21d	*Nco*I - *Xho*I	expression in *E.coli*
AtFBPase	At3g54050	full-length	pET21d	*Nco*I - *Bam*HI	expression in *E.coli*
AtTic62-Ct	At3g18890	Pro-334 to His-641	pET21d	*Nco*I - *Xho*I	expression in *E.coli*
AtpreFNR-L1	Küchler *et al.*, 2002				*in vitro* TK/TL
AtpreFNR-L2	Küchler *et al.*, 2002				*in vitro* TK/TL
PsmTic20-opt*	-	Ala-83 to Glu-253	pIVEX2.3	*Nco*I - *Sma*I	expression in RTS system / S12 lysate
AtmTic20-I*	At1g04940	Ala-103 to Asp-274	pCOLDII	*Nde*I - *Xba*I	expression in *E.coli*
pAR1219	T7-RNA polymerase (kind gift of Christoph Schwartz and Dr. Hüseyin Besir from the Dept. of Membrane Biochemistry, AG Prof. Dr. D.Oesterhelt, MPI for Biochemistry, Martinsried, Germany)				expression in *E.coli*

* for further information on codon-optimization, see section 1.3, for vector map, see Figure 8
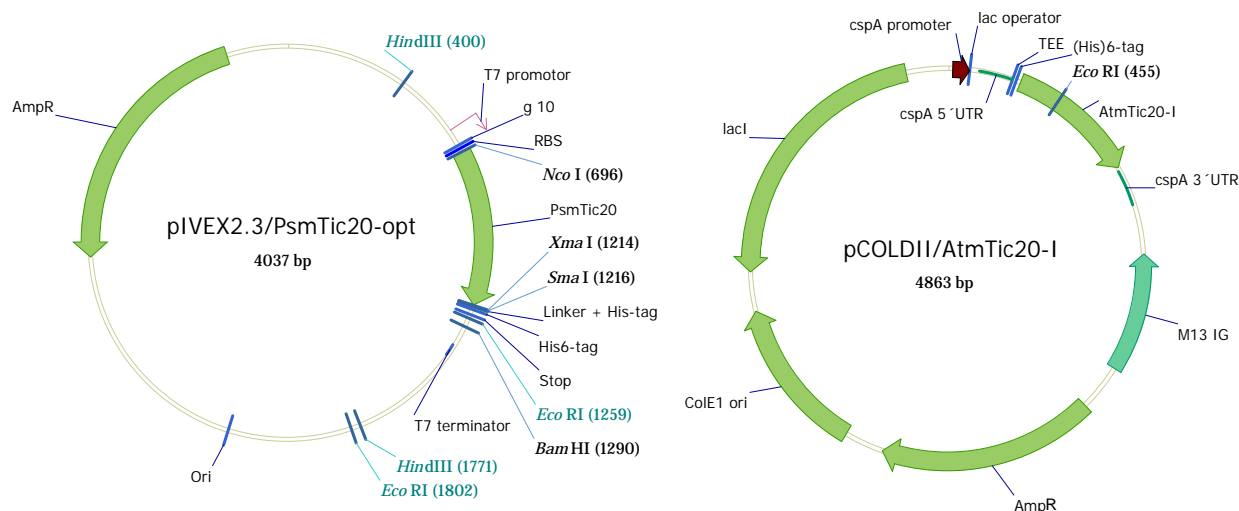
Figure 8: Vector maps of the Tic20 expression clones presented in this work. Vector maps were constructed for the two presented expression clones of Tic20 using the Vector NTI program (Invitrogen). pIVEX2.3/PsmTic20-opt was used for expression of the mature Tic20 protein from *Pisum sativum* (Ps) in the RTS *E. coli* HY Kit (Roche, Penzberg, Germany) as well as in the self-made *E. coli* S12 lysate. pCOLDII/AtmTic20-I was used for cold-induced expression of the mature Tic20 ortholog from *Arabidopsis thaliana* (At) in intact *E. coli* BL21 (DE3) cells. AmpR, ampicillin resistance (β-lactamase); ColE1 ori/Ori, origin of replication; cspA, cold-shock protein A; g10, initiation-enhancer region; lac*I*, lac repressor gene; RBS, ribosomal binding site; TEE, transcription enhancer element.

1.3 Generation of a codon-optimized PsmTic20 gene

For optimization of the Tic20 gene for the *E. coli* codon bias, the sequence coding for the mature part of Tic20 from *Pisum sativum* (PsmTic20), Ala-83 to Glu-253, was analyzed with the Leto 1.0 program by Entelechon (Regensburg, Germany). It analyzes gene sequences based on a genetic algorithm, allowing for the simultaneous optimization of a large set of competing parameters. Besides codon usage, the following features were optimized in parallel: (I) all internal restriction sites that could interfere with cloning were erased, (II) the number of codon tandem repeats was reduced, (III) potential helices in the mRNA secondary structure were reduced in size and abundance, (IV) the GC-content was adjusted to decrease local concentration peaks, and (V) AT/GC-stretches longer than four nucleotides in a row were avoided. The optimized gene was then synthesized by Entelechon and delivered as an insert in the pCR4-TOPO vector (Invitrogen).

For comparison, the native and optimized gene sequences are depicted in an alignment in Figure 9.

Figure 9: Sequence alignment of the PsmTic20 gene in its native state and in the codon-optimized form. A sequence alignment was performed with the cDNA sequence of Tic20 from *Pisum sativum* (PsTic20; AF095285) coding for the mature part of the protein (Ala-83 to Glu-253) and the codon-optimized version obtained from Entelechon (Regensburg, Germany). The *Pisum* sequence was retrieved from GenBank. The representation of the alignment is the "conserved" mode from the Genedoc program. Identical nucleotides are indicated by black boxes.

1.4 Preparation of genomic DNA from *Arabidopsis thaliana* for PCR genotyping

A small *Arabidopsis* leaf piece (~ 0.5 x 0.5 cm) was cut and transferred to a 1.5 ml microtube. 200 µl extraction buffer (200 mM Tris-HCl (pH 7.5), 250 mM NaCl, 25 mM ethylenediaminetetraacetic acid (EDTA), 0.5% SDS) and one small iron bead was added to the tube and the sample lysed in a TissueLyser (Qiagen, Hilden, Germany) for three minutes at max. speed. After pelleting of the debris for 15 min at 15,000 rpm and room temperature (RT), 100 µl of the supernatant was transferred to a fresh tube. To precipitate the genomic DNA, one volume of -20°C isopropanol was added to the sample, carefully mixed and centrifuged for another 15 min at 15,000 rpm and +4°C. The resulting pellet was washed once with 70% ethanol, subsequently air-dried and finally resuspended in 50 µl of sterilized H_2O or 10 mM Tris-HCl (pH 8.5). Immediately preceding use of the sample in PCR, residual non-dissolved debris was pelleted for 1 min at full speed in a table-top centrifuge. 0.5 µl of the DNA sample supernatant was then added to a standard 25 µl PCR.

1.5 Characterization of plant T-DNA insertion lines

Genomic DNA of the T-DNA insertion lines was screened by PCR genotyping. To identify plants with the T-DNA insertion in both alleles (homozygous), we used a combination of gene-specific primers flanking the predicted T-DNA insertion sites and T-DNA-specific left border (LB) primers (see Table 2). Usage of a LB primer (in combination with a corresponding gene-specific primer) will only generate an amplification product in plants

carrying at least one T-DNA allele (heterozygous or homozygous for the T-DNA). The combination of two gene-specific primers, on the other hand, will generate a PCR product only in DNA of plants carrying alleles without a T-DNA (WT and heterozygous for the T-DNA). For positions and orientations of the T-DNA inserts and oligonucleotide primers in *tic62-1* and *tic62-2*, see Figure 14. For *lfnr1-1* and *lfnr1-2*, see Lintala *et al*., 2007. To verify PCR products and T-DNA insertion sites, amplified DNA fragments were sequenced.

Table 2: List of used oligonucleotides for PCR genotyping of *Arabidopsis* T-DNA lines

allele	PCR for…	primer	seq. (5`-3`)
tic62-1	WT	Ex5fwd	GATCTCCGATATTACCGGTCCTTAC
		Ex6/8rev	AGTTTCTTTGTATGCATCAGTCG
	T-DNA	Ex5fwd	see above
		SAIL LB1	GCCTTTTCAGAAATGGATAAATAGCCTTGCTTCC
tic62-2	WT	atTic62fwd-NcoI	GAGCCATGGAAGGAACTTGTTTTCTCCGTGGACAACC
		Ex2rev	TTGCTTCTGTTACTACAGAGCTTG
	T-DNA	T-DNA-GABI	GGACGTGAATGTAGACACGTCG
		Ex2rev	see above
lfnr1-1	WT	FNR-L1_salk1_for	TTGAATTGTGTGGATAATGG
		FNR-L1_salk1_rev	CAACAAGTGAGAAAGAGTAG
	T-DNA	LBa1	TGGTTCACGTAGTGGGCCATCG
		FNR-L1_salk1_rev	see above
lfnr1-2	WT	FNR-L1 salk2_hinten_for	CTTATCTGGAAATGGATCCT
		FNR-L1 salk2_hinten_rev	GGCAACAACAGTGTCTAGAGA
	T-DNA	LBa1	see above
		FNR-L1 salk2_hinten_rev	see above

1.6 RNA extraction form *Arabidopsis thaliana* and RT-PCR

Total RNA from leaves of four-week-old *Arabidopsis* plants was isolated using the Plant RNeasy Extraction kit (Qiagen, Hilden, Germany). The RNA was digested with RNase-free DNase I (Qiagen) and transcribed into cDNA using MMLV Reverse transcriptase (Promega, Mannheim). Detection and quantification of transcripts were performed as described previously (Philippar *et al*., 2004) using a LightCycler (Roche, Penzberg). For Tic62, the gene-specific primers Ex3fwd (5`CTGGGATTTCGGGTTAGAG 3`) and Ex7rev (5`CGTAATTAAGACCGCTTTCA 3`) were constructed, amplifying a product of 416 bp, spanning both sites of the T-DNA insertion of *tic62-1*.

1.7 Affymetrix microarray-analysis

For microarray analysis, two rosette leaves each (number 6 & 7) from 20 five-week-old plants grown on soil under short-day conditions (8 h light, 100 μmol photons m^{-2} sec^{-1} at +21°C / 16 h dark at +16°C) were harvested, pooled and used for preparation of RNA. Three independent samples (n = 3) from both WT (Col-0) and *tic62-1* were taken from plants sown and harvested

in three consecutive weeks. Five µg RNA each were used and hybridized on Affymetrix „GeneChip *Arabidopsis* ATH1 Genome Arrays" using the Affymetrix „One-Cycle Labeling and Control" (Target) kits (Affymetrix UK, High Wycombe, UK) following the supplier`s protocols. Signal data were analyzed using the Affymetrix „Data Mining Tool" and „GeneChip Operating Software" (see *e.g.* Clausen *et al.*, 2004). The statistical significance of signal change was calculated using the SAM software (Tusher *et al.*, 2001) as described in Duy *et al.*, 2007. The isolation of RNA and hybridization of the microarrays were performed by D. Eder. Evaluation of the data was done by Dr. U. Oster and Dr. K. Philippar (all Dept. Biologie I, Botany, LMU München).

1.8 *In vitro* transcription and translation

Transcription of linearised plasmids was carried out as previously described (Firlej-Kwoka *et al.*, 2008).

Translation was carried out using the Flexi Rabbit Reticulocyte Lysate System from Promega (Madison, USA) following the manufacturers protocol in presence of [^{35}S]-methionine for radioactive labeling.

2 Biochemical methods

2.1 General biochemical methods

SDS-PAGE was performed according to Laemmli, 1970.

Gels were stained either by Coomassie Brilliant Blue R250 (Sambrook *et al.*, 1989) or silver-stained using a protocol according to Blum *et al.*, 1987 with modifications.

Determination of chlorophyll (Chl) concentration was carried out as described by Arnon, 1949.

Determination of protein concentration was performed as follows: For soluble proteins, the concentration was determined with the help of the Bio-Rad Protein Essay Kit (Bio-Rad, München, Germany). Concentration of proteins in membrane samples were determined according to Lowry *et al.*, 1951.

2.2 Preparation of whole-leaf protein extracts

Rosette leaves (0.1 g) of three to five-week-old plants were harvested and flash-frozen in liquid N_2. The frozen material was thoroughly ground with mortar and pestle and extracted by addition of either 750 µl SDS buffer (50 mM Tris (pH 8), 0.2 mM EDTA, 1% SDS) or sequential addition of first 400 µl Urea buffer (50 mM Tris (pH 8), 0.2 mM EDTA, 6 M urea) and subsequently 200 µl of SDS buffer. In the first case, both soluble and membrane proteins

are extracted in one step. In the latter case, first soluble and membrane-attached proteins are recovered by urea-treatment and only in the second step membrane proteins solubilized from the urea-insoluble pellet. Generally, the sample is incubated with the respective buffer for 15 min at room temperature (RT) and the insoluble material sedimented by centrifugation at full-speed in a table-top centrifuge for 10 min.

2.3 Two-dimensional blue native (BN) / SDS-PAGE and immunoblotting

Blue native gel electrophoresis (BN-PAGE) was carried out essentially as described in Schagger and von Jagow, 1991 and Wittig *et al.*, 2006 with the following modifications: Chloroplasts, thylakoids (equivalent to 5-50 μg of Chl) or IE membranes (50-200 μg protein) were solubilized in 50 mM Bis-Tris/HCl (pH 7.0), 750 mM 6-aminocaproic acid, 1% *n*-dodecyl-β-D-maltoside. After incubation on ice for 15 min, samples were centrifuged at 256,000 x g for 10 min at +4°C. The supernatant was supplemented with 0.1 vol. of a Coomassie Blue G solution (5% Coomassie Brilliant Blue G-250, 750 mM 6-aminocaproic acid) and loaded on a polyacrylamide gradient gel. Electrophoresis was carried out at increasing voltage (stacking gel: 100 V max.; separating gel: 15 mA/400 V max. for a 12 x 14 cm gel, 8 mA max. for a 6 x 8 cm gel) at +4°C. The cathode buffer contained 0.02% dye, and was replaced by buffer lacking dye after approximately one-third of the electrophoresis run. For 2D BN/SDS-PAGE the lanes were cut out after the run and incubated in 1% SDS, 1 mM β-mercaptoethanol (β-ME) for 15 min, followed by 15 min in 1% SDS without β-ME and 15 min in SDS-PAGE electrophoresis buffer (25 mM Tris, 192 mM glycine, 0.1% SDS) at RT. Single lanes were then placed on top of SDS-PAGE gels (10 or 12.5% polyacrylamide), and the individual complexes were separated into their constituent subunits by electrophoresis. For antibody detection, proteins were electro-blotted onto polyvinylidene fluoride (PVDF; Immobilon-P; Zefa, Harthausen) or nitrocellulose membrane (Protran; Whatman, Dassel) using a semi-dry Western blotting system (Hoefer TE 77; Amersham Biosciences, Freiburg) and Towbin buffer (25 mM Tris/HCl (pH 8.2-8.4), 192 mM glycine, 0.1% SDS, 20% methanol). Labeling with protein-specific primary antibodies was carried out by standard techniques, and bound antibodies were visualized either with alkaline phosphatase (AP)-conjugated secondary antibodies (goat anti-rabbit IgG (whole molecule)-AP conjugated; Sigma-Aldrich Chemie GmbH, Taufkirchen) or using a chemiluminescence detection system (see below) in combination with a horseradish peroxidase-conjugated secondary antibody (goat anti-rabbit (whole molecule)-peroxidase conjugated; Sigma).

2.4 BN-PAGE (Turku, Finland)

BN-PAGE was performed as described previously (Rokka *et al.*, 2005; Sirpiö *et al.*, 2007) with small modifications: Thylakoid membranes were resuspended in 25BTH20G buffer (25 mM BisTris/HCl (pH 7.0), 20% (w/v) glycerol and 0.25 mg/ml Pefabloc) to a final Chl concentration of 1 mg/ml. An equal volume of 2% (w/v) *n*-dodecyl-β-D-maltoside was added and the thylakoids were solubilized on ice for 3 min. Traces of unsolubilized material was removed by centrifugation at 18,000 x g at +4°C for 20 min. The supernatant was supplemented with 1/10 volume of 100 mM BisTris/HCl (pH 7.0), 0.5 M ε-amino-*n*-hexanoic acid, 30% (w/v) sucrose and 50 mg/ml Coomassie Blue G. Proteins were loaded on BN-PAGE in amounts corresponding to 3 μg of Chl per well. Electrophoresis (Hoefer Mighty Small, Amersham Pharmacia Biotech, Uppsala, Sweden) was performed at 0°C by gradually increasing the voltages as follows: 75 V for 30 min, 100 V for 30 min, 125 V for 30 min, 150 V for 60 min, 175 V for 30 min, and 200 V for 45–60 min or until the stain reached the end of the gel. After electrophoresis, proteins from the gel were electroblotted to PVDF membrane and Tic62 and FNR were detected using protein specific antibodies.

2.5 Immunoblot development

2.5.1 Enhanced Chemiluminescence (ECL)

Peroxidase-conjugated antibody signals were visualized by ECL detection. For this, solution 1 (100 mM Tis-HCl (pH 8.5), 1% (w/v) luminol, 0.44% (w/v) coomaric acid) and solution 2 (100 mM Tris-HCl (pH 8.5), 0.018% (v/v) H_2O_2) were mixed in a 1:1 ratio and added to the blot membrane (1-2 ml per small gel). After incubation for 1 min at RT (in the dark) the solution was removed and the luminescence detected with a film (Kodak Biomax MR; PerkinElmer, Rodgau, Germany).

2.5.1 Alkaline phosphatase detection

Detection of AP signals was performed in a buffer containing 66 μl / 10 ml NBT (nitro blue tetrazolium chloride, 50 mg/ml in 70% N,N-dimethylformamide) and 132 μl / 10 ml BCIP (5-bromo-4-chloro-3-indolyl phosphate, 12.5 mg/ml in 100% N,N-dimethylformamide) in 100 mM Tris-HCl (pH 9.5), 100 mM NaCl, 5 mM $MgCl_2$ buffer.

2.6 Isoelectric focusing (IEF)

2.6.1 Preparation of stroma samples

Rehydration buffer (7 M urea, 2 M thiourea, 0.2% biolytes 3-10 (Bio-Rad, München), 2% CHAPS, 100 mM dithiothreitol (DTT), bromophenol blue) is supplemented just before use with protease inhibitors (for 3.0 ml buffer: 2.88 ml urea/thiourea rehydration buffer, 0.06 ml

50x complete (in H_2O), 0.03 ml 100 mM phenylmethylsulfonyl fluoride (PMSF; in isopropanol), 0.003 ml pepstatin 1 mg/ml (in pure ethanol)). 200 µg soluble protein (with a concentration of at least 6 mg/ml) is filled up with this buffer to a total volume of 200 µl and incubated at RT for 1 h. The samples are centrifuged for 10 min at 20,000 x g at RT and the supernatant is loaded into an IEF-tray (for 11 cm strips).

2.6.2 Preparation of thylakoid samples

For membrane samples, delipidation has to be performed to improve the quality and resolution of the gels. For this purpose, thylakoids according to 200 µg Chl are pelleted and resuspended in 1 ml delipidation solution (tri-*n*-butylphosphate : acetone : methanol = 1:12:1). The samples are incubated for 90 min at +4°C and centrifuged for 15 min at 2,800 x g, +4°C. The white pellet is subsequently washed in first 1 ml tri-*n*-butylphosphate, then 1 ml acetone and finally 1 ml methanol (resuspend pellet, centrifuge for 5 min at 2,800 x g). After air-drying of the pellet, it is resuspended in 200 µl rehydration/protease buffer (see above) containing 4% CHAPS, incubated for 5 min at +90°C and subsequently for 15 min at +35°C (in block-heater, shaking). The samples are centrifuged for 10 min at 20,000 x g at RT and the supernatant is loaded into an IEF-tray (for 11 cm strips).

2.6.3 First dimension IEF

The samples (200 µl) are loaded into the IEF-tray, the protection foil is removed from the strips (ReadyStrip IPG strips, pH range 3-10, Bio-Rad, München) and gel strips are put on top of the sample avoiding air bubbles between the strip and the sample (gel side on bottom, writing on the left hand side). After incubation for 1 h at RT, the strips are covered with mineral oil and the run is started (Protean IEF Cell; Bio-Rad; settings: preset method; rapid; rehydration: yes, active; gel length 11 cm; pause after rehydration: yes; hold at 500V: yes). After 12 h of rehydration, the run pauses and wet wicks (use 10 µl H_2O per wick) are inserted between strips and electrodes. Then the program is continued for ~ 9.5 h (35,000 Vh, end voltage: 8,000 V). After the run finishes, the strips are drained on a tissue to remove oil and transferred into a clean tray (with gel side facing up). They can either be applied directly to the second dimension or stored at -80°C for several weeks.

2.6.4 Second dimension SDS-PAGE

The strips are transferred to a clean tray and equilibrated for 20 min in equilibration buffer I (6 M urea, 2 % SDS, 50 mM Tris (pH 8.8), 20% glycerol, 2% DTT). After incubation in equilibration buffer II (6 M urea, 2% SDS, 50 mM Tris (pH 8.8), 20% glycerol, 2.5% iodoacetamide) for 10 min, the strips are covered with running buffer. SDS-gels (with Rotiphorese Gel 40 (29:1) acrylamide; Carl Roth GmbH, Karlsruhe) contain 0.1% SDS in

both the stacking and separating gel and are poured in a Bio-Rad gel system (Criterion Cassette). After application of the IEF strip to the top of the stacking gel, it is directly overlaid with 1% agarose (in running buffer). Electrophoresis is performed in a Criterion Cell (Bio-Rad) at 35 mA per gel.

2.6.5 Staining of gels (colloidal Coomassie)

For staining, the gels are first fixed in 30% ethanol, 2% phosphoric acid (100 ml per gel) for at least 5 h or overnight on a shaker at RT. The gels are then washed in H_2O three times for 20 min each (or longer). Subsequently, gels are incubated in staining solution (120 ml per gel; 17% ammonium sulfate, 2% phosphoric acid, 34% methanol) for 1 h before 120 mg Coomassie Blue G-250 (1 mg dye/ml) are sprinkled onto the surface. After incubation for 3 days (on a shaker at RT), the gels are washed for 1 h in H_2O and are then ready for scanning and analysis.

2.7 Protein identification by mass spectrometry (MS)

Coomassie- or silver-stained protein spots were cut from SDS-PAGE gels and send for identification to the "Zentrallabor für Proteinanalytik" (ZfP, Adolf-Butenandt-Institut, LMU München). There, tryptic peptides were detected either by Peptide Mass Fingerprint (MALDI, <u>M</u>atrix <u>A</u>ssisted <u>L</u>aser <u>D</u>esorption/<u>I</u>onization) or LC-MS/MS (<u>L</u>iquid <u>C</u>hromatography with MS) runs. Protein identification was then accomplished with a Mascot software assisted database search. Only hits displaying a threshold score of >= 60 were analyzed further.

2.8 Sucrose density gradient centrifugation

250 µg of IE vesicles were incubated with either H_2O, 1 mM $NADP^+$ or 1 mM NADPH for 15 min at 25°C, followed by solubilisation with 1.5% *n*-decyl-β-maltoside for 15 min on ice. Linear sucrose gradients (10-50% w/v sucrose in 25 mM Hepes-KOH (pH 7.6), 1 mM EDTA, 1 mM PMSF, ± 0.1 mM NADP(H)) were centrifuged at 342.000 x g for 16 h at 4°C. Fractions of 200 µl were collected, precipitated with trichloroacetic acid (TCA) and analyzed by SDS-PAGE and immunoblotting.

2.9 Pea thylakoid isolation and redox treatment

Chloroplasts from pea were isolated from leaves of 9-11 days old pea seedlings (*Pisum sativum* var. Arvica) and purified through Percoll density gradients as previously described (Keegstra and Youssif, 1986; Waegemann and Soll, 1995). Chloroplasts were subsequently lysed by incubation in 5 mM Hepes-KOH (pH 7.6) (100 µg Chl/1 ml) for 20 min on ice and thylakoids separated from the stroma by centrifugation (5 min 5,000 x g at +4°C).

For the redox assay, thylakoids (10 μg Chl) were resuspended in 100 mM Tris-HCl (pH 7.6), 10 mM $MgCl_2$, 1 mM EDTA, 0.1% *n*-decyl-β-D-maltoside and incubated for 10 min on ice. Subsequently, 1 mM of the respective pyridine nucleotides was added (or mock treatment with H_2O) and incubated for 30 min at +25°C followed by ultra-centrifugation (256,000 x g, +4°C for 10 min) to separate soluble from insoluble proteins.

2.10 Enzymatic assays

2.10.1 Cyt c reduction

Fd-dependent cytochrome c (Cyt c) reductase activity was determined by an assay consisting of 20 μM Cyt c (horse heart), 0.1 μM Fd (spinach) and 100 μM NADPH in 1 ml of a 50 mM Tris-HCl (pH 7.5), 100 mM NaCl, 1 mM $MgCl_2$ reaction buffer. The reduction of Cyt c was monitored with a spectrophotometer (Ultrospec 3100pro, Amersham Biosciences, Freiburg, Germany) at 550 nm in kinetic mode over a course of 120 sec. The amount of reduced Cyt c was calculated from the extinction coefficient $\varepsilon = 21.1$ mM^{-1} cm^{-1}.

2.10.2 NADP-malate dehydrogenase activity

The NADP-malate dehydrogenase (MDH) activity was measured basically as described by Scheibe and Stitt, 1988. *Arabidopsis* leaves (~ 100 mg) from ~ three-week-old plants grown under standard long-day conditions on soil were shock-frozen in liquid N_2 and used for the assay. The leaves were ground in liquid N_2 using mortar and pestle and the powder transferred to a microtube. 500 μl isolation buffer (50 mM sodium acetate (pH 6.0), 1 mg/ml BSA, 0.2 mg/ml Pefablock, 4 mM DTT, 0.1% TX-100; degassed and bubbled with N_2) were added to the powder, mixed until homogenous and incubated on a laboratory wheel for 5-10 min at RT. An aliquot was used for Chl-determination, before the insoluble debris was pelleted by centrifugation (1 min, 15,000 rpm). The resultant supernatant was transferred into a fresh tube and used for the assay. Three measurements were performed with each sample, each in a vol. of 1 ml: (1) NADP(H)-MDH initial activity, (2) maximal activity, and (3) NAD(H)-MDH (background) activity. The oxidation of NADPH/NADH was monitored with a spectrophotometer (Ultrospec 3100pro, Amersham Biosciences) at 340 nm in kinetic mode over a course of 180 sec. Samples were shortly bubbled with N_2 just before measurement and tightly closed with Parafilm to avoid oxidation. (1) 931 μl standard assay mix (100 mM Tris-HCl (pH 8.0), 1 mM EDTA, degassed and bubbled with N_2; add fresh: 0.2 mM NADPH) was added to 50 μl of sample. Just before measurement, 19 μl 100 mM oxaloacetate (endconc. 2 mM) was added (kept on ice; pre-warmed immediately before adding to buffer). (2) 50 μl sample were incubated with 25 μl 0.5 M DTT and 25 μl 1 M Tris-HCl (pH 9.0) for 40 min at RT. For measurement, 881 μl standard assay mix plus 19 μl oxaloacetate were added as

above. (3) Background activity was measured with 2 µl sample in 989 µl NAD-MDH assay mix (100 mM Tris-HCl (pH 8.0), 1 mM EDTA, 10 mM MgCl$_2$, 0.2 mM NADH) plus 9.5 µl oxaloacetate (endconc. 1 mM). NADP(H)-MDH activity was calculated from the following equation:

$$\text{NADP(H)-MDH activity} = (a - 0.002 \text{ x } b) / (c - 0.002 \text{ x } b)$$

a = NADP(H)-MDH initial activity

b = NAD(H)-MDH activity

c = NADP(H)-MDH maximal activity

2.11 Protein expression and purification

2.11.1 Expression of Tic20 in the RTS E. coli HY system

Expression of PsmTic20 in the RTS *E. coli* HY system (Roche, Penzberg, Germany) in absence and presence of detergents was performed according to the manufacturer`s instructions.

2.11.2 Preparation of an E. coli cell-free (S12) lysate

The set-up of the system and initial experiments were done with technical help of Christoph Schwartz and Dr. Hüseyin Besir from the Dept. of Membrane Biochemistry, AG Prof. Dr. Dieter Oesterhelt, at the MPI for Biochemistry (Martinsried). The final protocol is a modification of the protocol by Kim *et al.*, 2006.

The cell extracts were prepared from *E. coli* strains BL21 (DE3) and BL21 (DE3) RIL (Novagen/Merck) for production of the uninduced or T7-RNA polymerase induced lysate, respectively. BL21 (DE3) RIL were therefore previously transformed with the pAR1219 construct. The bacteria (BL21 (DE3) without antibiotics, BL21 (DE3) RIL-pAR1219 with 50 µg/ml chloramphenicole, 100 µg/ml ampicillin) were grown first at +37°C in a small (10 ml LB medium) overnight culture and then diluted (1:100) into 1 L main culture in KYGT medium (per 1L: 5.6 g KH$_2$PO$_4$, 28.9 g K$_2$HPO$_4$, 10 g yeast extract; after autoclaving add (filter-sterilized) 25 ml 40% glucose and 15 mg thiamine). The main culture was grown at +37°C with vigorous agitation and aeration (250 rpm). When the cell density (OD$_{600}$) reached 0.6, 1 mM isopropyl-1-thio-β-D-galactopyranoside (IPTG) was added to BL21 (DE3) RIL-pAR1219 to express the T7-RNA polymerase, and cells were further grown until OD$_{600}$ ≈ 4.5 (mid-log phase). Uninduced BL21 (DE3) were only grown until OD$_{600}$ ≈ 1.5 and then harvested by centrifugation at 3,000 x *g* for 10 min at +4°C. All following steps were performed on ice. The weight of the wet cell pellets was determined and cells were carefully washed three times with 20 ml/g of ice-cold buffer A (10 mM Tris-acetate buffer (pH 8.2), 60 mM potassium glutamate, 14 mM magnesium acetate, 1 mM DTT, and 0.05% β-ME; prepare

with diethylpyrocarbonate (DEPC)-H_2O; add DTT and β-ME fresh) by shaking or knocking by hand, *not* pipetting. After the last wash (with only half of β-ME), the weight of the wet cell pellet was determined again and could be stored at -80°C at this point. Alternatively (or after thawing), cells were resuspended carefully in 1.27 ml/g of buffer B (same as buffer A without β-ME) and disrupted in a French press cell (SLM-Aminco/Thermo Scientific, Langenselbold, Germany) in a *single* run at constant pressure of 20,000 psi (settings at 1,200 psi at high ratio). Subsequently, the lysate was cleared at 12,000 x *g* for 10 min at +4°C and the recovered supernatant incubated for 30 min at +37°C in the dark (wrapped in aluminum foil; rolling). The resulting extract was divided into small aliquots, shock-frozen in liquid N_2, and stored at -80°C for later use in cell-free protein synthesis.

2.11.3 Cell-free protein synthesis in the S12 lysate

Basic components of the *in vitro* system are (I) the *E. coli* lysate providing the basic transcription and translation machinery (*e.g.* ribosomes), (II) an efficient RNA polymerase driving the transcription of the GOI (*e.g.* T7-RNA polymerase), (III) an energy-regenerating system (*e.g.* creatine phosphate and creatine kinase), (IV) a supply of nucleotides, tRNAs and amino acids, as well as (V) further additives and buffering components.

Expression of soluble PsmTic20 in presence of detergent: Cell-free protein synthesis was carried out in a 1.5 or 2.0 ml microtube in a 100-200 µl volume at +30°C for 1-2 h with constant rolling. The plasmid pIVEX2.3-PsmTic20 was used as template for the reaction. The standard reaction mixture consisted of the following components: 57 mM Hepes-KOH (pH 8.2), 1.2 mM ATP, 0.85 mM each of CTP, GTP, and UTP, 2 mM DTT, 0.17 mg/ml *E. coli* total tRNA mixture (from strain MRE600), 0.65 mM cAMP, 90 mM potassium glutamate, 80 mM ammonium acetate, 15 mM magnesium acetate, 34 µg/ml ʟ-5-formyl-5,6,7,8-tetrahydrofolic acid (folinic acid), 0.75 mM each of 20 amino acids, 2% polyethylene glycol 8000 (PEG), 100 mM creatine phosphate (CP), 0.27 mg/ml creatine kinase (CK), ~ 10 µg/ml plasmid DNA (1µl of 0.5-1µg/µl in 100 µl rct.), 25% BL21 (DE3) and 2% BL21 (DE3) RIL-pAR1219 cell extract. Detergent was added as shown in results, section 2.2.

For visualization of the reaction products, 5 µl of the reaction were centrifuged for 10 min at 10,000 x g. The supernatant was precipitated by addition of 50 µl (-20°C) acetone for 5 min on ice (to separate protein and PEG) and again centrifuged for 5 min at 10,000 rpm at +4°C. The resulting pellet was air-dried for 10 min and both pellets resuspended in 20 µl of SDS-PAGE sample buffer.

For purification of the PsmTic20 protein, 50-100 reactions were pooled and insoluble material removed by centrifugation at 10,000 x g for 10 min at +4°C. The supernatant (5-10 ml) was

then diluted 1:3 with buffer S1 (50 mM NaH_2PO_4-NaOH (pH 8.0), 300 mM NaCl, 0.8% Brij-35, 20 mM imidazole) and incubated for 1 h in presence of 3 mM ATP with 20-100 µl Ni-NTA-Sepharose (GE Healthcare, Munich, Germany), rolling, in the cold-room. Subsequently, the beads were washed five times with 1 ml each of buffer S1 and transferred to a clean micro-column (Mobicols; MoBiTec, Göttingen, Germany). Elution was carried out by a step-wise increase of imidazole concentration in buffer S1 (50, 100, 200, 250, 500, 1000 mM) in 100-200 µl volume each.

For immunization of rabbits, the protein was dialysed (two times 1 l each) against 20 mM Tris-HCl (pH 7.0), 154 mM NaCl and for reconstitution assays (at the University Osnabrück) against 10 mM MOPS/Tris (pH 7.0), 120 mM KCl using a dialysis membrane with a MWCO of 3,500 Da (Spectra/Por, Spectrum Laboratories, Rancho Dominguez, CA, USA). For CD-spectroscopy, see section 5.1.

2.11.4 Cold-induced expression of AtmTic20-I

AtmTic20-I/pCOLDII was transformed in BL21 (DE3) cells (Novagen/Merck) and grown at +37°C with vigorous shaking (240 rpm) in M9ZB medium to an OD_{600} of 0.4. Cells were then shifted for 30 min to +15°C, subsequently induced by addition of 1 mM IPTG and further grown at the same temperature for overnight. Cells were harvested and resuspended in 50 mM Tris-HCl (pH 8.0), 150 mM NaCl and lysed by two passages through a M-110L Microfluidizer Processor (Microfluidics, Newton, MA, USA). Cell membranes and inclusion bodies were pelleted by centrifugation at 20,000 x g and +4°C for 20 min and solubilized in 50 mM Tris-HCl (pH 8.0), 300 mM NaCl, 1% *n*-lauroylsarcosine (N-LS) for 1 h, rotating in the cold-room. Unsolubilized material was removed by centrifugation at 20,000 x g and +4°C for 15 min, and the cleared supernatant used for batch Ni^{2+}-affinity purification using Ni-NTA-Sepharose (GE Healthcare, Munich, Germany). Tic20 was bound to Ni^{2+} for 1 h at +4°C without imidazole, the beads were then washed five times with 30 bead volumes each of 50 mM Tris-HCl (pH 8.0), 300 mM NaCl, 0.3% N-LS, 10 mM imidazole and two times with three bead volumes each of 50 mM Tris-HCl (pH 8.0), 150 mM NaCl, 0.3% N-LS, 10 mM imidazole. Elution was carried out six times with one bead volume each of 50 mM Tris-HCl (pH 8.0), 150 mM NaCl, 0.3% N-LS, 100 mM imidazole and checked by SDS-PAGE and Coomassie-staining. The best elutions were pooled, filtered and subjected to size-exclusion chromatography on a Superdex 75 HR 10/30 column (GE Healthcare) using 50 mM Tris-HCl (pH 8.0), 150 mM NaCl, 0.3% N-LS as buffer with a flow rate of 0.5 ml/min.

2.11.5 Other constructs

For heterologous expression, constructs were transformed in *E. coli* BL21 (DE3) cells (Novagen/Merck) and grown at +37°C in the presence of 100 µg/ml ampicillin to an OD_{600} of 0.5 (PsTic62-IA1, PsmFNR-L and FBPase in LB medium and LeTic62-fl as well as LeTic62-Nt in M9ZB medium). Expression was induced by addition of 1 mM IPTG, and cells were grown for 3 h at +37°C (PsTic62-IA1 and FBPase) or at +12°C for overnight (LeTic62-fl, LeTic62-Nt, and PsmFNR-L), respectively. All proteins were purified via their C-terminal polyhistidine tags using Ni-NTA-Sepharose (GE Healthcare, Munich, Germany) under native conditions and eluted with 100-400 mM imidazole. The proteins were always used fresh, concentrated and buffer was exchanged for 50 mM Tris-HCl (pH 8.0), 150 mM NaCl prior to binding or activity assays.

In preparation for the Cyt c reduction assay, 10 µg of purified FNR was incubated for overnight at +4°C in a rotary shaker in 1 ml of reaction buffer, supplied with or without the indicated molar amounts of Tic62 or control (egg albumin) protein.

2.12 Tic62 affinity chromatography

AtTic62-Ct/pET21d was expressed in *E. coli* BL21 (DE3) (Novagen, USA). The expressed peptide was purified under native conditions by its C-terminal polyhistidine tag using Ni-NTA-Sepharose (GE Healthcare, Munich, Germany) and subsequent size-exclusion chromatography using a Superdex 75 column (GE-Healthcare) in 50 mM Na_2HPO_4/NaH_2PO_4 buffer (pH 8.0), 150 mM NaCl. The purest fractions were again bound to Ni-NTA-Sepharose beads and washed three times with 30 bead volumes each (50 mM Na_2HPO_4/NaH_2PO_4 buffer (pH 8.0), 300 mM NaCl), followed by three washes with 1% egg albumin in the same buffer to saturate unspecific binding sites and five washes without albumin. An empty column without the addition of His-tagged protein was used as negative control. The columns were then incubated with concentrated stroma from *tic62-1 Arabidopsis* plants (lacking endogenous Tic62 protein) for 1 h at +4°C followed by 8 washes and elution by sequential addition of 750 mM NaCl (E1), 1 M NaCl (E2), 4 M urea (E3), 8 M urea (E4), 200 mM imidazole (E5) and 400 mM imidazole (E6). Proteins were subsequently separated on a 12% acrylamide, 4 M urea-SDS-PAGE, blotted and probed for FNR using an antibody raised against LFNR1 (reacting with both leaf isoforms).

2.13 PEGylation assay

IE vesicles were treated with 40 mM metoxypolyethylenglycol-maleimide 5,000 Da (PEG-MAL, Laysan Bio, Arab, AL) in a buffer containing 100 mM Tris/HCl (pH 7.0), 1 mM

EDTA, for 0, 5, 10, and 30 min, at 4° C in the dark in absence or presence of 1% SDS. The PEGylation reaction was stopped by addition of 100 mM DTT and SDS-PAGE sample buffer. Bis-Tris gels (0.36 M Bis-Tris-HCl (pH 6.5-6.8), 10% acrylamide), were employed using a MES running buffer (50 mM MES, 50 mM Tris, 1 mM EDTA, 1 mM sodium bisulfite, 0.1% SDS). The protein was detected by immunoblotting.

3 Cell biological methods

3.1 GUS-reporter gene detection

For the histochemical localization of β-glucuronidase activity (GUS) whole seedlings or plants were submerged in staining solution consisting of 25 mM Na_2HPO_4/NaH_2PO_4 buffer (pH 7.0), 2 mM 5-bromo-4-chloro-3-indolyl-β-d-glucuronide cyclohexylamine salt (X-gluc), 0.5 mM ferricyanide, 0.5 mM ferrocyanide, and 10 mM EDTA at +37°C for 4 h to overnight. The β-glucuronidase (GUS) staining solution was removed and changed for 70% ethanol to "bleach" the tissue.

3.2 Preparation of inner and outer envelope vesicles from *Pisum sativum*

For isolation of IE and OE vesicles from chloroplasts, pea seedlings grown for 9-11 days on sand, under a 12/12 hours dark/light regime, were used. All procedures were carried out at 4°C. Pea leaves cut from ~ 20 trays were ground in a kitchen blender in 10-15 l isolation medium (330 mM sorbitol, 20 mM MOPS, 13 mM Tris, 0.1 mM $MgCl_2$, 0.02% (w/v) BSA) and filtered through four layers of mull and one layer of gauze (30 μm pore size). The filtrate was centrifuged for 5 min at 1,500 x g, the pellet gently resuspended with a brush and intact chloroplasts reisolated via a discontinuous Percoll gradient (40% and 80%). Intact chloroplasts were washed twice with wash medium (330 mM sorbitol, Tris-base (~ pH 7.6)), homogenized and further treated according to the modification (Waegemann *et al.*, 1992) of the previously described method (Keegstra and Youssif, 1986).

3.3 Isolation and fractionation of *Arabidopsis* chloroplasts

Intact *Arabidopsis* chloroplasts were prepared from ~ 150 g fresh weight leaf material of four-week-old plants grown in soil essentially as described in Seigneurin-Berny *et al.*, 2008. Chloroplasts were subsequently taken up in 15 ml of 10 mM Hepes-KOH (pH 7.6), 5 mM $MgCl_2$ and lysed using 50 strokes in a small (15 ml) Dounce-homogenizer (Wheaton, Millville, NJ, USA). Further separation in stroma, thylakoids, and envelopes was done according to Li *et al.*, 1991.

For high ionic-strength washes of *Arabidopsis* thylakoids, chloroplasts were isolated with the above protocol, ruptured by incubation in 10 mM Hepes-KOH (pH 7.6), 5 mM $MgCl_2$ for 20 min on ice, and separated in membranes and supernatant by centrifugation at 5,000 x g for 5 min at +4°C. The membrane fraction was washed several times (in Hepes/Mg buffer without additional salt) to get rid of stroma proteins, and then incubated, rotating, for 30 min at +4°C in the dark with Hepes/Mg buffer incl. 500mM NaCl. The supernatant was then used in sprectrophotometric Cyt c reduction assays and for immunoblotting. The pellet was resuspended in Hepes/Mg buffer and likewise saved for immunoblotting.

3.4 Isolation of thylakoid membranes from *Arabidopsis* (Turku, Finland)

Frozen leaves were ground in buffer containing 0.1% BSA, 50 mM Hepes-NaOH (pH 7.4), 300 mM sucrose, 5 mM $MgCl_2$, 5 mM EDTA, filtered through one layer Miracloth and pelleted at 6,000 x g at +4°C for 5 min. The pellet was resuspended in shock buffer (5 mM sucrose, 50 mM Hepes-NaOH (pH 7.4), 5 mM $MgCl_2$), centrifuged at 6,000 x g at +4°C for 5 min, and this pellet resuspended in storing buffer (100 mM sucrose, 10 mM Hepes-NaOH (pH 7.4), 10 mM $MgCl_2$). Thylakoids were stored at -70°C for later use.

3.5 *Arabidopsis* thylakoid sub-fractionation

Arabidopsis leaves were homogenized in 25 ml of isolation buffer (0.4 M sorbitol, 0.1 M Tricine-KOH (pH 7.8), 0.3 mM PMSF). After two rounds of filtration through a layer of gauze, the homogenate was pelleted at 1,400 x g for 10 min at +4°C, resuspended and washed once in isolation buffer. Chloroplasts were resuspended in lysis buffer (25 mM Hepes-KOH (pH 7.8), 5 mM $MgCl_2$, 0.3 mM PMSF) and incubated for 15 min on ice in the dark. After centrifugation at 10,000 x g for 10 min at +4°C, thylakoids were resuspended in buffer B (15 mM Tricine-KOH (pH 7.9), 0.1 M sorbitol, 10 mM NaCl, 5 mM $MgCl_2$).

To separate stroma thylakoids from grana thylakoids, the protocol of Ossenbühl *et al*., 2002 was followed. Briefly, isolated thylakoid membranes (0.2 mg/ml of Chl) were solubilised with 0.1 % digitonin in buffer B for exactly 5 min at RT. The incubation was stopped by adding 10 vol. buffer B. Fractionation was obtained by four rounds of centrifugation at +4°C, beginning with 1,000 x g for 30 min (1K, unlysed chloroplasts), 10,000 x g for 30 min (K10, grana), 40,000 x g for 1 h (40K, margins) and at 140,000 x g for 1.5 h (140K, stroma lamellae). The final supernatant was precipitated with TCA. Subfractions were used for immunoblots.

3.6 *Arabidopsis* chloroplast isolation and protein import

Chloroplasts were isolated from 17 to 18-days-old *Arabidopsis* plants (grown on plates) according to the protocol by Aronsson and Jarvis, 2002 with the following exceptions: all

buffers were supplied with 0.4 M sorbitol, and NaHCO$_3$ as well as gluconic acid were omitted. An import reaction (containing chloroplasts equivalent to 7.5 µg Chl) was subsequently carried out in 100 µl volume containing 3 mM ATP and 1-5% (v/v) [^{35}S]-labeled translation products. Import reactions were initiated by the addition of translation product to the import/chloroplast mix and carried out for the indicated time at +25°C. Reactions were terminated by the addition of 2 volumes ice-cold washing buffer. Chloroplasts were washed twice in wash medium (0.4 M sorbitol, 50 mM Hepes-KOH (pH 8.0), 3 mM MgSO$_4$) and finally resuspended in Laemmli buffer (50 mM Tris-HCl (pH 6.8), 100 mM β-ME, 2% (w/v) SDS, 0.1% bromophenol blue (w/v), 10% glycerol (v/v)). For BN-PAGE separation of thylakoid proteins, the import was performed as above (30 min import time), and the chloroplasts lysed after the second wash in 25 µl of shock buffer (10 mM Hepes-KOH (pH 8.0), 5 mM MgCl$_2$) for 10 min on ice. Stroma was separated from the membranes by ultracentrifugation (10 min 256,000 x g at +4°C). The supernatant was treated with BN-loading buffer and the pellet solubilized using standard procedures (see below).

Import products were separated by SDS-PAGE and radiolabeled proteins were analyzed by a phosphorimager or by exposure on autoradiography films (Kodak Biomax-MR).

4 Plant methods

4.1 Plant growth conditions and harvesting of samples

In Munich: To synchronize germination, all seeds were subjected to vernalization at +4°C for two days. Plants were grown on soil or on 0.3% Gelrite medium containing 1% D-sucrose and 0.5 x MS salts at pH 5.7. Unless stated otherwise, plant growth occurred in growth chambers with a 16 h light (+21°C; 100 µmol photons m^{-2} s^{-1}) and 8 h dark (+16°C) cycle. Before sowing on sterile plates, seeds were surface-sterilized with 70% ethanol, 0.05% Triton X-100 for 10 min and washed four times with 96% ethanol. If not stated otherwise, plants were harvested during the early light phase, shock-frozen in liquid N$_2$ and stored at -80°C until use.

In Turku, Finland: *Arabidopsis thaliana* ecotype Col-0 (WT), T-DNA insertion lines *tic62-1* and *lfnr1*, and RNAi line *lfnr2* were grown in soil/vermiculite mixture under short day conditions (8 h light / 16 h darkness) for five weeks under illumination of 100 µmol photons m^{-2} sec^{-1} at +23°C. Leaf samples were harvested from the darkness in the end of the dark period (dark), from the growth light conditions after four hours of onset of light (GL) or plants were transferred to 1000 µmol photons m^{-2} sec^{-1} for two hours after one hour exposure under GL light (high light, HL). Leaves were shock frozen in liquid nitrogen and stored for later use at -70°C.

4.2 Plant transformation

Plants were transformed with the Agrobacterium strain UIA143 (kind gift of PD Dr. C.Bolle, Dept. Biologie I, Botany, LMU München) using the floral dip procedure (Clough and Bent, 1998) and subsequently selected for positive transformation events on MS-plates containing 1% sucrose and the antibiotic kanamycin (Kan). The descendents of the initial Kan_R-plants were screened for a 3 Kan_R : 1 Kan_S ratio, indicating a single T-DNA insertion event. Homozygous lines (all descendants Kan_R) were produced in the next generation only from those plants and used for further analysis.

4.3 Preparation and transient transfection of *Arabidopsis* protoplasts

Arabidopsis mesophyll protoplasts were isolated from leaves of four-week-old plants and transiently transfected according to the protocol of Jen Sheen (available at http://genetics.mgh.harvard.edu/sheenweb/protocols_reg.html). GFP fluorescence was observed with a Leica TCS SP5 confocal laser-scanning microscope (Leica Microsystems, Wetzlar, Germany).

4.4 Chlorophyll fluorescence measurements

4.4.1 Chlorophyll fluorescence measurements of PSII (Munich)

In vivo Chl *a* fluorescence of single leaves was measured using a PAM 101/103 fluorometer (Walz, Effeltrich, Germany). Plants were dark adapted for 30 min and minimal fluorescence (F_0) was measured. Then pulses (0.8 sec) of saturating white light (5000 µmol photons m^{-2} sec^{-1}) were applied to determine maximal fluorescence (F_m) and calculate the ratio $F_v/F_m = (F_m − F_0)/F_m$ (max. quantum yield of PSII). A 15 min illumination with actinic light of 90 or 1100 µmol, respectively, was supplied to drive electron transport between PSII and PSI. Then the steady state fluorescence (F_s) and by a further saturating pulse the max fluorescence in the light (F_m`) were determined and the effective quantum yield of PSII ($\Phi_{PSII}$) was calculated as ($F_m$` - F_s)/F_m`. Additionally, the photosynthetic parameters 1-$qP$ (excitation pressure of PSII; $qP = (F_m$`- F_s)/(F_m`- $F_0$) ) and NPQ (non-photochemical quenching; ($F_m$ -$F_m$`)/F_m`) were determined.

4.4.2 Oxido-reduction of P700 (Turku, Finland)

The redox state of PSI reaction center Chl P700 was basically measured as in Lintala *et al*., 2009 with small modifications. A PAM-Fluorometer PAM-101/102/103 (Walz, Effeltrich, Germany) equipped with an ED-P700DW-E emitter-detector unit (Walz) was used to monitor the redox state of P700 by absorbance changes at 810 nm using 860 nm as a reference, at +23°C for plants grown in standard conditions, and at +10°C for low temperature-grown

plants. Prior to measurement leaves were kept in darkness for three min. P700 was oxidized by FR light from a photodiode (FR-102; Walz) for 30 sec, and the subsequent re-reduction of $P700^+$ in darkness was monitored.

4.4.3 F_0 'rise' measurements (Turku, Finland)

The transient post-illumination increase in Chl fluorescence (F_0 'rise') was measured basically as described in Allahverdiyeva *et al.*, 2005. The F_0 'rise' measurement was performed using a PAM101/103 Chlorophyll Fluorometer equipped with an ED-101 unit. Prior to measurement, detached leaves were kept in darkness for 15 min. Transient increase of dark-level Chl fluorescence was then monitored after actinic light illumination (100 μmol photons m^{-2} sec^{-1} for 5 min). The maximum Chl fluorescence level was induced by a saturating flash of white light.

5 Spectroscopy and microscopy

5.1 Circular dichroism – spectroscopy (CD)

The proteins (LeTic62-Nt, PsTic62-IA3, and PsmTic20) were always used fresh and dialysed against 20 mM Na_2HPO_4/NaH_2PO_4 buffer (pH 8.0) prior to CD analysis. Measurement of Tic20 was performed in presence of 0.8% Brij-35. CD experiments were carried out at RT (+20°C) using a J-810 spectropolarimeter (Jasco, Groß-Umstadt, Germany) flushed with N_2. Spectra were collected from 260 to 185 nm using a 1 mm path length of a cylindrical quartz cell. Each spectrum was the average of three (Tic62) to four (Tic20) scans taken at a scan rate of 50 nm/min (Tic62) or 20 nm/min (Tic20) with a spectral bandwidth of 1 nm. The concentration of proteins varied from 0.02 to 0.284 mg/ml. For the final representation, the baseline was subtracted from the spectrum. Experiments were done in duplicate or triplicate. The analysis was performed using the CDSSTR method (protein reference set 3 for Tic62 and reference set 4 for Tic20) from the DichroWeb server (Whitmore and Wallace, 2004; Whitmore and Wallace, 2008).

5.2 Transmission electron microscopy (TEM)

Arabidopsis seedlings (Col-0, *tic62-1* and *tic62-2*) were first grown on 0.5x MS-plates with sugar for one week and were then transplanted to soil and grown under standard long-day conditions (16 h light, 100 μmol photons m^{-2} sec^{-1} at +21°C / 8 h dark at +16°C) for another three weeks. Specimens were taken from rosette leaves.

Approximately 1 – 2 mm^2 segments of leaves (standardized segment at the first-third on top of the leaf) were prefixed in 2.5% (w/v) glutaraldehyde in 75 mM cacodylate buffer (pH 7.0).

Specimens were rinsed in cacodylate buffer and fixed in 1% (w/v) osmium tetroxide in the same buffer for 2.5 h at RT. The specimens were then stained en block with 1% (w/v) uranyl acetate in 20% acetone, dehydrated in a graded acetone series and embedded in Spurr's low viscosity epoxy resin (Spurr, 1969). First, semi-thin sections were cut with a glass knife on an LKB Pyramitome 11800 and light-microscopically analyzed (at 400 x magnification) to take an overview of the tissue. Ultra-thin sections of approximately 60 nm to 90 nm were then cut with a diamond knife on an LKB Ultratome III 8800 and post-stained with lead citrate (Reynolds, 1963). Micrographs were taken at 80 kV on an EM109R electron microscope (Zeiss, Göttingen, Germany)

6 Computational methods

6.1 Co-expression analysis

6.1.1 Arabidopsis thaliana Co-Response Database

Co-expression analysis with the *Arabidopsis thaliana* Co-Response Database (AthCoR@CSB.DB; http://csbdb.mpimp-golm.mpg.de/csbdb/dbcor/ath.html) was performed with the following settings: Single Gene Query - Matrix: Developmental Series (only WT); ATH1 chip; AtGenExpress; 12,200 genes - Coefficient: non-parametric Spearman's Rho rank correlation - Output: positive, significant co-responding genes (Bonferroni correction).

6.1.2 Hierarchical clustering

Co-expression analysis by hierarchical clustering of microarray data (Eisen *et al*., 1998) was performed as follows in the lab of Prof. Dr. A.Weber (Uni Osnabrück, Germany): gcRMA normalized (Irizarry *et al*., 2003), log2-transformed A*rabidopsis* microarray data of the AtGenExpress Developmental Series (Schmid *et al*., 2005) were downloaded from the AtGenExpress website (http://www.weigelworld.org/resources/microarray/AtGenExpress/) and arithmetic means were calculated for each of the triplicate values of the 79 tested conditions provided by AtGenExpress. The data were loaded into the program Cluster 3.0 (de Hoon *et al*., 2004) and then adjusted by median-centering rows (genes) and columns (arrays) (in this order) for five consecutive rounds each. After data adjustment, genes and arrays were hierarchically clustered, using a Spearman Rank Correlation similarity metric and Average Linkage as the clustering method. The clustered data file and the tree files were loaded into the program Java Treeview (Saldanha, 2004) for visualization and data mining.

Since Tic62 was found to be part of a big, well co-expressed cluster of genes (394 and 193 genes co-expressed with a Spearman rank $\rho >= 0.9$, respectively), the specificity of the assay was increased by concentrating only on those genes showing a significant co-expression

behavior (Spearman ρ >= 0.9) in both methods. By this way, the total number of genes was slightly decreased to 142. Only those genes were used for further analysis and grouped into bins based on MapMan annotation (Thimm *et al*., 2004).

6.2 Software, databases and algorithms used in the present study

Table 3: List of used software tools (freeware)

name	version	author/reference	URL
Chromas lite	2.01	Technelysium Pty Ltd.	http://www.technelysium.com.au/chromas_lite.html
Genedoc	2.6.002	Nicholas and Nicholas, 1997	http://www.nrbsc.org/gfx/genedoc/
AnnHyb	4.938	Olivier Friard	http://bioinformatics.org/annhyb
MapMan	2.2.0	Thimm *et al*., 2004	http://gabi.rzpd.de/projects/MapMan/

Table 4: List of used software tools (licensed)

name	version	Publisher/Licensor
Vector NTI	9.1.0	Invitrogen
AIDA (Advanced Image Data Analyzer)	3.25.001	raytest Isotopenmeßgeräte GmbH

Table 5: List of used databases and algorithms (available online)

name	version/ release	author/reference	URL
TMHMM	2.0	Sonnhammer *et al*., 1998	http://www.cbs.dtu.dk/services/TMHMM/
BLAST		Altschul *et al*., 1990; Altschul *et al*., 1997	http://www.ncbi.nlm.nih.gov/BLAST
ARAMEMNON	5.2	Schwacke *et al*., 2003	http://aramemnon.botanik.uni-koeln.de
AthCoR@CSB.DB		Steinhauser *et al*., 2004	http://csbdb.mpimp-golm.mpg.de/ csbdb/home/databases.html#athcor
NASCArrays			http://affymetrix.arabidopsis.info/narrays/ experimentbrowse.pl
AtEnsembl	49	Sanger Institute / EMBL-EBI	http://atensembl.arabidopsis.info/ Arabidopsis_thaliana_TAIR/index.html
Expasy		Gasteiger *et al*., 2003	http://www.expasy.org/
Dichroweb		Whitmore and Wallace, 2004; Whitmore and Wallace, 2008	http://dichroweb.cryst.bbk.ac.uk/ html/home.shtml
Graphical Codon Usage Analyser	2.0	Fuhrmann *et al*., 2004	http://gcua.schoedl.de/
E. coli Codon Usage Analyser	2.0	Morris Maduro	http://www.biology.ualberta.ca/ pilgrim.hp/links/usage2.0c.html

Results

1 The Tic62/FNR complex

Tic62 was initially identified as a component of the Tic complex of pea chloroplasts (Küchler *et al*., 2002). In addition, Tic62 was found to specifically interact with the photosynthetic oxido-reductase FNR. Based on these observations, Tic62 was considered to act as a redox-sensor protein for the Tic complex. Research so far focused on the function of Tic62 in the IE, its interactions with the Tic complex as well as its redox-dependent shuttling behavior into the stromal compartment (Küchler *et al*., 2002; Stengel *et al*., 2008). In *Arabidopsis*, Tic62 is encoded by the single-copy gene *AtTIC62* (At3g18890; Balsera *et al*., 2007). Interestingly, the corresponding protein was detected in an analysis of the thylakoid proteome (Peltier *et al*., 2004), possibly indicating an additional role of Tic62 beside import regulation in conjunction with FNR.

1.1 Tic62 is part of two well co-regulated gene clusters and exclusively present in photosynthetic tissue

Transcript co-expression analysis is a widely used tool assisting in the development of testable hypotheses about possible functional roles of gene-products of interest. Therefore, different databases were examined in order to identify *Arabidopsis* genes with a similar expression pattern as Tic62. Aim of this analysis was to obtain insights into possible regulatory pathways Tic62 might be involved in. To this end, co-expression analyses were performed using the *Arabidopsis* Co-Response database (AthCoR@CSB.DB) and hierarchical clustering analysis (Eisen *et al*., 1998) of the *Arabidopsis* AtGenExpress developmental series microarray dataset (Schmid *et al*., 2005), performed in collaboration with Prof. Dr. A. Weber (University Düsseldorf, Germany). In the intersection of both analyses, 142 genes were identified that displayed a significant co-expression behavior in both cases ($\rho >= 0.9$), the overwhelming majority of which coding for proteins either predicted or shown to be localized in the chloroplast (for a complete list see supplemental Table S1). Interestingly, when these co-expressed genes were functionally classified according to MapMan bins (Figure 10 A), more than 50% of the annotated genes fell in only two classified groups of about similar size: "photosynthesis" (bin 1) and "protein" (bin 29). Genes implicated in photosynthetic functions accounted for the largest group (~ 30% of the annotated genes), including most steps of the Calvin-Benson cycle (*e.g.* GAPDH or FBPase), several members of PSII (*e.g.* two PsbP-like proteins and PsbQ), as well as five constituents of the NDH-complex (NDH-N, NDH-L,

Ndf6, Ndf1 and CRR3). It is known that the genes encoding photosynthetic proteins represent a well-coordinated group (Biehl *et al.*, 2005), to which Tic62 is apparently closely connected.

A

27 - RNA
34 - transport
20 - stress
21 - redox regulation
31 - cell
16 - secondary metabolism
26 - misc.
13 - amino acid metabolism
3 - minor CHO metabolism
7 - OPP
18 - Co-factor and vitamine metabolism
19 - tetrapyrrole synthesis
28 - DNA
2 - major CHO metabolism
9 - mitochondrial e- transport/ATP synthesis
12 - N-metabolism
23 - nucleotide metabolism
33 - development
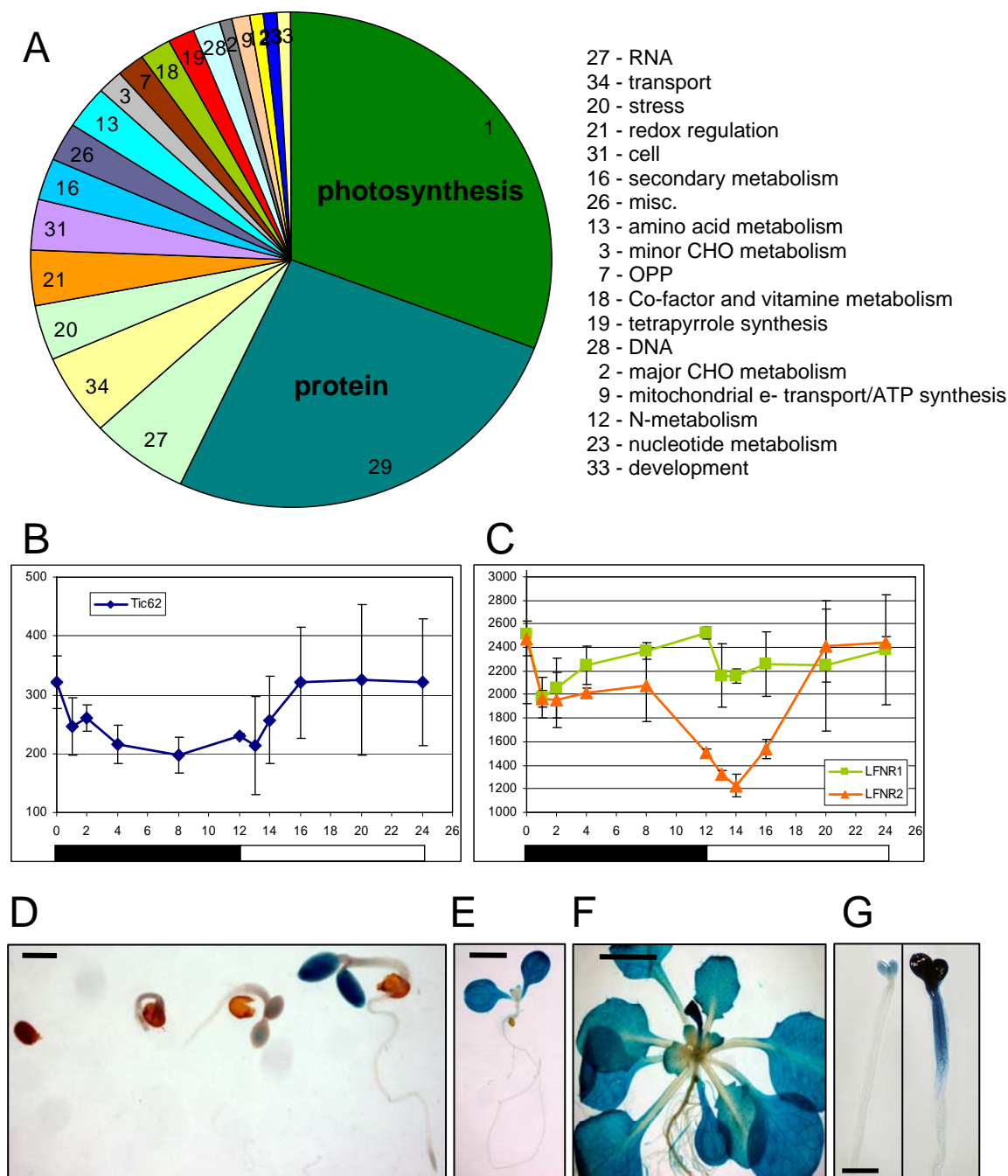
Figure 10: Expression analysis of Tic62 in *Arabidopsis thaliana*. The expression of Tic62 is tightly correlated with photosynthetic functions and tissue as well as protein turnover. (**A**) Pie chart displaying genes co-expressing with Tic62, functionally classified according to MapMan bins. Results are derived from a combination of the analysis of two databases (*Arabidopsis* Co-Response database (AthCoR@CSB.DB) and hierarchical clustering analysis of the *Arabidopsis* AtGenExpress developmental series microarray dataset; in collaboration with A. Weber, University Düsseldorf, Germany). Only genes showing significant co-expression (Spearman rank $\rho >= 0.9$) in both databases were grouped and displayed. For further information, see Supplementary Table S1. (**B,C**) Examination of transcriptional data on gene expression throughout the diurnal cycle (NASCArray data by Dr. Steve Smith, University of Edinburgh, UK). The experiment was done in two biological replicates and involved sampling of *Arabidopsis* leaves at eleven different time points as follows: 0, 1, 2, 4, 8, 12, 13, 14, 16, 20, and 24 h (where time 0 is the onset of dark and 12 h is the onset of light). The 24 h time point is a repeat of 0 h. Data for transcript abundance of Tic62 (At3g18890), LFNR1 (At5g66190) and LFNR2 (At1g20020) were extracted from the dataset and plotted as a function of the sampling time with

standard deviation. Night and day are indicated by a black or white bar at the bottom, respectively. (**D-G**) Tic62 is expressed exclusively in photosynthetic tissue. Tic62::*GUS* reporter gene analyses of *Arabidopsis* plants. GUS activity in (**D**) the cotyledons after staining of seedlings at various time points (one to four days) following germination, (**E**) in emerging true leaves of a one-week and (**F**) a mature three-week-old plant. (**G**) Expression of Tic62 is induced by light. GUS-staining of a seedling after five days of germination in darkness (left) and after one additional day in the light (right). The scale bar represents 1 mm (**D,G**), 4 mm (**E**) and 1 cm (**F**), respectively.

The second biggest bin ("protein") comprises a heterogeneous group, containing factors with functions in protein biosynthesis and turnover, such as translation, folding, post-translational modifications, intracellular targeting or degradation. Genes that were found to be co-regulated with Tic62 mainly belonged to sub-groups functioning in protein folding (*e.g.* four immunophilins and a cyclophilin belonging to a group of peptidyl-prolyl-isomerases acting among other things as chaperones/foldases for the photosynthetic complexes; Romano *et al.*, 2005), protein degradation (*e.g.* DEG5 and DEG8, which are involved in cleavage of photodamaged D2 of the PSII reaction center), and protein transport (*e.g.* SecA and another putative member of the Tic complex: AtTic20-V, which is a distant homolog of AtTic20-I). The remaining co-regulated genes were found to be distributed between 18 different functional groups, many of which contribute to chloroplast or thylakoid biogenesis and maintenance.

Considering the interaction of Tic62 with FNR on protein level, it was of special interest, whether a co-regulation of *TIC62* and any of the *FNR* isoforms could be observed. Both FNR leaf isoform genes (*AtLFNR1*, At5g66190, and *AtLFNR2*, At1g20020) were each part of only one of the database-groups displaying co-regulation with a Spearman's rank $\rho >=$ 0.9 and thus fell below the cut-off for the final analysis. They can therefore only be considered to have a weakly similar expression behavior to *AtTIC62*. This fact was also reflected when the diurnal regulation of the genes was analyzed (Figure 10 B/C). The respective data were extracted from the openly available Affymetrix database NASCArrays (http://affymetrix.arabidopsis.info/narrays/ experimentbrowse.pl; dataset of Dr. Steve Smith, University of Edinburgh, UK: "Gene expression and carbohydrate metabolism through the diurnal cycle"; reference number 60). In this experiment, *AtTIC62* displays a weak but regular change of expression level over the course of the day, with lower expression at night and an enhanced transcriptional activity starting at the beginning of the day, indicating a moderate light-induction of expression (Figure 10 B). Both *AtLFNR* genes on the other hand show a completely different pattern. Transcriptional activity in general is much stronger for both *AtLFNR*s than for *AtTIC62*, and both display a drop in expression strength in the beginning of the night as well as in the beginning of the day with a kind of transcriptional "recovery" in between (Figure 10 C).

To complement the *in silico* expression analysis of Tic62 (focusing on a developmental gradient) with data on tissue specific expression, *Arabidopsis* plants were transformed with a transgene composed of the native *AtTIC62* promoter region driving the expression of a GUS-reporter gene (Figure 10 D-G). GUS activity was initially detected around day three of seedling development in the cotyledons, which was at about the same time when the seedlings started greening (Figure 10 D). Signal intensity increased over the next days but was limited to the cotyledons and true leaves. No signal was visible in the roots and in the vascular veins of the leaf petioles (Figure 10 E/F). Closer examination revealed that the GUS signal generally started to appear at the leaf tips (Figure 10 E/F). Fully grown plants showed a GUS expression pattern that was almost exclusively restricted to green plant tissue (Figure 1 F). In addition to the assessment of developmental regulation of Tic62 expression, the induction of Tic62 expression by light was verified by GUS analysis. Etiolated seedlings, generated by germination of transgenic *AtTIC62* promoter-GUS plants for five days in the dark, were transferred to the light for an additional 24 h (Figure 10 G). Comparison of GUS-stained seedlings from before (left) and after (right) light-treatment revealed a strong increase in GUS-activity in the cotyledons, supporting the data from the Genechip analyses (Figure 10 B). Taken together, it appears that Tic62 expression correlates with the development of photosynthetic tissue, indicating a role in light-regulated and thus with high probability photosynthesis-related processes.

1.2 Tic62 and FNR are present at the envelope, in the stroma and at the thylakoids

Tic62 had originally been described as an IE-localized part of the Tic translocon (Küchler *et al.*, 2002), which was later demonstrated to shuttle into the stroma dependent on the redox status of the chloroplast (Stengel *et al.*, 2008). Since Tic62 had been furthermore detected in thylakoid membranes in a proteomics study (Peltier *et al.*, 2004), the sub-cellular localization was re-assessed. Sub-fractions were prepared from *Arabidopsis* chloroplasts and analyzed by immunoblotting (Figure 11). Indeed, Tic62 displayed a triple localization in the envelope, stroma and thylakoids, which was very similar to the chloroplastic distribution of FNR. However, FNR was predominantly present in the stroma while less protein could be detected in the envelope- and thylakoid membranes. In contrast, Tic62 was found to be mostly membrane-associated.
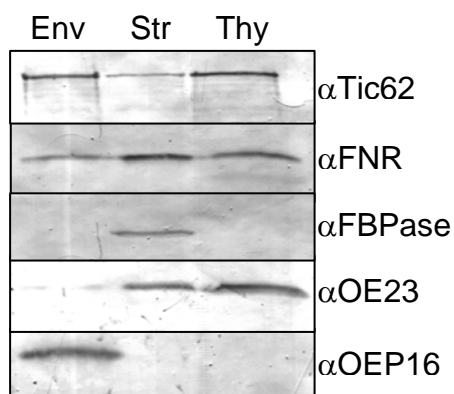
Figure 11: Tic62 and FNR show a triple localization in chloroplasts. Immunoblot analysis of the *Arabidopsis* chloroplast sub-fractions envelope (Env), stroma (Str) and thylakoids (Thy) using antibodies generated against Tic62, FNR, FBPase (stroma marker), OE23 (thylakoid marker; soluble lumenal protein and thus also detected in minor amounts in the stroma) and OEP16 (envelope marker).

In addition to the biochemical fractionation, transient transformation of *Arabidopsis* mesophyll protoplasts was employed to analyze the localization of Tic62 (Figure 12). For this purpose, the localization of partial or full-length Tic62 constructs, both leaf isoforms of FNR as well as Tic55 were monitored. The Tic62-GFP signal was visible exclusively within the chloroplasts, clearly overlapping with the red autofluorescence emitted from the thylakoid membranes. The strong signal intensity made it impossible to distinguish any additional signals from the envelopes which closely encompass the thylakoids, as can be seen with the exclusively envelope-localized construct Tic55-GFP. No signal was detected in the stromal compartment, possibly due to highly oxidized conditions present in the protoplasts. These might have been caused by the rather long incubation in the dark, leading to preferential membrane-attachment of the redox-sensitive Tic62 (Stengel *et al*., 2008). Interestingly, the Tic62-GFP signal was not distributed evenly throughout the entire thylakoids. Instead, areas with the strongest autofluorescence, which likely represent the grana stacks, were mostly free of GFP signal, indicating that the protein associates with the stroma lamellae. The N-terminal half of Tic62 fused to GFP (Tic62-Nt) produced a very similar signal like the full-length construct, albeit with a reduced signal intensity. Expression of Tic62-Ct, on the other hand, N-terminally fused to the native transit peptide and C-terminally to GFP, resulted in a signal reminiscent of soluble stromal proteins. These results confirm that Tic62 is indeed able to bind to the thylakoid membrane system and demonstrate that the Nt of Tic62 contains all the necessary information for the internal targeting of the protein within the chloroplast.

Expression of both leaf-type isoforms of FNR (LFNR1 and LFNR2) as C-terminal RFP-fusions, resulted in a very similar signal pattern for both constructs. The signals were associated with the thylakoid membranes, but formed an irregular, spotted pattern and had the tendency to accumulate at the thylakoid-to-stroma border.
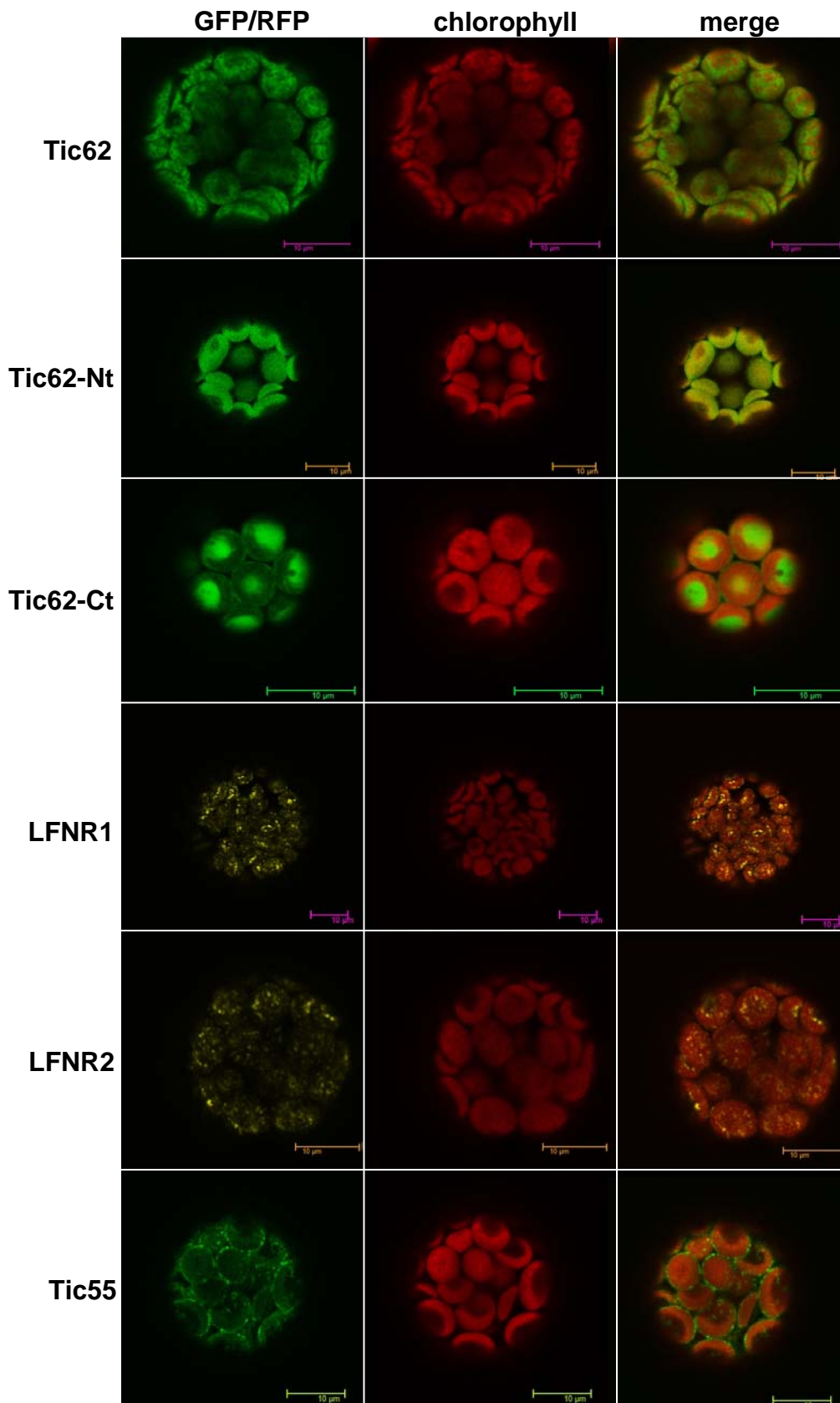
Figure 12: Localization of Tic62 and FNR in *Arabidopsis* chloroplasts. *Arabidopsis* mesophyll protoplasts were transiently transformed with various GFP- or RFP fusion constructs (Tic62 full-length, Tic62-Nt, Tic62-Ct (including the native transit peptide), and Tic55 as envelope control (GFP constructs); LFNR1 and LFNR2 as RFP constructs) and the resulting localization of the constructs was analyzed using a confocal microscope. One representative transformed protoplast is depicted for each construct. The first column shows the GFP/RFP signal, the second column the Chl autofluorescence and the third column the merge picture. All signals were detected exclusively in chloroplasts. Tic62 and FNR both localize to (stroma-) thylakoids. The N-terminal module of Tic62 is necessary and sufficient for the targeting. The scale bar in each picture represents 10 μm.

Taken together, the data verify the presence of a Tic62 pool at the thylakoid membranes in proximity to both FNR isoforms and support the idea of Tic62 having functions beyond its role as a translocon component, potentially affecting the fate of photosynthesis-related proteins.

1.3 Tic62 is part of high molecular weight complexes at the thylakoids, which are exclusively associated with FNR

Having established that a pool of Tic62 is located at the thylakoid membranes, the question arose whether it might interact with other proteins or protein complexes present in the same compartment. For this purpose, mildly solubilized chloroplast membranes were used for 2D BN/SDS-PAGE analyses. As the signal intensity resulting from detection of AtTic62 with an antibody raised against the Ct of Tic62 from pea was quite weak when used in second dimension blots from *Arabidopsis*, pea thylakoids were used in addition to *Arabidopsis* samples. The visible migration pattern of the thylakoid complexes was extremely similar in samples from both organisms (compare Figures 13 A and B). The same was true for the Tic62 signal, which was mainly detected in three to four complexes ranging from roughly 250 kDa to 500 kDa. When using antibodies against FNR, it was found that the migration behavior of both proteins matched extremely well in the entire high molecular weight (HMW) range (Figure 13 A, indicated by red lines). Since FNR had already been found associated with components of PSI, the $Cytb_6f$ complex and the NDH complex in various studies (*e.g.* Andersen *et al.*, 1992; Guedeney *et al.*, 1996; Zhang *et al.*, 2001; Okutani *et al.*, 2005), potential co-migration of Tic62 and FNR with representatives from those complexes was investigated. PSI subunits generally migrate together with LHCI in a single complex at around 550 - 600 kDa, which is readily visible in the first BN dimension due to its dark green color (indicated by a dotted line in Figure 13 A). As mentioned above, the largest complex containing Tic62 and FNR displayed a significantly faster movement in the first dimension and could be found at only ~ 500 kDa. Thus, no co-migration of either component with PSI could be observed in this assay. Antibodies directed against a component of the NDH complex (Ndh-H) revealed two distinct signals: one migrating with a size of around 1,000 kDa and another at about 500 kDa, possibly corresponding to monomeric and dimeric NDH complexes, respectively (Figure 13 B; compare Aro *et al.*, 2005; Darie *et al.*, 2005; Ishihara *et al.*, 2007). The monomeric complex had similar mobility like the largest Tic62/FNR complexes. An expected signal at the size of the dimeric NDH complex for Tic62 (or FNR) was however not detectable, arguing against a stable association. The $Cytb_6f$ complex was detected in a monomeric and a dimeric form after solubilization as well, migrating in the same

molecular weight range as Tic62. At closer inspection however, the signal peaks only partially overlapped (Figure 13 C), probably due to high signal strength rather than co-localization.
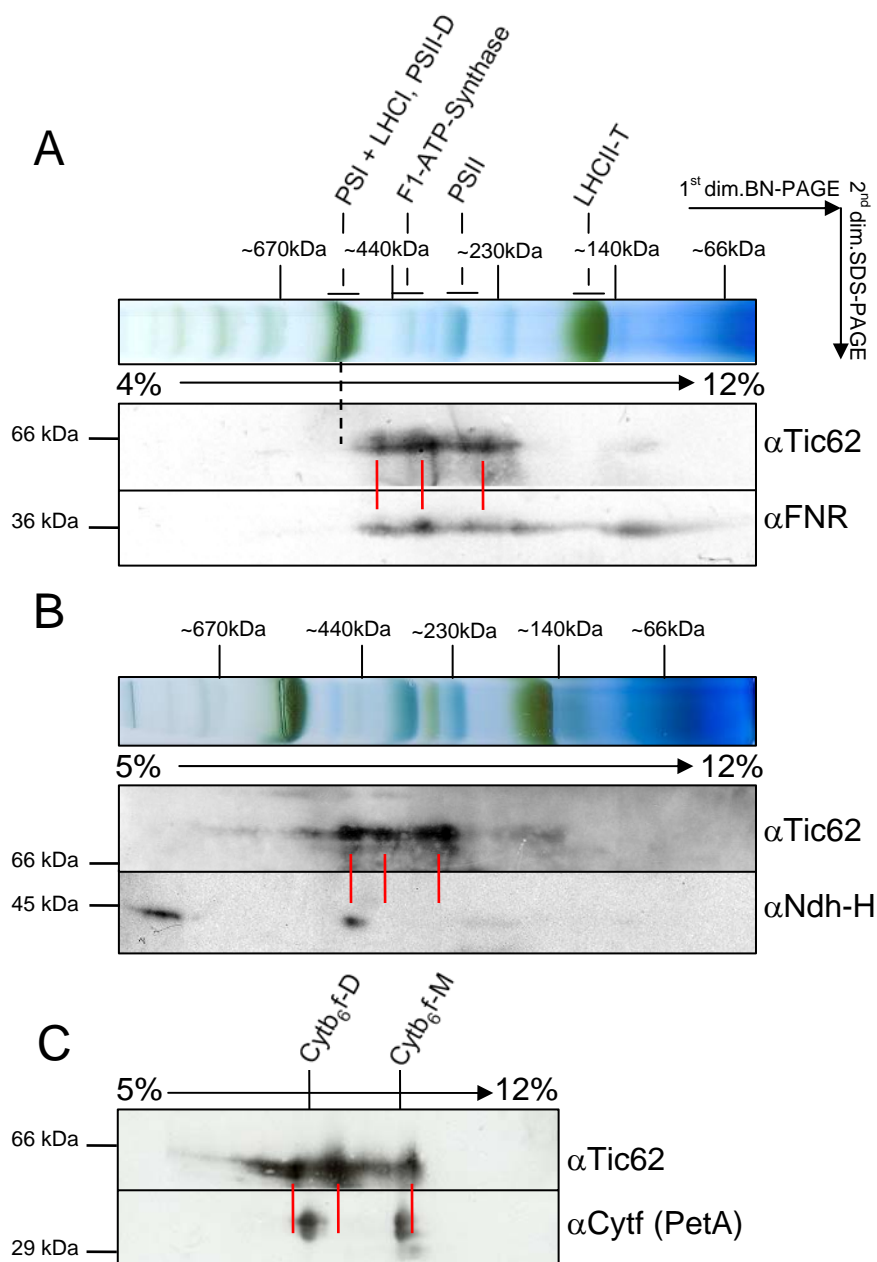
Figure 13: Thylakoidal Tic62 co-migrates almost exclusively with FNR. (**A**) Co-migration of Tic62 and FNR was observed in 2D BN/SDS-PAGE of pea thylakoids solubilized with 1% DDM. The first dimension (10 µg Chl) and immunoblots of the second dimension with αTic62 and αFNR antibodies are shown with the positions of the major thylakoidal complexes indicated. Red lines represent the main signals detected for Tic62, the dashed line the location of PSI, which displays a slower mobility than Tic62 and FNR. (**B,C**) Tic62 does not co-migrate with the high-molecular weight NDH complex or the Cytb$_6$f complex. (**B**) The first dimension and immunoblots of the second dimension of 2D BN/SDS-PAGE of *Arabidopsis* chloroplasts (20 µg Chl) with αTic62 and αNdh-H antibodies are shown. The NDH complex was detected in two complexes, probably representing a dimeric and a monomeric form. (**C**) The immunoblot of the second dimension of a 2D BN/SDS-PAGE of pea thylakoids (15 µg Chl) is depicted, incubated with antibodies generated against Tic62 and Cytf (PetA). The Cytb$_6$f complex is found in a monomeric (Cytb$_6$f-M) and a dimeric (Cytb$_6$f-D) form. Positions of molecular weight marker bands in the first and second dimensions are indicated (in kDa) as well as the acrylamide concentration gradient used for the BN-PAGEs.

In summary, the BN-PAGE analysis suggests that Tic62 and FNR form several HMW complexes at the thylakoid membrane. Analyzing the migration behavior of thylakoid protein complexes, which have been implicated with FNR-binding to the thylakoids, no specific association could be verified. However, more transient or dynamic interactions with one or several of the respective complexes cannot be ruled out.

1.4 Absence of Tic62 results in reduced FNR protein content and a drastic loss of FNR binding to chloroplast membranes

To obtain further insight into the role of Tic62, two *Arabidopsis* lines, *tic62-1* (SAIL_124G04) and *tic62-2* (GABI_439H04), containing a T-DNA insertion within the genomic sequence of the *AtTIC62* gene (At3g18890) were analyzed (Figure 14 A). Immunodecoration with Tic62 antiserum verified that no Tic62 protein was present in both lines (Figure 14 B), even though RT-PCR analysis indicated a small amount (~ 5%) of residual transcript in *tic62-2*, which nevertheless most likely represents truncated mRNA (Figure 14 C).
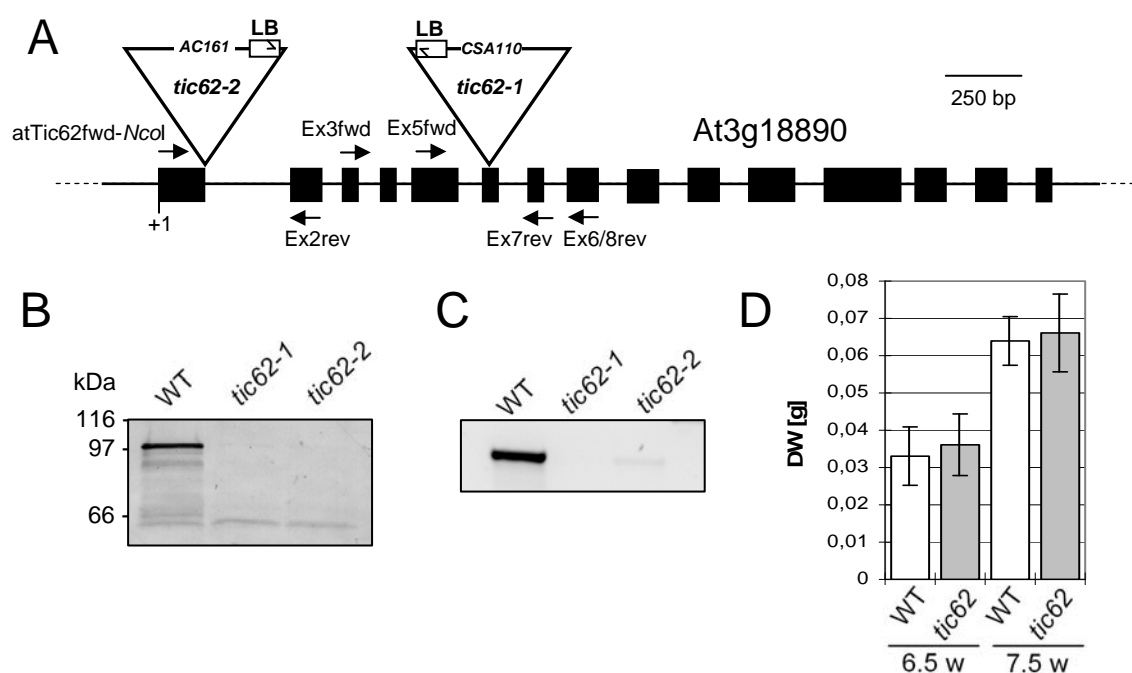
Figure 14: Identification and initial characterization of Tic62 knockout lines. (**A**) Genomic structure of Tic62 from *Arabidopsis thaliana* (At3g18890). Black boxes denote exons, black lines introns and dotted lines 5`and 3` untranslated regions (not to scale). The insertion sites of T-DNAs in lines SAIL_124G04 (*tic62-1*) and GABI_439H04 (*tic62-2*) are indicated by triangles. Furthermore, binding sites for Tic62 gene-specific primers and T-DNA-specific left border (LB) primers used for screening are depicted. (**B**) No Tic62 protein can be detected in *tic62* mutants, demonstrated by an immunoblot analysis of WT, *tic62-1* and *tic62-2* chloroplast extracts (5 μg Chl). Note that the *Arabidopsis* Tic62 protein displays an aberrant mobility and is found at ~ 98 kDa in SDS-PAGE gels. (**C**) Tic62 transcript is almost completely absent in *tic62* knockout lines. An RT-PCR experiment performed with the Ex3fwd-Ex7rev primers (being 3′ of the *tic62-2* and flanking the *tic62-1* T-DNA insertion site) of WT, *tic62-1* and *tic62-2* RNA is shown. (**D**) Growth phenotype. The dry weight (DW, in g per plant) of 6.5 and 7.5-week-old plants grown under short-day conditions was determined (± SD; n = 16 to 27).

To ensure that any observation on the mutant plants is due to the disruption of *AtTIC62*, most of the following experiments were performed with both *tic62* lines. Since practically identical results were obtained, not all data are presented separately. If not stated otherwise, the results obtained with line *tic62-1* are shown.

Knockout plants had the same appearance as wild type (WT) plants in all conditions tested, including long-day (16 h light), short-day (8 h light), constant light (24 h light), low light (< 30 µmol photons m^{-2} sec^{-1}), high light (> 300 µmol photons m^{-2} sec^{-1}), cold stress (+10°C on soil, +4°C on plates) or addition of methylviologen (data not shown). Interestingly, in some conditions the mutant plants had the tendency to be slightly, but not significantly, larger than the WT, as exemplified by the measurement of the dry weight of 6.5 and 7.5-week-old plants grown under short-day conditions (Figure 14 D). In addition to visual examination, the ultrastructure of mesophyll chloroplasts was investigated by transmission electron microscopy (TEM; preparation and pictures by Dr. Irene Gügel), but no major sub-cellular phenotypes were obvious in both knockout lines (compare Figures 15 A/B, C/D and E/F).

Figure 15: Ultrastructural analysis of WT and *tic62* mesophyll chloroplasts by transmission electron microscopy. Rosette leaves from four-week-old *Arabidopsis* WT (Col-0; **A/B**), *tic62-1* (**C/D**) and *tic62-2* (**E/F**) plants grown under standard long-day conditions were prepared for transmission electron microscopy (TEM) as described in Methods. Representative pictures from ultra-thin cuts of each line are depicted. Photographs taken with 1,100 x magnification (left) give an overview of the leaf mesophyll cell architecture and content. A 7,000 x magnification (right) provides a detailed view of two representative chloroplast sections each. No obvious phenotype could be detected in the *tic62* knockout lines as compared to the WT.

To screen for changes in the proteome of *tic62* chloroplasts, 2D IEF/SDS-PAGE of stroma and thylakoid samples from both WT and mutants was performed. Protein spots that displayed an apparent increase/decrease compared to the WT samples were analyzed by mass spectrometry at the "Zentrallabor für Proteinanalytik" at the LMU München (Head: Dr. Axel Imhof). Of six proteins spots from the stroma samples, three could be unequivocally identified as cp33, PGK1 and RuBisCO activase (Figure 16 A). Changes in the steady-state amounts of a putative RNA-binding protein (spot 3; cp33) were unexpected but interesting, since the corresponding gene belongs to the group of genes that are highly co-regulated with Tic62 (At2g35410; see Table S1). A decreased amount of phosphoglycerate kinase (PGK1) and RuBisCO activase, on the other hand, could be an indication for an effect in carbohydrate metabolism in the mutants, which is closely linked to the metabolic redox-status. In the thylakoid sample, two protein spots were chosen for sequencing, one at around 26 kDa and another one migrating at 36 kDa, the latter being the most prominent in a series of four spots migrating very close to each other, all being less abundant in the mutant (Figure 16 B; underlined). Only the 36 kDa protein could be identified and was sequenced as LFNR2. Since Lintala *et al.*, 2007 had already demonstrated that the FNR leaf isoforms LFNR1 and LFNR2 migrate next to each other in four distinct spots in 2D IEF/SDS-PAGE, it is very likely that also the protein spots surrounding the identified LFNR2 are FNR isoforms which are likewise diminished in abundance in *tic62* thylakoids.
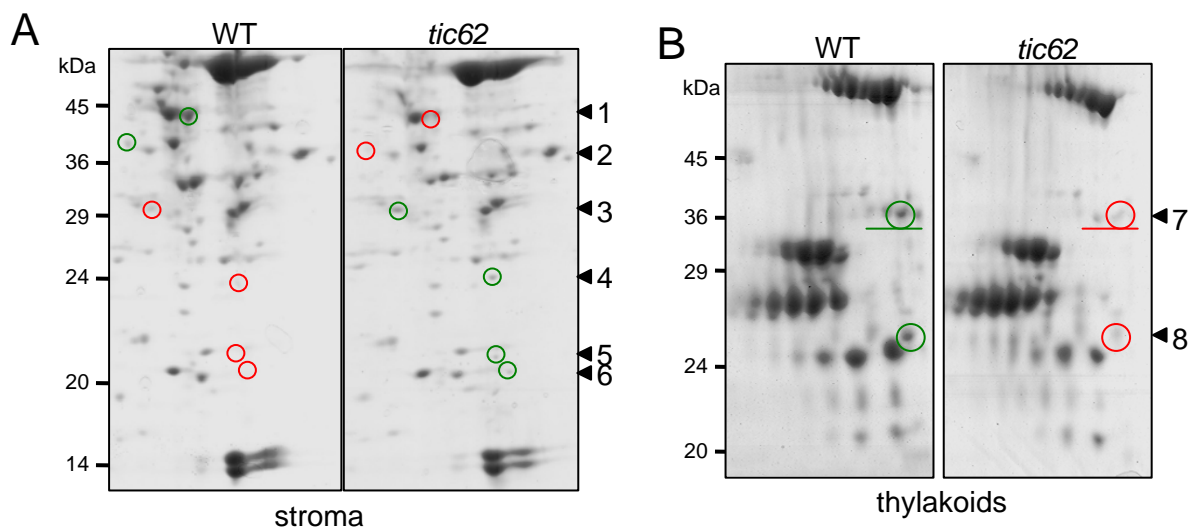
Figure 16: Tic62 knockout lines display a specific reduction of FNR in the thylakoids. Comparative 2D IEF/SDS-PAGE analysis of stroma (**A**) and thylakoid (**B**) samples prepared from WT and *tic62* chloroplasts. Protein spots with an apparent increase (green circles) or decrease (red circles) in protein amount relative to the WT sample were cut and identified by mass spectrometry: 1, RuBisCO activase; 2, PGK1; 3, put. RNA-binding protein cp33 and PsbO-2 (OE33; thylakoid lumen contamination); 4, not identified; 5+6, RuBisCO large subunit (LSU) contamination; 7, LFNR2; 8, not identified. The experiment was performed once with thylakoids and twice with stroma samples. PGK1 was identified in both replicas.

To verify this result in another context, immunoblotting of fractionated chloroplasts from WT and mutant plants was performed, revealing a distinct molecular phenotype (Figure 17 A). In particular the membrane-bound pools of FNR were severely affected: the envelope-bound fraction of FNR was barely visible in the mutant samples (<20% of WT) while the thylakoid-localized pool was about halved (~ 50% of WT). Interestingly, the soluble pool of FNR in the stroma remained unchanged. When testing for the Tic complex, the subunits were likewise found to be present at unchanged levels in the mutants compared with the WT (Figure 17 B). Taken together, the molecular phenotype of *tic62* plants confirms the close link between Tic62 and FNR. Particularly the attachment of FNR to chloroplast membranes is impaired in the mutant plants.
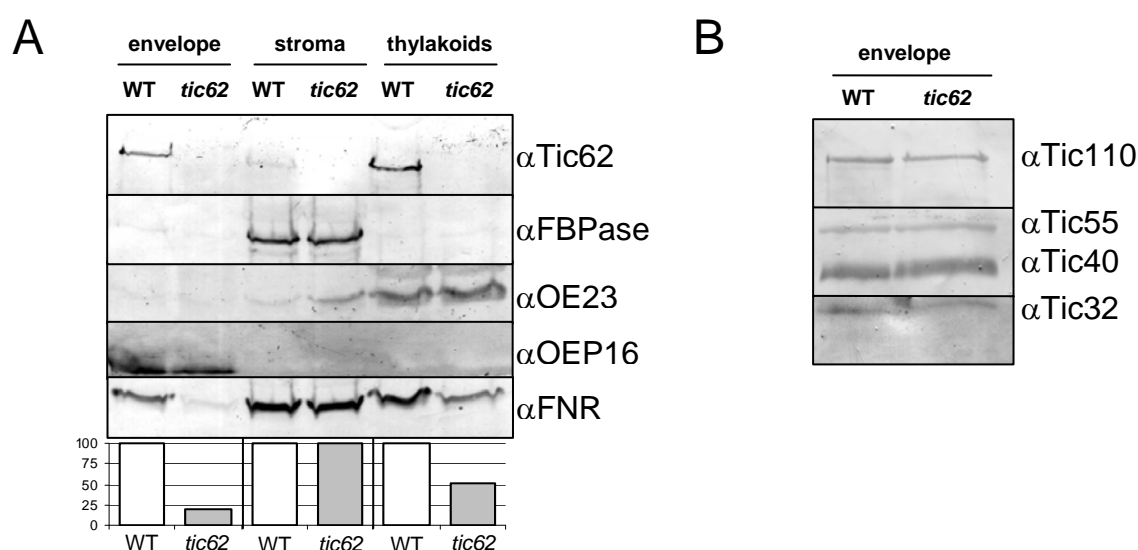
Figure 17: Tic62 knockout lines display a specific reduction of FNR in the membrane fractions. (**A**) Detection of Tic62 and FNR in sub-fractions of *Arabidopsis* chloroplasts isolated from WT and *tic62* plants. 5 µg of protein were used for envelope and thylakoid fractions and 10 µg protein in stroma samples. The immunoblot shows the signals obtained with antibodies generated against Tic62, FBPase (stroma marker), OE23 (thylakoid marker, soluble lumenal protein), OEP16 (envelope marker) and FNR of envelope, stroma and thylakoids. The histogram below shows the quantification of FNR amount in WT (white) and *tic62* (grey) samples. The WT value was arbitrarily set to 100% in each sample pair. The depicted result is one representative of four independent preparations. (**B**) The Tic complex is not affected in *tic62* plants. Immunoblot of WT and *tic62* envelopes (5 µg protein) with Tic110, Tic55, Tic40 and Tic32 antibodies.

1.5 FNR is specifically lost from high-molecular-weight thylakoid complexes and from stroma lamellae

To investigate how the loss of Tic62 in the knockout plants might effect the sub-thylakoidal localization of FNR in more detail, thylakoid sub-fractionations of both WT and *tic62* chloroplasts were performed (adapted from Ossenbühl *et al*., 2002; Figure 18). The assay resulted in thylakoid fractions enriched in heavy grana thylakoids (10K fraction), intermediate margin regions (40K), the low density stroma lamellae (140K), as well as the final supernatant of the fractionation, containing those components that are attached to membrane

protein complexes but readily dissociated during the procedure (as *e.g.* the CF_1 part of the ATPase). Success of the fractionation was confirmed by Coomassie-staining of the respective samples separated in SDS-PAGE, determination of the Chl *a:b* ratio (increasing with enrichment of PSI/LHCI), and immunoblotting. The PSII supercomplexes are known to be preferentially located in the grana thylakoids and, accordingly, components of PSII were found to be enriched in the 10K fraction (*e.g.* D1/D2 and LHCII proteins). In contrast, subunits of PSI (PsaA/B/D/F), the ATPase ($CF_1\alpha/\beta$), and (to a lesser degree) the NDH complex (Ndh-H) were found to accumulate in the lower-density fractions, in agreement with published data (Dekker and Boekema, 2005; Aro *et al.*, 2005). Analysis of Tic62 distribution revealed a fractionation pattern similar to the PSI and ATPase marker proteins, clearly indicating a stroma-thylakoid localization and thus supporting the data from the confocal analysis of GFP-tagged constructs in transformed protoplasts (Figure 12).
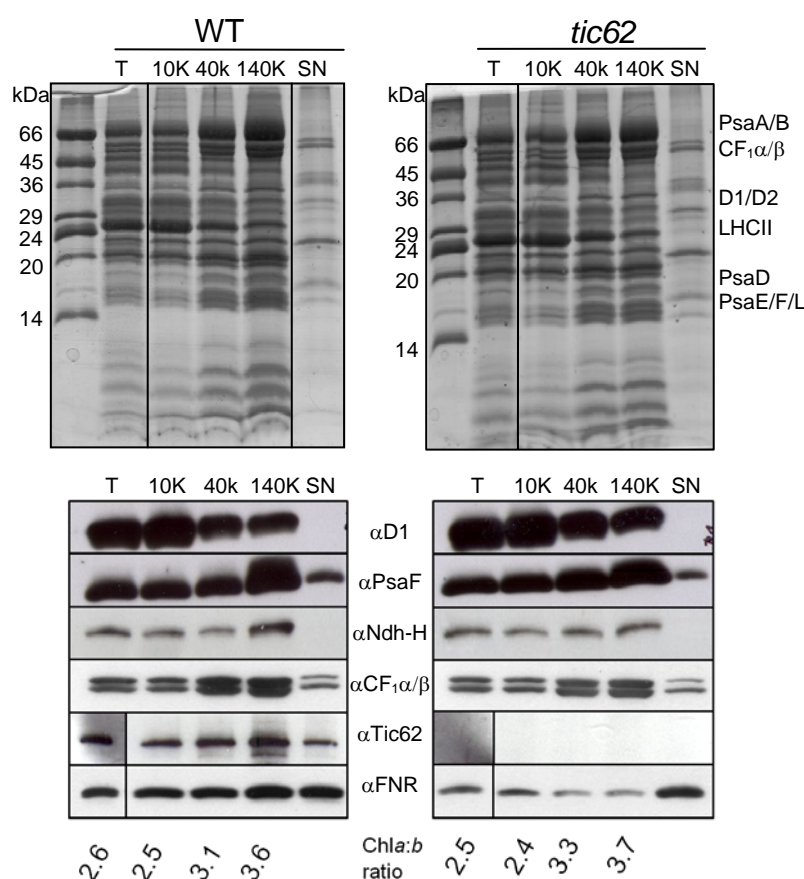
Figure 18: FNR and Tic62 co-localize to stroma-thylakoids. *Arabidopsis* thylakoids from WT and *tic62* plants were sub-fractionated by differential centrifugation after a short solubilization with 0.1% digitonin (according to Ossenbühl *et al.*, 2002). A Coomassie-stained 15% Urea-SDS gel (major thylakoid proteins are indicated) and an immunoblot of the obtained fractions is shown: T, untreated thylakoids; 10K, centrifugation at 10,000 x g, containing grana thylakoids; 40K, centrifugation at 40,000 x g, representing margins; 140K, centrifugation at 140,000 x g, enriching stroma lamellae; SN, final TCA-precipitated supernatant. For the immunoblots, 5 µg Chl and 10 µg protein of the supernatant were used per lane and probed with antibodies against Tic62, FNR and representatives of the main thylakoidal protein complexes: PSII (αD1) PSI (αPsaF), NDH complex (αNdh-H) and the ATPase ($\alpha CF_1\alpha/\beta$). The indicated Chl *a:b* ratio is a measure for the successful enrichment of grana (low *a:b* ratio) or stroma thylakoids (high *a:b* ratio). The figure shows one of two independent repetitions with essentially identical results.

As expected, the samples from *tic62* mutant thylakoids were devoid of any detectable Tic62 signal. Detection of FNR displayed a more evenly distributed signal with minor enrichment in the stroma lamellae fraction of the WT, equally reminiscent of the more irregular RFP signal in the confocal analysis. Probing the *tic62* samples for FNR, the pattern differed again markedly from the WT as the membrane-bound pool was reduced while similar amounts were found in the supernatant. Interestingly, the remaining signal was strongest in the 10K fraction of *tic62* and thus proportionally the least diminished, indicating that the stroma lamellae pool of FNR was affected most by the loss of Tic62.

In addition to the localization of Tic62 and FNR in the thylakoid system, the assembly into protein complexes within the membrane was investigated. To that end, chloroplasts of WT and both *tic62* lines were solubilized and protein complexes separated by 2D BN/SDS-PAGE (Figure 19). Examination of the first dimensions after BN-PAGE revealed no differences in the migration behavior or amount of any visible protein complex (Figure 19 A). Immunodetection of FNR in the second dimension, on the other hand, demonstrated a drastic change in complex assembly in the mutants compared to the WT: FNR containing complexes with the highest molecular weight were not detectable in *tic62* thylakoids (Figure 19 B). Only two smaller complexes of ~ 250 kDa and 140 kDa remained present, even though in varying amounts, as well as the low molecular weight signals most likely representing monomers or dimers of FNR. These results clearly establish that the formation of HMW complexes containing FNR depends on the presence of Tic62. Moreover, in combination with the data derived from the thylakoid sub-fractionation, these Tic62/FNR complexes seem to be preferentially located in the stroma lamellae of thylakoids.
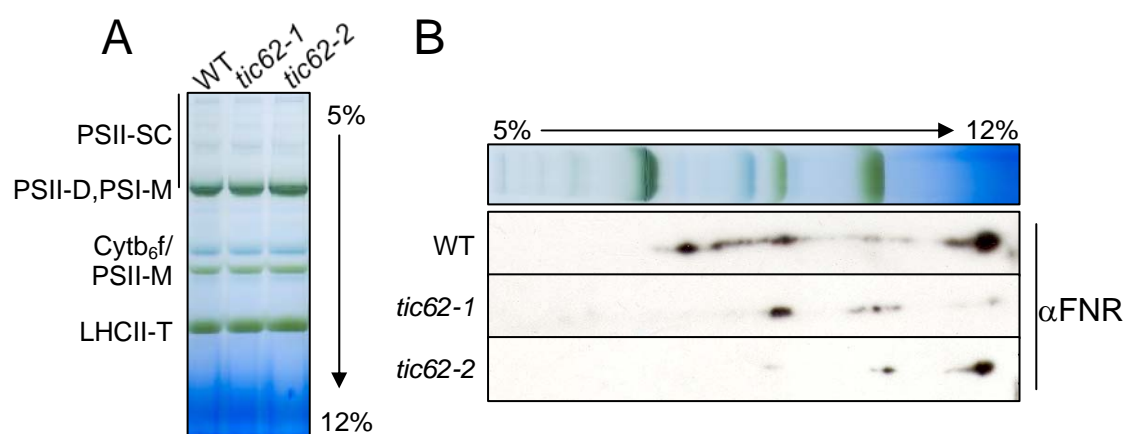
Figure 19: FNR is specifically lost from high-molecular-weight complexes in *tic62* thylakoids. (**A**) The major thylakoidal protein complexes are intact in *tic62* mutants. BN-PAGE gel (5–12%) of chloroplasts (6.5 µg Chl) isolated from WT and *tic62* plants without prior import. Positions of the major thylakoidal complexes are indicated. (**B**) Immunoblot with αFNR antibodies of chloroplasts from WT and *tic62*, separated in a first dimension using BN-PAGE (same as in A) followed by a SDS-PAGE (10%) in the second dimension.

1.6 The incorporation of FNR into high-molecular-weight complexes is specifically defective in *tic62* thylakoids

The present data suggest that the binding of FNR to the internal chloroplast membrane systems is less efficient in *tic62* chloroplasts. At the same time, FNR does not seem to accumulate in a soluble form in the stroma. Hence, the overall amount of FNR in the mutant chloroplasts is reduced. However, assessment of the transcriptional activity of the *tic62* plants by an Affymetrix analysis did not result in the detection of a drastically changed expression pattern (see Table 6). Except Tic62 itself and a cytosolic n-methyltransferase involved in the biosynthesis of phosphatidylcholine (XIPOTL1; Cruz-Ramirez *et al.*, 2004) no other gene displayed a clear change in transcript level, including both FNR leaf isoforms (At5g66190 and At1g20020). Interestingly, as one exception a gene coding for a small protein of 59 amino acids was found as being down-regulated (At3g30720). Since this had been detected likewise in a number of other Affymetrix assays performed in the lab (personal communication with Katrin Philippar) and the function of this peptide is completely unknown, it was not further analyzed. It is thus concluded that the loss of FNR in the *tic62* chloroplasts cannot be ascribed to a reduction in transcript level of the FNRs themselves or any component involved in protein biogenesis or transport. Notably, the absence of other hits displaying a significant reduction in expression at the same time indicates that the knockout line *tic62-1* is specifically defective in Tic62 and most likely does not carry any additional T-DNA insertions in the genome.

Table 6: Regulation of gene expression in *tic62* mutants.
The Affymetrix ATH1 microarray analysis was performed as described in Methods. AGI code (<u>A</u>rabidopsis <u>G</u>enome <u>I</u>nitiative), the average signal values (n = 3; ± SD), signal change direction and times change (signal (*tic62*) / signal (WT)) are specified. Both At3g17990 and At3g18000 code for the same polypeptide.

AGI code	corresponding protein name	signal (WT)	signal (*tic62*)	change direction	times change
At3g17990	XIPOTL1	74 ± 9	150 ± 21	up	2.03
At3g18000		191 ± 16	356 ± 24	up	1.86
At3g30720	unknown protein of 59 amino acids	148 ± 32	32 ± 3	down	0.22
At3g18890	AtTic62	659 ± 18	9 ± 3	down	0.01
At5g66190	AtLFNR1	1967 ± 234	1910 ± 137	-	(0.97)
At1g20020	AtLFNR2	2833 ± 141	2680 ± 100	-	(0.95)

Another possible reason for the reduction in FNR could be a defect in preprotein import, caused by loss of Tic62. To test this hypothesis, preLFNR1 and preLFNR2 constructs

were subjected to *in vitro* chloroplast import assays. However, as depicted in Figure 20 (A), the import efficiency of preLFNR1 into *tic62* chloroplasts was equal to WT. A similar result was obtained for preLFNR2, although with a lower overall import efficiency (data not shown). These data demonstrate that (I) the expression of the FNR isoforms is not affected in the *tic62* mutants and (II) both FNR preproteins do not seem to be imported in a strictly Tic62-dependent manner, suggesting that differences in the turnover of the FNRs exist between WT and *tic62* mutants *inside* of the chloroplast.
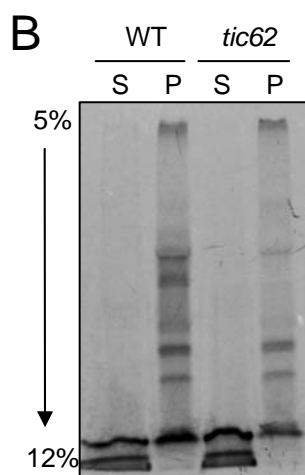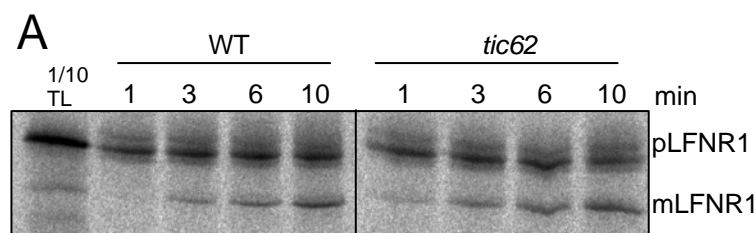
Figure 20: The integration step of FNR into HMW complexes is defective in *tic62* thylakoids. (**A**) The loss of Tic62 does not affect the chloroplast import of FNR preprotein. Import into isolated WT and *tic62* *Arabidopsis* chloroplasts (6.5 µg Chl) was started by the addition of translation product (pLFNR1) and carried out at 25°C for the indicated time. Import products, including 10% of translation product (TL), were separated by SDS-PAGE, and radiolabeled proteins were analyzed by a phosphorimager. pLFNR1: precursor form of LFNR1; mLFNR1: mature form of LFNR1. (**B**) Incorporation of FNR into thylakoid complexes was monitored by import of radiolabeled FNR precursor followed by BN-PAGE. pLFNR1 protein was first imported into WT and *tic62* chloroplasts (10 µg Chl) for 30 min at 25°C and the membranes were subsequently separated from the stroma compartment by disruption of the chloroplasts in 10 mM Hepes-KOH (pH 7.6), 5 mM $MgCl_2$ for 10 min and centrifugation at 256,000 x g for 10 min. The resulting fractions of supernatant (S) and pellet (P) were separated by a BN-PAGE gel (5–12%) and analyzed on a phosphorimager.

Having established that the steady state levels of FNR at the membranes were reduced in the *tic62* mutants, it was analyzed if the initial binding to the thylakoid membranes after import was affected or whether the effect is caused at a later stage (*e.g.* decreased complex stability). For this purpose, preLFNR1 was imported into WT and *tic62* chloroplasts, followed by separation of the membranes from the stroma compartment. The resulting fractions were analyzed on a BN-PAGE gel (Figure 20 B). Comparison of the samples showed that the overall binding of FNR to membranes was diminished in the Tic62-depleted chloroplasts. Moreover, the HMW FNR complexes were completely absent. Two lower molecular weight complexes were detected that seemed unchanged and the monomeric/dimeric pool of FNR was present, albeit in reduced amounts. The signal in the soluble fraction was stronger in *tic62* chloroplasts than in WT, indicating that the excess FNR that could not be incorporated into

the HMW complexes at least initially accumulates in the stroma, where it might be proteolytically degraded later on.

1.7 High-molecular-weight Tic62/FNR complexes are dependent on the presence of Tic62 and both leaf FNR isoforms

Since the overall amount of FNR was found to be reduced in *tic62* chloroplasts, the converse situation was investigated, testing for the fate of Tic62 in absence of one of the LFNR isoforms. Accordingly, protein extracts from WT and *lfnr1* leaves were prepared and analyzed by immunoblotting (Figure 21 A). In contrast to the WT, the amount of Tic62 was found to be drastically reduced. Taken together, this reciprocal phenotype indicates that the absence of either Tic62 or FNR affects the accumulation of the remaining interaction partner(s) in the chloroplasts.
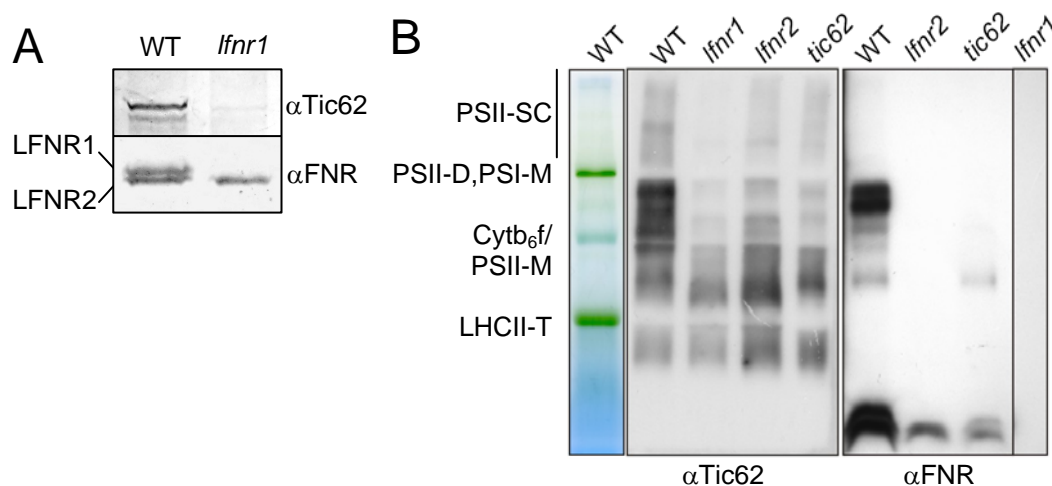
Figure 21: The HMW Tic62/FNR complexes depend on the presence of *tic62*, *lfnr1*, and *lfnr2*. (**A**) Tic62 is reduced in *lfnr1* plants. Total protein extracts (Urea/SDS) were prepared from WT and *lfnr1* plants and applied to Urea/SDS-PAGE to separate the two leaf FNR isoforms. An immunoblot with αTic62 and αFNR antibodies is shown. (**B**) BN-PAGE (5–13.5%) of thylakoids isolated from WT, *tic62*, *lfnr1*, and *lfnr2* plants (3 μg Chl each). An unstained gel lane indicating the major thylakoidal complexes and immunoblots with αTic62 and αFNR antibodies are shown. Blot (B) by courtesy of Minna Lintala & Paula Mulo, University of Turku, FIN.

This observation on the level of total chloroplast protein raised the question how this effect might be reflected more specifically at the thylakoids. In two recent reports (Lintala *et al*., 2007; Lintala *et al*., 2009) it was demonstrated that in *lfnr1* and *lfnr2* mutants, thylakoid binding of the respective other isoform was affected. Similar to the *tic62* phenotype, several HMW complexes were missing in *lfnr2* thylakoids. Moreover, in *lfnr1* knockout lines, binding of LFNR2 to the thylakoids was completely abolished. To examine these apparent similarities in parallel, the Tic62/FNR complex assembly in the thylakoids was compared in *tic62*, *lfnr1*, and *lfnr2* mutants using BN-PAGE, which was done in collaboration with Minna Lintala and Dr. Paula Mulo from the University of Turku, Finland (Figure 21 B). Comparison

of FNR and Tic62 protein pattern in the WT samples corroborated the co-migration in the HMW range (compare both first lanes). FNR was lost from these complexes in *tic62* and *lfnr2* plants, and absolutely no FNR could be detected in *lfnr1* thylakoids. Similarly, Tic62 was absent from the HMW complexes co-migrating with FNR in any of the mutant lines, demonstrating that Tic62 is likewise lost from the thylakoids of both *lfnr* mutants as the FNRs are in the *tic62* background. This fact indicates that the thylakoid-bound HMW complexes are dependent on Tic62 and both FNR isoforms, LFNR1 and LFNR2. The complexes therefore most probably represent hetero-oligomers comprised of all three components in varying composition or stoichiometry.

1.8 The localization of Tic62 as well as its association with interaction partners is regulated by the metabolic redox status

It was next analyzed whether the thylakoid-localized Tic62/FNR complexes represent a static entity or dynamically react to regulatory signals. Tic62 and FNR were shown to react to oxidizing or reducing agents with a re-localization between the membrane and stromal compartments (Stengel *et al.*, 2008). Since the metabolic $NADP^+$/NADPH ratio was demonstrated to be the likely signal inducing the dissociation of Tic62 and FNR from the envelope, it was investigated whether this redox-related signal is also effective in the detachment of FNR and Tic62 from the thylakoids. To this end, isolated pea thylakoids were incubated with either $NADP^+$ or NADPH (simulating oxidized and reduced conditions, respectively), NADH (as selectivity control) or mock-treated with buffer only (H_2O). After separation of soluble and membrane-bound proteins, both fractions were analyzed by immunoblotting (Figure 22). In the mock-treated control, Tic62 and FNR remained mostly membrane-bound. Incubation with NADH had only minor dissociating effects, but $NADP^+$ as well as NADPH led to a definite release of both proteins from the membrane. For FNR, both $NADP^+$ as well as NADPH caused approximately equal dissociation. The behavior of Tic62 on the other hand seemed more selective, as it reacted stronger to addition of NADPH than to $NADP^+$. Hence the reaction of Tic62 to different redox conditions is similar to what had been shown for the envelope-bound pool of Tic62, although less stringent. Notably, comparing both proteins, FNR was found to dissociate easier from the thylakoids in this experiment than Tic62.
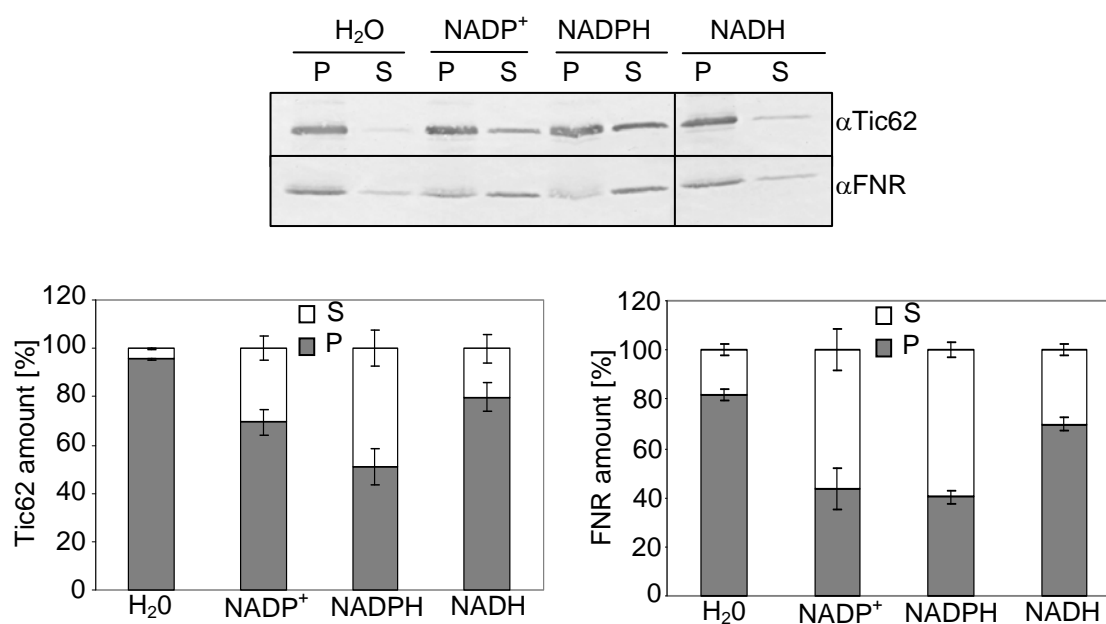
Figure 22: The attachment of Tic62 and FNR to thylakoids is dependent on redox conditions. Isolated pea thylakoids (10 μg Chl) were mildly solubilized with 0.1% DeMa for 10 min on ice and subsequently incubated for 30 min at 25°C with either 1 mM $NADP^+$, NADPH, NADH or H_2O as control. After separation of soluble and membrane-bound proteins by ultra-centrifugation (256,000 x g, 4°C for 10 min), pellets (P) and supernatants (S) were analyzed by immunoblotting with antibodies against Tic62 and FNR. A typical result of four independent experiments is shown. Furthermore, the amount of Tic62 and FNR in the pellet (grey) and supernatant (white) of all experiments (n = 4) was quantified (including standard error bars) and is depicted as fraction of total sample (100%).

In the course of the redox experiments the question arose whether changes in the redox environment also have an influence on the interactions of Tic62 with its partner proteins. Since no interaction partner other than FNR was known in the thylakoids, the experiments were performed with IE vesicles from pea. The redox-dependent association of Tic62 with Tic110 on the one and FNR on the other hand was analyzed by sucrose density centrifugation. Comparable to the assay above, the IE vesicles were preincubated with either $NADP^+$, NADPH or buffer as control, mildly solubilized, and the migration of proteins analyzed after centrifugation to equilibrium on linear sucrose density gradients (Figure 23). In untreated or $NADP^+$-treated IE vesicles, Tic62 was found to co-localize with Tic110. In contrast, preincubation with NADPH resulted in a shift of Tic62 toward lower density fractions and a co-localization with FNR. Thus, redox-changes indeed not only induce re-localization of Tic62 (as shown in Stengel *et al.*, 2008 for the IE and in this study for the thylakoids) but also lead to altered association with interaction partner proteins *within* the membrane. Whether this is also the case for potential interactions of Tic62 with further proteins in the thylakoids remains to be shown.
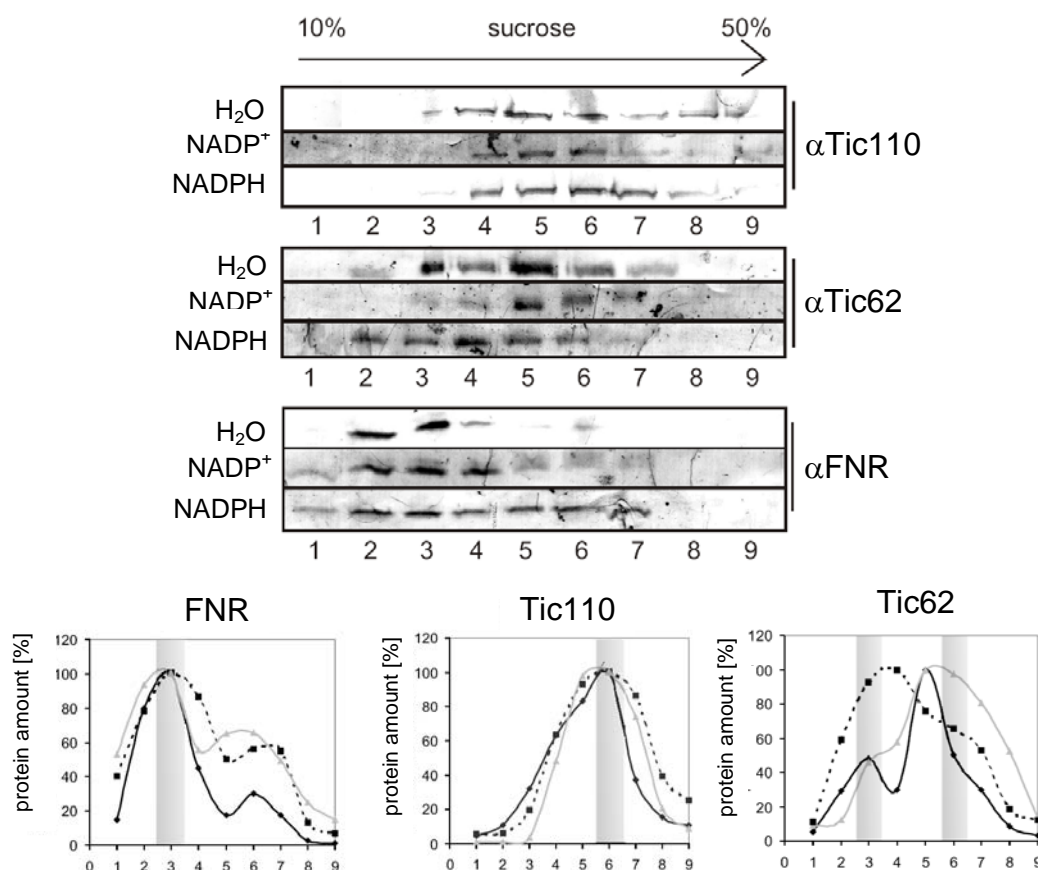
Figure 23: Redox conditions affect the interaction properties of Tic62. Co-localization of Tic62 with either Tic110 or FNR in sucrose density gradients is redox-dependent. IE vesicles were incubated with 1 mM NADP$^+$, NADPH or H$_2$O as control, solubilised with 1.5% DeMa and loaded on linear sucrose gradients. The presence of Tic110, Tic62 and FNR was analyzed in the fractions resulting after centrifugation to equilibrium (0 = lowest density; 9 = highest density). Immunoblots with αTic110, αTic62 and αFNR of one experiment and quantifications of this experiment are shown. For the quantifications, the highest value of each blot was arbitrarily set as 100% and the other values were calculated proportionally. Sucrose gradient analyses were performed five times, a typical result is shown. Experiment was published previously in Stengel *et al.*, 2008.

1.9 The high-molecular-weight Tic62/FNR complexes assemble in a light-dependent manner but are not involved in photosynthetic electron transport

Since light-regulation is common for thylakoidal protein complexes, in particular those involved in photosynthesis, the behavior of the Tic62/FNR complexes in response to light was investigated. Thylakoids prepared from dark-adapted chloroplasts were thus compared to light treated samples and analyzed by BN-PAGE (Figure 24); again in collaboration with Minna Lintala and Dr. Paula Mulo from the University of Turku, Finland. Visualization of the Tic62/FNR complexes by immunoblotting revealed that the Tic62-dependent FNR complexes decreased markedly in abundance upon irradiation (growth-light; GL). The effect was proportional to the light intensity and led to an almost complete loss of FNR from the HMW complexes under high-light (HL). The amount of Tic62 at the thylakoids likewise diminished in irradiated samples, but interestingly a fraction remained attached to the membranes even under HL. These observations confirm that Tic62 and FNR are not immobilized at the

thylakoid membranes but react dynamically, yet differentially, in response to light-dependent stimuli.
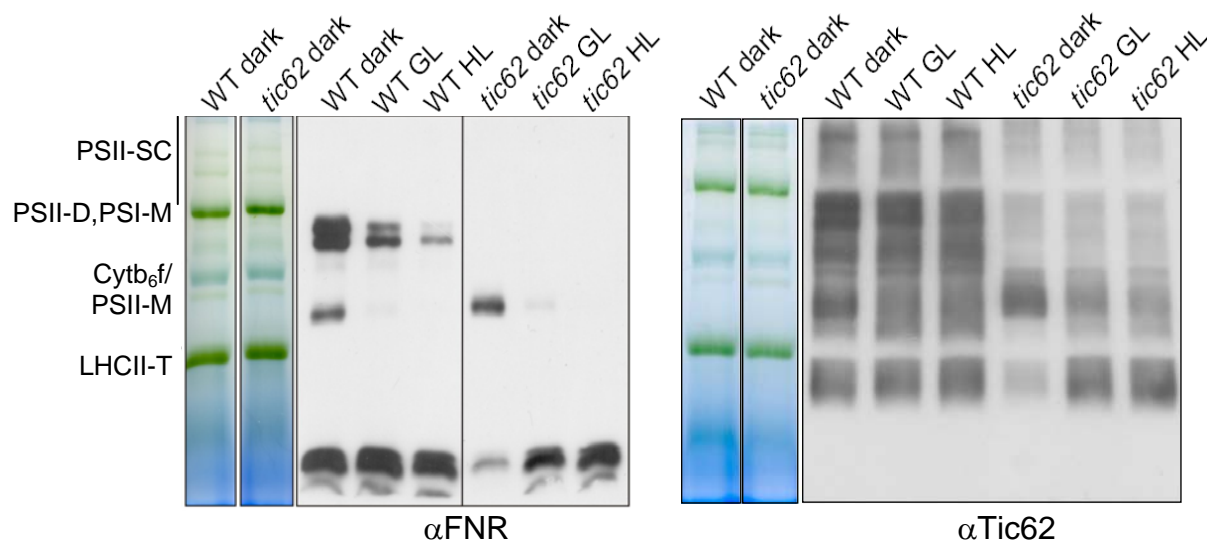
Figure 24: The thylakoidal Tic62/FNR complexes are dynamic in response to light. The HMW Tic62/FNR complexes dissociate in response to light-irradiation as demonstrated by BN-PAGE analysis (5–13.5%) of thylakoids isolated from WT and *tic62* plants (3 µg Chl each). Thylakoids were prepared from the dark and compared to growth-light (GL) or high-light (HL) treated samples (see Methods). An original BN-PAGE gel lane from WT and *tic62* thylakoids with the major photosynthetic protein complexes indicated and immunoblots with αTic62 and αFNR antibodies are shown. Blots by courtesy of Minna Lintala & Paula Mulo, University of Turku, FIN.

The ability of the thylakoidal Tic62/FNR complexes to react to changes in light and redox status raised the question whether the loss of Tic62 – and the joint reduction of FNR at the thylakoids – had any influence on the light-driven electron transport. PSII performance of intact leaves from growth-light or high-light treated WT and *tic62* mutant plants was measured using a PAM-Fluorometer (Table 7). However, no differences could be detected, as deduced from the ratio of variable to maximum fluorescence (F_v/F_m), the quantum yield of PSII (Φ_{PSII}), the degree of non-photochemical quenching (NPQ) and the excitation pressure of PSII (1-qP).

Table 7: Photosynthetic properties of *Arabidopsis* WT and *tic62* plants.
Chl *a* fluorescence parameters of plants grown under standard growth conditions and measured using either growth-light (90 µmol photons m^{-2} sec^{-1}) or high-light irradiation (1,100 µmol photons m^{-2} sec^{-1}). Values are means from four independent measurements of distinct plants. F_v/F_m, max. quantum yield of PSII; Φ_{PSII}, quantum yield of PSII; NPQ, non-photochemical quenching; 1-qP, excitation pressure of PSII.

irradiation	parameter	WT	*tic62*
90 µmol photons m^{-2} sec^{-1}	F_v/F_m	0.816 ± 0.007	0.819 ± 0.008
	Φ_{PSII}	0.717 ± 0.008	0.717 ± 0.017
	NPQ	0.276 ± 0.038	0.276 ± 0.016
	1-qP	0.064 ± 0.007	0.066 ± 0.014
1100 µmol photons m^{-2} sec^{-1}	Φ_{PSII}	0.296 ± 0.022	0.286 ± 0.023
	NPQ	1.886 ± 0.248	1.949 ± 0.094
	1-qP	0.449 ± 0.034	0.466 ± 0.047

58

In addition to these measurements of PSII activity, the post-illumination rise in Chl fluorescence (F_0 ´rise`) was monitored, which has been used as an indication for cyclic electron flow mediated by the NDH complex (Figure 25 A; Shikanai *et al*., 1998; Lintala *et al*., 2009). Furthermore, the kinetics of the dark-induced re-reduction of P700$^+$ was determined as a parameter for PSI-driven cyclic electron flow (Figure 25 B; Lintala *et al*., 2007; Lintala *et al*., 2009). Both analyses did not result in any obvious differences between WT and mutant plants, and it was thus concluded that Tic62 itself as well as the Tic62-dependent pools of FNR do not directly participate in linear or cyclic photosynthetic electron transport.
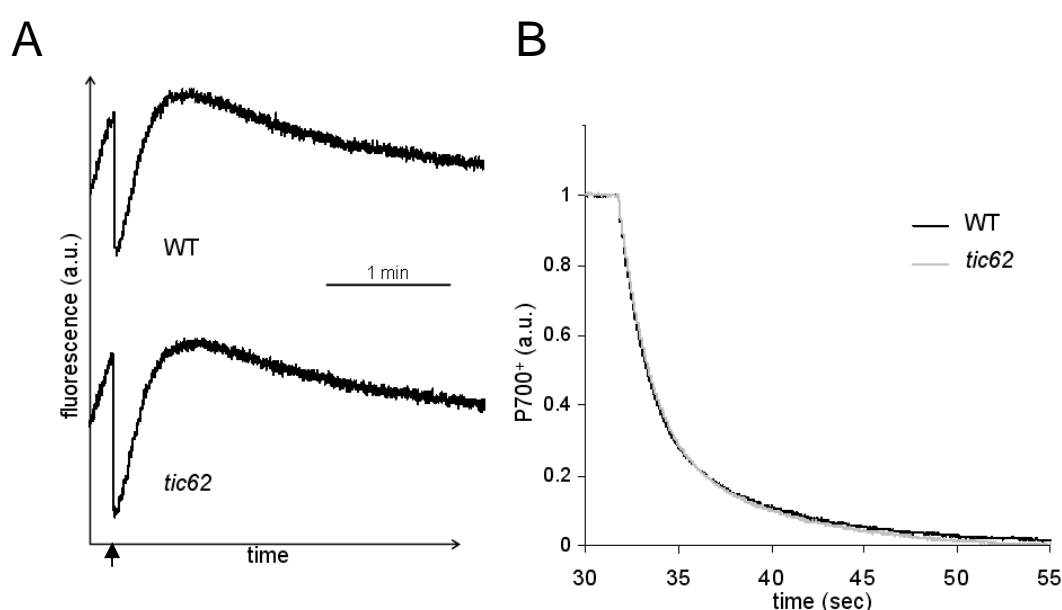
Figure 25: Cyclic electron transfer is not inhibited *tic62* plants. (**A**) Transient post-illumination increase in Chl fluorescence (F_0 'rise') from plants grown under standard short-day conditions. The F_0 'rise' was monitored in darkness after the termination of actinic light (arrow). The visible transient increase in Chl fluorescence is due to NDH activity. (**B**) Dark re-reduction of P700$^+$ in WT and *tic62* plants. The P700$^+$ re-reduction was monitored from plants grown under short-day conditions with standard illumination (100 µmol photons m^{-2} sec^{-1}). P700 was oxidized by FR light for 30 sec and P700$^+$ re-reduction was monitored in darkness. Curves were normalized to the maximal signal. a.u., arbitrary units.

1.10 Loss of Tic62 leads to an altered stromal redox poise

As mentioned in the introduction, FNR is in constant competition with FTR, which is likewise dependent on the presence of reduced Fd, and functions in recharging oxidized Trx. Reduced levels of FNR, as is the case in *tic62* plants, could cause an increased flow of electrons via FTR to Trx, potentially changing their reduction status. The stromal Trx redox status was therefore determined at three different time points throughout the day (Figure 26). The most accepted assay does so indirectly by measuring the activation state of the Trx-dependent

enzyme NADP$^+$-malate dehydrogenase (MDH) (Scheibe and Stitt, 1988; Miginiac-Maslow and Lancelin, 2002). *lfnr1* plants were used as a control since they had already been shown to have an impaired Trx-related redox-status under short-day conditions (Lintala *et al.*, 2007). Interestingly, using long-day grown plants for this assay, the Trx pool was found to be constantly *more* reduced in the *lfnr1* plants than in the WT, the effect being strongest after three hours of light. This result is in conflict with the observed effect by Lintala *et al.*, 2007, who detected a decreased MDH-activity in their assay, but this could be due to the differing growth conditions. Analysis of *tic62* knockout plants revealed a similar increase in MDH-activity as seen in *lfnr1*, which was likewise visible already after 30 min of illumination and became strongest after three hours of light, but then decreased to almost WT levels in the afternoon. It is worth noting that the overall activation of the MDH in the *tic62* plants was less pronounced than in the *lfnr1* mutants. This observation could reflect the differences in extend of FNR being lost from the thylakoids. In *lfnr1* plants, FNR is completely absent from the thylakoid membranes, whereas ~ 50% is still present in the *tic62* knockouts.
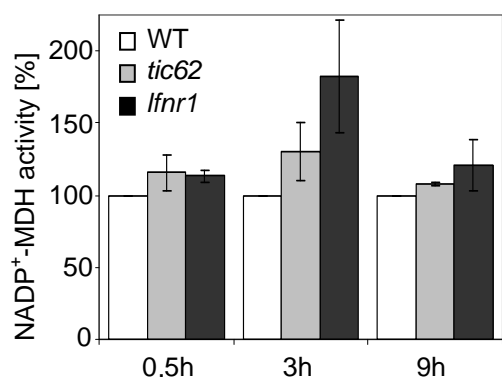
Figure 26: Loss of Tic62 and/or FNR affects the redox-homeostasis of the cell. The NADP$^+$-malate dehydrogenase (NADP$^+$-MDH) activity is increased in *tic62* and *lfnr1* plants. NADP$^+$-MDH activity, measured in *Arabidopsis* WT (white), *tic62* (grey) and *lfnr1* (black) leaf extracts at 0.5 h, 3 h and 9 h after start of illumination. The result of triplicate measurements including standard error bars is shown. The values obtained for the WT samples were arbitrarily set to 100% and the other values were normalized accordingly.

In summary, the thylakoidal Tic62/FNR complexes are able to respond to environmental signals such as light or changes in the redox state, but are apparently not directly involved in processes connected with linear or cyclic electron flow. Furthermore, the presented results demonstrate that changes in the FNR pool have a distinct effect on the redox-homeostasis of the organelle, as exemplified by its impact on the redox-dependent MDH-activity.

1.11 Tic62 exerts a stabilizing effect on FNR

The activity of many enzymes is modulated by conformational changes upon binding of effector molecules or proteins to allosteric sites, or by blocking of the active site directly. To investigate potential enzymatic effects of the Tic62/FNR interaction, the catalytic activity of heterologously expressed and purified FNR was measured *in vitro* using a cytochrome c (Cyt

c)-reduction assay in presence or absence of varying amounts of recombinant Tic62 protein (full-length or Ct; Figure 27). However, none of the tested Tic62 concentrations resulted in a measurable change of FNR activity in this assay after a 10 min preincubation time (data not shown). The preincubation period was then extended to overnight in the cold-room, allowing both proteins to get into a binding equilibrium. When the Cyt c activity was then measured, it was discovered that the samples containing FNR only had lost most of their catalytic activity (< 5% residual activity). In contrast to this, samples with saturating amounts of Tic62 present (ratio Tic62 : FNR = 2 : 1) were much more active, still showing ~ 80% of the original Cyt c reduction capacity. Similarly, in presence of Tic62 Ct ~ 64% of FNR activity was retained. To test whether the observed effect was specific for the Tic62/FNR interaction or simply due to an increased protein concentration in the overnight reaction, FNR was additionally incubated with equal molar amounts of egg albumin as a control protein using otherwise identical conditions. In this case, a portion of FNR stayed active, but to a much lower extend than seen for the Tic62 constructs (< 25% original activity). When the amount of added protein was decreased to a ratio of 1 : 0.5 (FNR : protein), activity in the presence of egg albumin was indistinguishable to the values without protein. Under the same conditions however, the Tic62 constructs still had a considerable effect on FNR activity: ~ 42 % or ~ 29 % activity, respectively.
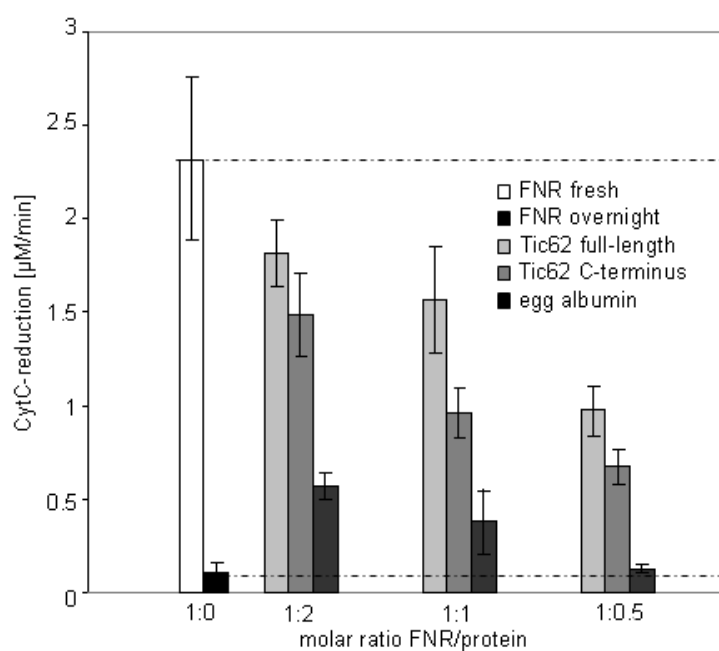
Figure 27: Tic62 is stabilizing FNR *in vitro*. Catalytic activity of overexpressed and purified FNR was measured *in vitro* using the Fd-dependent Cyt c-reduction assay. 10 μg of FNR were either used fresh (white) or activity was determined after overnight incubation, rotating at 4°C (black). Both values are additionally represented by dotted lines for comparison with the other results. Various amounts (molar ratio of FNR:used protein was 1:2, 1:1, 1:0.5) of full-length Tic62 (light grey), Tic62 C-terminus (grey) or egg albumin as control (dark grey) were added to FNR before overnight incubation and activity was measured the next day. None of the interacting proteins displayed any detectable Cyt c-reductase activity independently of FNR (data not shown). The mean values of triplicate experiments with standard error bars are depicted.

The observable effect of Tic62 (full-length or Ct) on FNR activity implies that the interaction helps to stabilize FNR under otherwise adverse conditions. An additional modulating activity of Tic62 exceeding this stabilizing function could nevertheless not be detected in this assay.

1.12 The two modules of Tic62 are not only evolutionary but also structurally different

Tic62 consists of two modules with distinct function and evolutionary origin (Küchler *et al.*, 2002; Balsera *et al.*, 2007). To get insight into the structure of these modules, circular dichroism (CD) measurements of representative constructs (LeTic62-Nt and PsTic62-IA3; Figure 28 A/B) were performed. The CD data obtained for LeTic62-Nt as analyzed by the CDSSTR software from DichroWeb (Whitmore and Wallace, 2004; Whitmore and Wallace, 2008) indicated a structure consisting of roughly 28% α-helices, 21% β-sheets, and 19% turns (Figure 28 A). In contrast, PsTic62-IA3 (corresponding to the Ct of Tic62) revealed a disordered structure possibly involving poly (Pro) II helix features (Figure 28 B; analyzed according to Kelly *et al.*, 2005), which would be in agreement with the high Pro-content in the FNR binding repeats. Altogether, the recorded spectra demonstrate that Tic62 consists of two structurally very different domains. The tightly folded conformation of the Tic62-Nt, including a Rossman-fold (Balsera *et al.*, 2007), is probably necessary for the enzymatic activity of the protein, which was demonstrated *in vitro* (Stengel *et al.*, 2008). The extremely loose, non-regular structure of the Ct, on the other hand, could aid in the binding to the FNR partner protein.
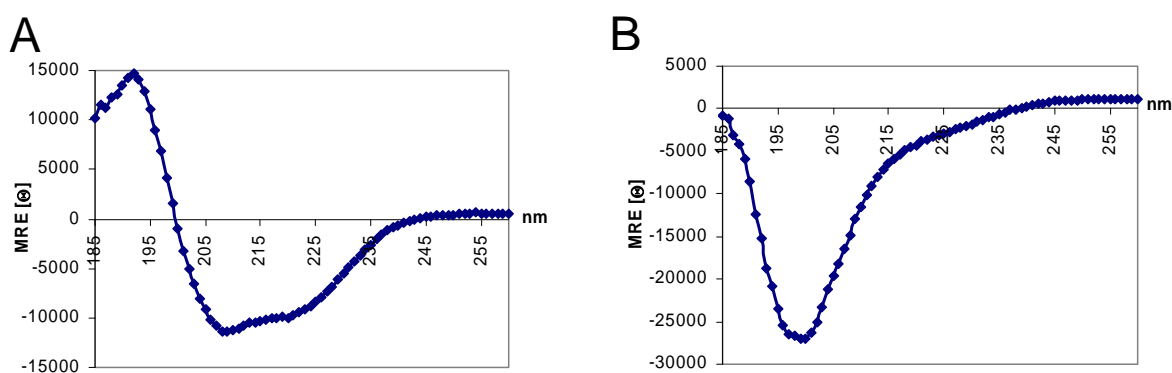
Figure 28: The N- and C-termini of Tic62 are structurally different. Analysis of secondary structure composition by circular dichroism spectroscopy of an N-terminal (LeTic62-Nt, **A**) and of a C-terminal construct (PsTic62-IA3, **B**). The analysis of one typical spectrum (an average of three scans with a spectral bandwidth of 1 nm) is shown. Data were converted to mean residue ellipticity (MRE [Θ] in degrees cm^2 dmol^{-1} residue^{-1}). Data were published previously in Stengel *et al.*, 2008.

1.13 The Tic62/FNR complex involves hydrophobic interactions, and Tic62 does not distinguish between the *Arabidopsis* FNR isoforms *in vitro*

Thylakoid-bound FNR can be sub-divided into fractions with differential binding affinities. Washing with salt readily releases a fraction of the enzyme, whereas another, stronger bound sub-pool is not affected by such a treatment (Matthijs *et al.*, 1986). Comparison of the dissociation of FNR from isolated thylakoids of WT and *tic62* mutant plants using high ionic-strength buffer was employed to investigate which of those fractions contains the Tic62-bound FNR, possibly allowing to extract information about the binding mode. For quantification of the amount of solubilized enzyme, a fraction of the supernatant after high-salt wash was used in Cyt c-reduction assays (Figure 29 C). In parallel, supernatant and pellet were immunoblotted and probed with antibodies against FNR (Figure 29 A/B).
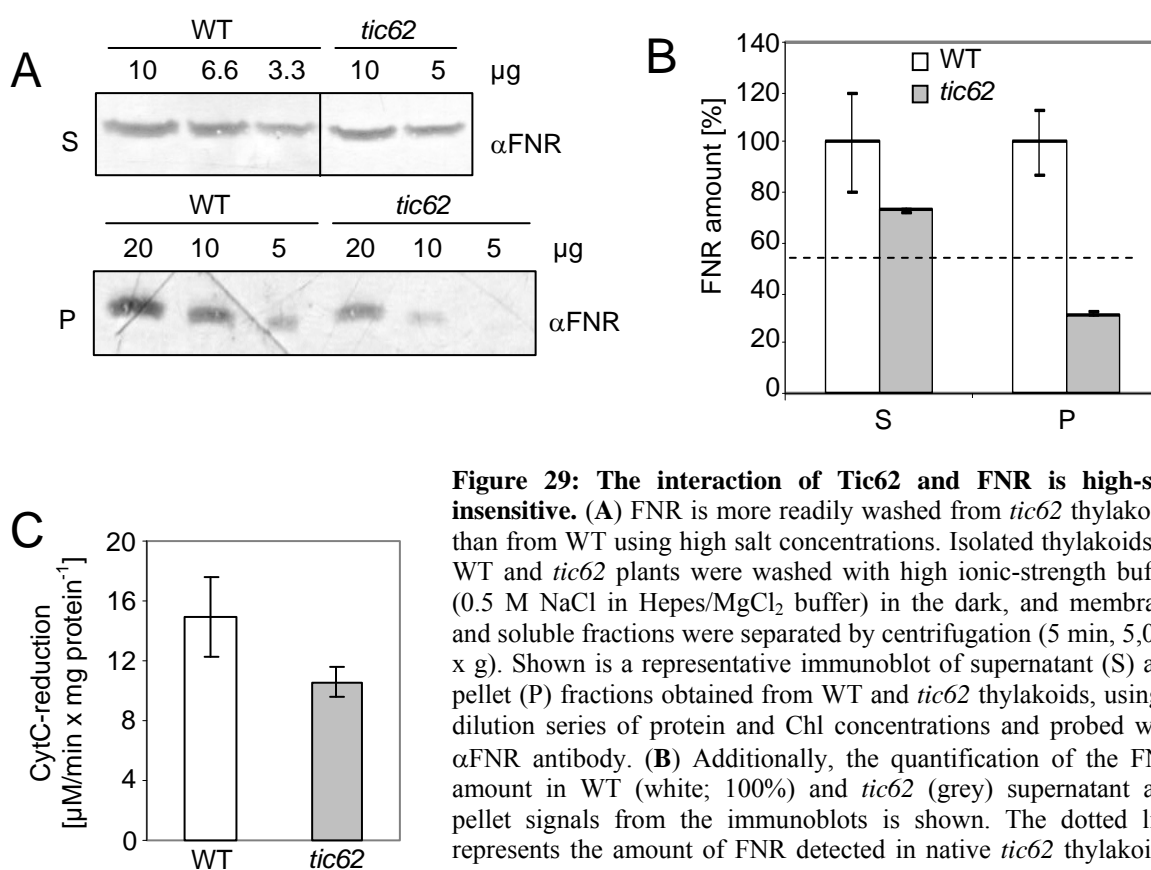
Figure 29: The interaction of Tic62 and FNR is high-salt insensitive. (**A**) FNR is more readily washed from *tic62* thylakoids than from WT using high salt concentrations. Isolated thylakoids of WT and *tic62* plants were washed with high ionic-strength buffer (0.5 M NaCl in Hepes/MgCl$_2$ buffer) in the dark, and membrane and soluble fractions were separated by centrifugation (5 min, 5,000 x g). Shown is a representative immunoblot of supernatant (S) and pellet (P) fractions obtained from WT and *tic62* thylakoids, using a dilution series of protein and Chl concentrations and probed with αFNR antibody. (**B**) Additionally, the quantification of the FNR amount in WT (white; 100%) and *tic62* (grey) supernatant and pellet signals from the immunoblots is shown. The dotted line represents the amount of FNR detected in native *tic62* thylakoids. Standard error bars are included; the experiment was performed in triplicate. (**C**) The FNR activity in the supernatant was determined by Fd-dependent Cyt c-reduction, monitored with a spectrophotometer at 550 nm. The experiment was performed in triplicate, standard error bars are included.

As the presented data demonstrate, the Cyt c-activity of the high-salt washes prepared from *tic62* thylakoids was ~ 70% of WT level, consistent with the amount of FNR in the supernatant as determined by immunoblotting (compare Figure 29 B and C). Provided that

FNR was equally well solubilized from the thylakoids in all samples, the resulting activity in the supernatant should match the difference in total quantity present in the membrane. This was estimated to ~ 50% in both mutant lines compared to the WT (see Figure 17 A), indicating that FNR was more readily washed from the mutant thylakoids than from WT samples, leading to an overrepresentation in the supernatant fraction. Accordingly, less FNR than expected remained in the pellet fraction (~ 30% of WT). Analysis of the second *tic62* knockout line (*tic62-2*) confirmed the results presented above, displaying an even stronger effect (only ~ 20% residual FNR in the pellet; data not shown). Thus, FNR is more readily washed from the thylakoid membranes in presence of high ionic-strength when Tic62 is not present, indicating a strong binding between the two proteins in the WT.

In the following, it was investigated whether Tic62 preferentially binds to one leaf FNR isoform over the other. For this purpose, heterologously expressed and purified Tic62 Ct, containing the FNR-binding repeats, was bound via its $(His)_6$-tag to Ni^{2+}-beads. These were used as an affinity matrix for LFNR1 and LFNR2 from *Arabidopsis tic62* stroma, being devoid of endogenous Tic62 (Figure 30). Elution was carried out by increasing first the ionic-strength of the solution and subsequent addition of 4 M or 8 M urea, respectively, to denature the proteins still bound to the matrix. Finally, the column was stripped with imidazole. Analysis of the resulting fractions by immunoblotting revealed that both FNR isoforms eluted equally well from the Tic62-Ct matrix (Figure 30, upper lane), indicating a similar affinity for Tic62. In addition, only little FNR could be eluted with salt, in line with the findings from the dissociation experiments from thylakoids. For a major fraction of bound FNR, denaturation with urea was necessary to release the protein from Tic62. As controls, stroma was also incubated with equal amounts of immobilized fructose-1,6-bisphosphatase (FBPase) or with Ni^{2+}-sepharose only. No (unspecific) FNR binding was detected in either sample.
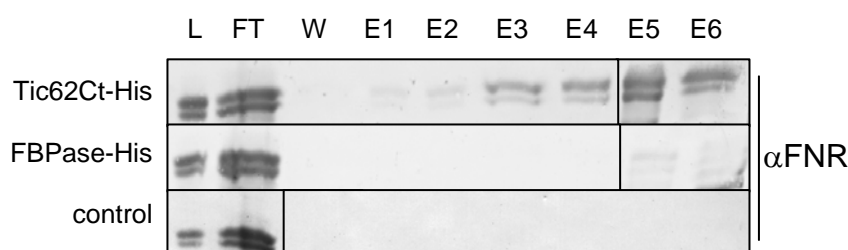
Figure 30: Tic62 binds both LFNR1 and LFNR2 equally well. LFNR1/ LFNR2 binding assay on Tic62Ct-His affinity matrix. Overexpressed and purified Tic62 Ct and FBPase were bound via a $(His)_6$-tag to Ni^{2+}-beads and used as an affinity matrix for LFNR1 and LFNR2 from *tic62 Arabidopsis* stroma. An empty column without the addition of His-tagged protein was used as additional negative control. After incubation for 1 h at 4°C the matrix was washed (W, last wash), and bound proteins were eluted by addition of 750 mM NaCl (E1), 1 M NaCl (E2), 4 M urea (E3), 8 M urea (E4), 200 mM imidazole (E5) and 400 mM imidazole (E6). The resulting samples including 1/40 of load (L) and 2/5 of flow-through (FT) were subjected to Urea/SDS-PAGE and immunoblotting with FNR antibody.

2 Heterologous expression and initial characterization of Tic20

As described above (Introduction, chapter 2.1), Tic20 was proposed to act as an alternative preprotein import channel in the IE next to, or in combination with, Tic110 (Inaba *et al.*, 2003). However, all studies so far were based on database predictions, immunological detection of the protein after cross-linking reactions, or the phenotypical characterization of plants with drastically reduced amounts of Tic20 (Ma *et al.*, 1996; Kouranov and Schnell, 1997; Kouranov *et al.*, 1998; Chen *et al.*, 2002; Reumann *et al.*, 2005; Teng *et al.*, 2006; van Dooren *et al.*, 2008). No direct biochemical evidence has been brought forward either demonstrating that Tic20 indeed has channel activity *in vitro* (or *in vivo*) or verifying any of the *in silico* predictions regarding *e.g.* topology or structure of the protein.

Production of pure protein therefore is a prerequisite for the investigation of biochemical and (electro-) physiological functions in more detail but no successful protocol has been published yet. Therefore, several new heterologous expression and purification strategies for Tic20 were tested, two of which are presented in the following: (I) expression of a codon-optimized Tic20 from *Pisum sativum* in a self-made *Escherichia coli* (*E. coli*) cell-free coupled transcription-translation system (S12-lysate) and (II) expression of Tic20 from *Arabidopsis thaliana* in standard *E. coli* cultures using a cold-induced promoter system.

2.1 Production of a codon-optimized Tic20 gene

A computational analysis of the *Pisum sativum* Tic20 gene codon usage in the target organism *E. coli* (Figure 31 A; *E. coli* Codon Usage Analyzer 2.0 by Morris Maduro) revealed that 42% of the codons present in the pea sequence are rarely used codons in *E. coli* (below 25% usage). Such inefficient codon usage is known to inhibit translation in heterologous expression systems. It was therefore attempted to increase the expression efficiency by optimization of the Tic20 gene for the *E. coli* codon bias. An optimized sequence was constructed with the help of a specialized software (Leto 1.0 by Entelechon, Regensburg), finally containing only 14% of rarely used codons (compare Figure 31 A and B). Furthermore, a more uniform AT/GC-content and distribution as well as a lower potential to form mRNA secondary structures such as hairpin loops was achieved (see chapter 1.3 in Methods). A PsmTic20 clone with the altered gene sequence was subsequently ordered from Entelechon and used for sub-cloning into several expression vectors.
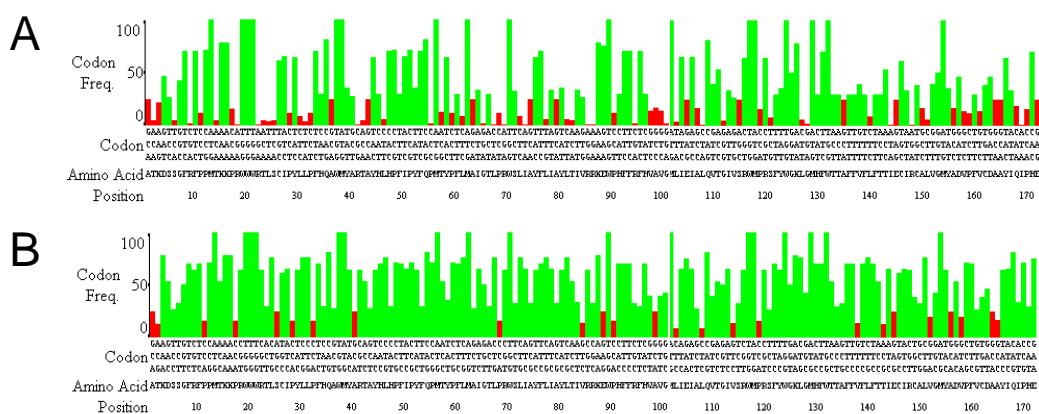
Figure 31: Analysis of the Tic20 gene codon usage. The sequence of the Tic20 gene from *Pisum sativum* coding for the mature part of the protein (Ala-83 to Glu-253) was analyzed in respect of its codon usage in the expression host organism *E. coli* using the "*E. coli* Codon Usage Analyzer 2.0" tool (by Morris Maduro). The codon usage frequency in *E. coli* for each codon of the sequence is displayed as a graphic report (red bars: frequency below 25% (threshold for rare usage), green bars: frequency above 25%). (**A**) Codon usage of the native Tic20 sequence before optimization. The fraction of codons below threshold is 42% (73 out of 171 codons). (**B**) In the optimized sequence, the fraction of codons below the frequency threshold is decreased to 14% (25 out of 171 codons) with a concomitant increase of the average usage frequency.

2.2 Set-up of a cell-free *E. coli* expression system for Tic20

Unfortunately, even the use of the codon-optimized Tic20 expression clones did not yield any significant improvement in the standard expression systems, while some strains displayed symptoms of toxicity (data not shown). It was therefore decided to test a cell-free expression system, using transcription and translation competent *E. coli* extracts instead of intact bacteria, thereby avoiding any possible toxic affects for the expression host. For this purpose, the sequence-optimized Tic20 was cloned into a vector of the pIVEX series (Roche Diagnostics, Penzberg), which contains all regulatory elements necessary for *in vitro* expression in a prokaryotic system as well as a C-terminal His-tag to allow for subsequent protein purification (pIVEX2.3/*Ps*mTic20-opt; Figure 8). The corresponding *in vitro* expression system, the RTS *E. coli* HY kit (Rapid Translation System *E. coli* High Yield) from Roche, was used for the initial cell-free expression experiments.

An advantage of the open nature of the cell-free system is that all kinds of additives can be easily screened for their effects on expression yield and protein availability (for review see Klammt *et al*., 2006). In addition, the screening process can be sped-up considerably by incorporation of (radioactively) labeled markers, which can be readily visualized after expression. This strategy was exploited to screen for suitable detergents assisting in the solubilization of the Tic20 protein already *during* the reaction (Figure 32 A). Radiolabeled methionine was added as a marker to follow the production process. Five different detergents, for which the suitability in the expression system had been shown previously either directly or for a similar derivative of the same detergent class (Klammt *et al*., 2005; Ishihara *et al*.,

2005), were thus tested. Two of these, Brij-35 (polyoxyethyleneglycol dodecyl ether) and digitonin (a steroid-derivative), were found to be particularly useful in the inhibition of Tic20 precipitation (Figure 32 A). Triton X-100 (polyethylene-glycol P-1,1,3,3-tetramethyl-butylphenyl-ether) and DeMa (n-decyl-β-D-maltoside) did not increase the amount of soluble protein compared to the control reaction, whereas DoPG (dodecyl-phospho-rac-glycerol), a long chain-phosphoglycerole, inhibited the whole reaction considerably. Since Brij-35 is more convenient to work with than digitonin (and also the less expensive detergent), this compound was chosen for the follow-up experiments. In a subsequent screen for the most suitable concentration, Brij-35 was found not to inhibit the reaction over a broad concentration range from 0.2% (~ 20 times above the critical micelle concentration (CMC)) up to 2.0% (Figure 32 B). However, 0.8% and 1.5% seemed to work best for the production of solubilized Tic20 and therefore 0.8% Brij-35 was chosen for all subsequent experiments.
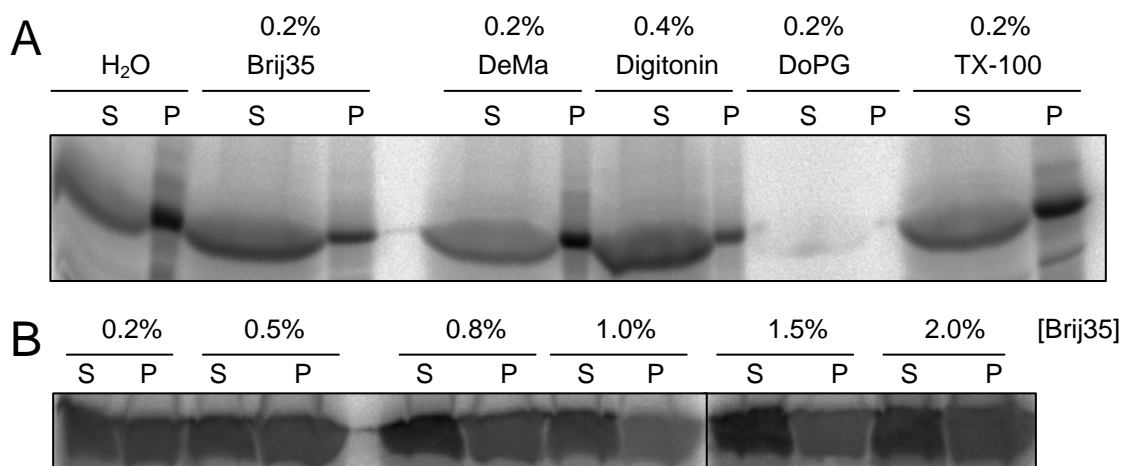
Figure 32: Screen for soluble cell-free expression of PsmTic20 in presence of detergents. Sequence-optimized PsmTic20 was expressed in the RTS *E.coli* HY Kit (Roche) in presence of radiolabeled methionine. After expression, insoluble material was sedimented by centrifugation at 20,000 x g for 15 min, the resulting pellet (P) and supernatant (S) applied to SDS-PAGE and tested for presence of expressed Tic20 protein by autoradiography. (**A**) Expression of Tic20 in absence (first two lanes; H$_2$O) or presence of several detergents (in the indicated concentrations). The amount of soluble Tic20 was highest in combination with Brij-35 and digitonin. DoPG inhibited the reaction completely. (**B**) Soluble expression of Tic20 in presence of Brij-35 added in different concentrations. 0.8% and 1.5% Brij-35 were most effective in solubilization of the protein.

The success of the commercial cell-free system prompted the decision to produce a self-made *E. coli* lysate. First, established protocols were tested (in collaboration with the AG Prof. Dr. D.Oesterhelt, at the MPI for Biochemistry, Martinsried), but in the following the protocol was adjusted to a more simple, rapid and cost-effective procedure that had been published only recently (Kim *et al.*, 2006). In contrast to the preparation of the standard so-called "S30"-lysate (*e.g.* Pratt, 1984), involving high-speed centrifugation (at 30K = 30,000 x g), long pre-incubation and dialysis, the new protocol only performs a low-speed centrifugation step (12,000 x g) after cell lysis to clear the extract from all membranes and

uses a shortened preincubation time to decrease background expression from endogenous RNAs still present in the lysate (for the detailed protocol see chapter 2.11.2 in Methods). Finally, the production of Coomassie-stainable amounts of Tic20 protein from the lysate was achieved after just one hour of reaction time at 30°C (see Figure 33 A). Subsequently, the quantity of recombinant protein could be further increased by keeping the reaction in a constant rolling motion in contrast to a static incubation (Figure 33 B).
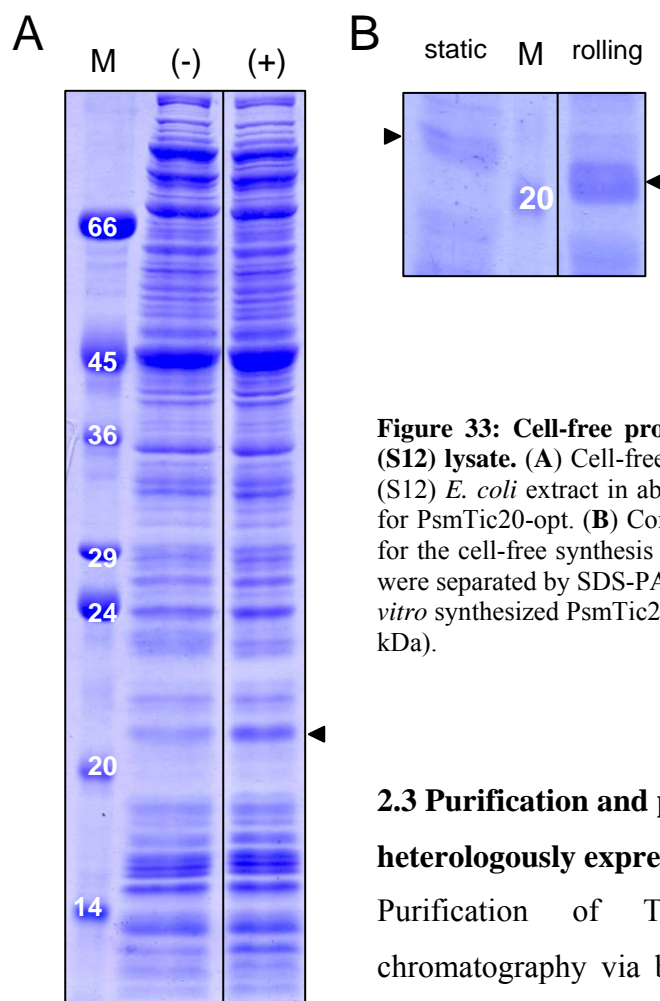
Figure 33: Cell-free protein synthesis of Tic20 in a self-made *E. coli* (S12) lysate. (**A**) Cell-free expression was performed for 1 h in a self-made (S12) *E. coli* extract in absence (-) or presence (+) of plasmid DNA coding for PsmTic20-opt. (**B**) Comparison of static or rolling incubation conditions for the cell-free synthesis reaction. Five µl samples of the reaction products were separated by SDS-PAGE and visualized by Coomassie-blue staining. *In vitro* synthesized PsmTic20 is indicated by an arrowhead. M, marker lane (in kDa).

2.3 Purification and partial characterization of heterologously expressed Tic20

Purification of Tic20 was performed by affinity chromatography via binding of the poly-(His)$_6$-tag to a Ni^{2+}-sepharose matrix in presence of Brij-35 (see chapter 2.11.3 in Methods). As the PsmTic20-(His)$_6$ construct was found to associate tightly with the matrix, stringent binding and washing conditions could be applied (Figure 34). In this way, the recombinant protein could be purified in soluble form to almost homogeneity in just one purification step. The resulting protein was sufficient in quantity for (I) the production of an antibody (directed against the full-length sequence as opposed to peptide antibodies available so far), (II) the first structural investigations of a Tic20-ortholog by CD spectroscopy, and (III) investigation of putative channel properties after reconstitution into a lipid bilayer.
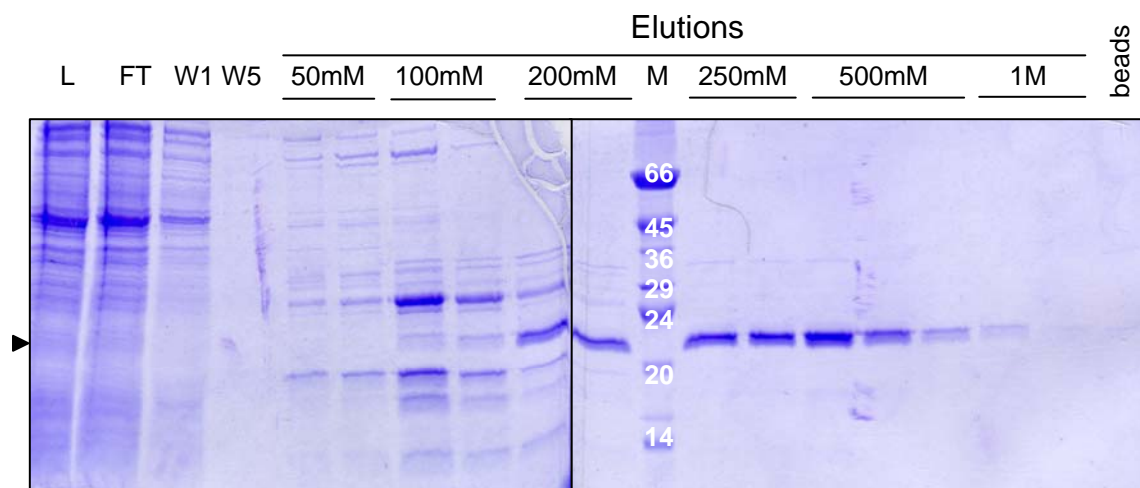
Figure 34: Purification of cell-free expressed PsmTic20 by Ni^{2+}-affinity chromatography. PsmTic20 was first expressed in the self-made (S12) *E. coli* lysate and the reaction incubated with Ni^{2+}-sepharose. The matrix was subsequently washed and bound proteins finally eluted from the matrix by addition of gradually increasing concentrations of imidazole as described in Methods. PsmTic20 is indicated by an arrowhead. L, 2 µl of reaction (load); FT, 6 µl of flow-through; W1 & W5, 15 µl each of first and last wash; M, marker lane (in kDa).

Antiserum resulting from the immunization of a rabbit with the purified PsmTic20 protein was tested against several samples containing the endogenous or recombinant protein and compared to the signal of pre-immune serum from the same animal. Already the first bleeding specifically detected Tic20 in the S12-lysate and in IE of pea (Figure 35). No signal was visible in whole chloroplasts, on the other hand, indicating that either the antibody titer was not sufficiently high or that the protein is not abundant enough to be detectable in these samples.
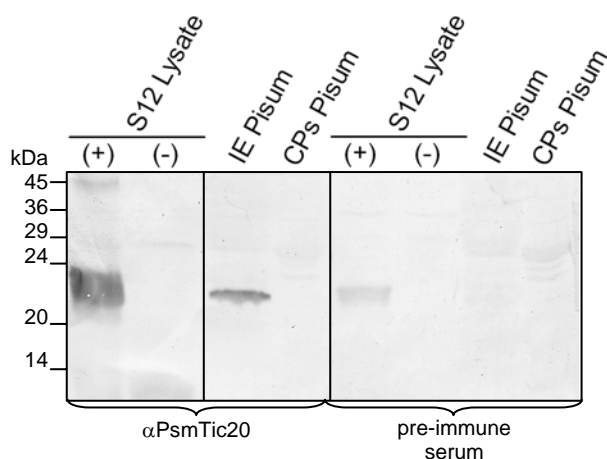
Figure 35: Test of the new PsmTic20 antiserum. Antiserum generated by immunization of a rabbit with purified PsmTic20 (first four lanes) was compared to the corresponding pre-immune serum (last four lanes) in an immunoblot with the following samples: 5 µl each of a S12 lysate used for expression of PsmTic20 (+) or a control reaction (-), 2 µl IE vesicles from pea (IE *Pisum*) or pea chloroplasts corresponding to 3 µg Chl (CPs *Pisum*). Signals were detected by incubation first with antiserum (first bleeding; 1:250 in TBS-T) followed by an alkaline phosphatase coupled secondary antibody (see Methods). The antiserum specifically detects Tic20 in the IE. TBST: 1 x Tris-buffered saline + 0.05% Tween-20 + 0.1% BSA.

To elucidate the secondary structure of PsmTic20, the re-buffered, solubilized protein was analyzed by CD spectroscopy (Figure 36). The recorded spectra, displaying two minima at 210 and 222 nm and a large peak of positive ellipticity centered at 193 nm, are characteristic of α-helical proteins and thus demonstrate that the protein exists in a folded

state in the S12-lysate in presence of Brij-35. A fitting of the spectrum to reference data sets using the DichroWeb server (http://dichroweb.cryst.bbk.ac.uk/html/home.shtml; Whitmore & Wallace 2008) allowed estimating the secondary structure composition of Tic20. Even though concentration determination was complicated by the presence of Brij-35, the result of ~ 78% α-helical content fits well to the prediction of Tic20 as a small helix-bundle protein.
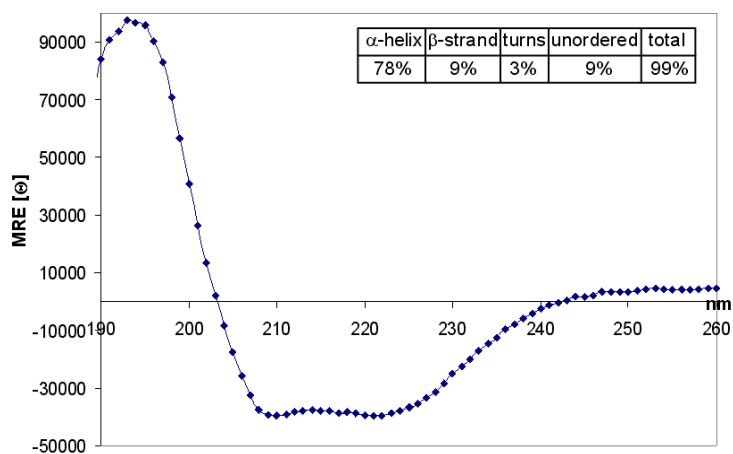
Figure 36: Cell-free expressed Tic20 is folded in presence of Brij-35. Structural analysis by circular dichroism spectroscopy of the cell-free expressed and purified PsmTic20 (183 amino acids; MW: 21,727.93 Da; concentration: ~ 0.02 mg/ml) in presence of Brij-35. The analysis of one typical spectrum (an average of four scans with a spectral bandwidth of 1 nm) is shown. Data were converted to mean residue ellipticity (MRE [Θ] in degrees cm^2 $dmol^{-1}$ $residue^{-1}$). Two minima at 210 and 222 nm and a maximum at 193 nm are very characteristic of α-helical proteins. (**Inset**) The content of secondary structure elements in PsmTic20 was calculated from the spectral data by help of the DichroWeb server software as described in Methods.

Regarding the electrophysiological characterization of Tic20, pure protein as well as control samples lacking Tic20 were analyzed in lipid bilayer experiments (in collaboration with Tom Alexander Götze, AG Prof. Dr. R. Wagner, Dept. for Biophysics, University Osnabrück, Germany). Data from preliminary trial experiments revealed that reconstitution of Tic20 into liposomes is inefficient, and therefore further experiments are necessary to acquire a sufficient dataset (data not shown).

2.4 Cold-induced expression of Tic20

In parallel to the cell-free translation experiments, it was further tried to establish an alternative expression system using intact *E. coli* cells. Among other things, the expression clone was switched from pea Tic20 to its *Arabidopsis* ortholog, AtTic20-I (At1g04940). In addition, a new kind of vector system was employed (pCOLDII; Takara Bio, Kyoto, JP), using the cold-induced promoter of a bacterial cold-shock protein, cspA (for a vector map of the construct pCOLDII/AtmTic20-I see Figure 8). This way, Coomassie-stainable amounts of Tic20 protein could be produced in an overnight reaction (Figure 37 A), which were however present in the membrane fraction. The insoluble pellet was treated with various detergents to test their effect on Tic20 solubilization (Figure 37 B). Apart from SDS, which served as

positive control and solubilized the pellet completely, also the addition of 8 M urea clearly increased the effect of the added detergents (Figure 37 B: compare DDM and Mega-9 in absence or presence of urea). The only substance that efficiently solubilized Tic20 without added urea, and thus in a more ´native` conformation, was the anionic detergent *n*-lauroylsarcosine (N-LS), which was therefore chosen for all subsequent assays.
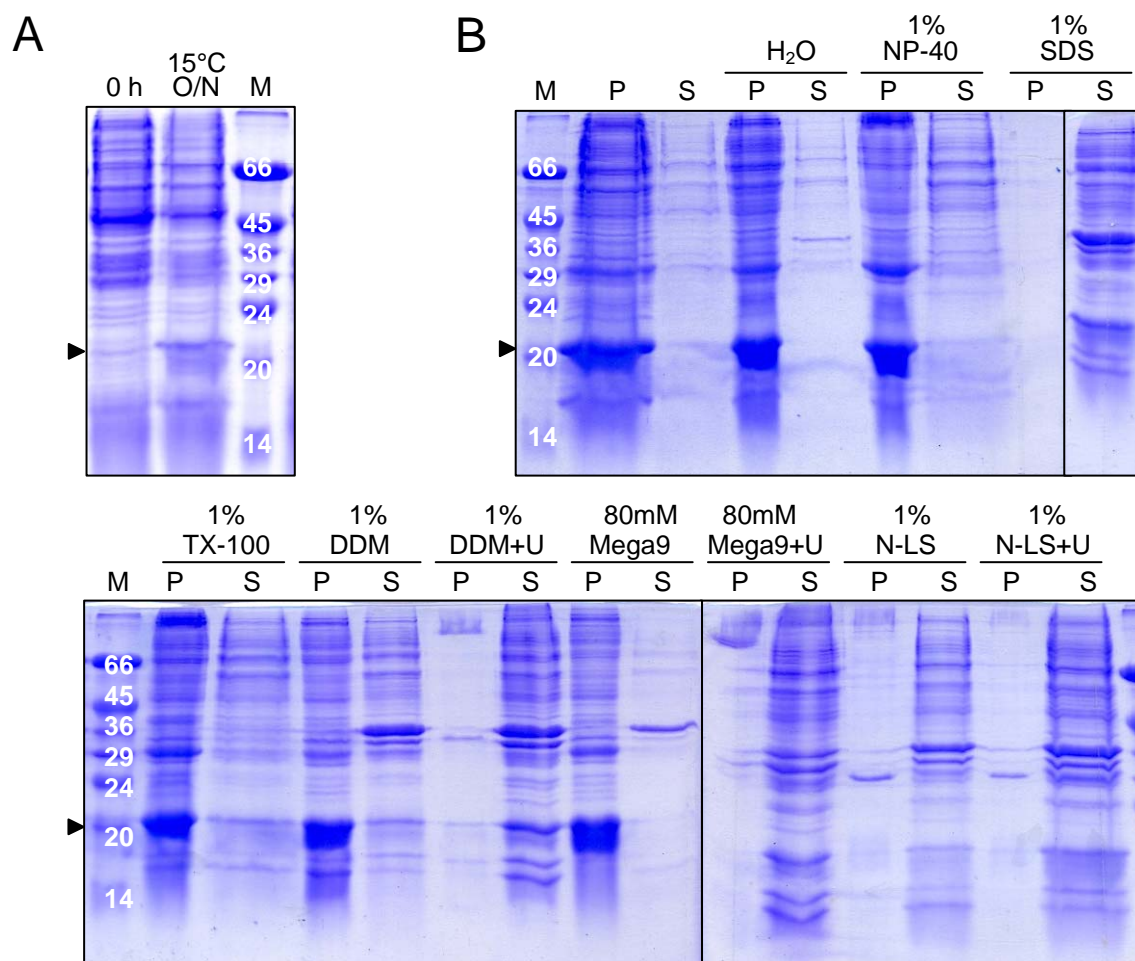
Figure 37: Cold-induced expression of AtmTic20-I in intact bacteria and solubilisation from the bacterial membranes with detergents. (**A**) Expression of AtmTic20-I/pIVEX2.3 in BL21 (DE3) cells leads to the production of Coomassie-stainable amounts of protein. Total bacterial lysate from before induction of expression (0 h) is compared to a sample taken after overnight incubation at 15°C (O/N). (**B**) After overnight expression of AtmTic20-I, bacteria were lysed and the total membrane fraction sedimented by centrifugation at 20,000 x g for 20 min. The resulting pellet was divided in 10 samples of equal size und subsequently incubated with various detergents in absence or presence of 8 M urea (addition of urea is indicated by "+U") in 50 mM Tris-HCl (pH 8.0), 150 mM NaCl for 1 h at RT. Insoluble material was again pelleted by centrifugation and 1/10 of each resulting pellet (P) and supernatant (S) applied to SDS-PAGE and Coomassie-staining. H$_2$O: control reaction without detergent or urea. AtmTic20-I is indicated by an arrowhead. M, marker lane (in kDa).

After initial solubilization of Tic20 from the membranes with 1% N-LS, the protein was purified via Ni^{2+}-affinity chromatography in presence of reduced amounts of detergents (0.3% N-LS; see Figure 38 A). Although silver-staining after Ni^{2+}-affinity chromatography did not reveal any additional protein bands in the eluates of the Ni^{2+}-column (Figure 38 A, last lane), an additional size-exclusion chromatography was performed to minimize potential

contaminations by other membrane channel proteins (Figure 38 B; see chapter 2.11.4 in Methods for detailed protocol). The resulting fractions yielded almost pure Tic20 protein in a single peak with only a slight shoulder in the early elutions, which might represent a Tic20 homo-dimer, also indicated by an additional band at ~ 40 kD in the Coomassie-stained SDS-PAGE of the respective peak fractions (see asterisk in Figure 38 B).
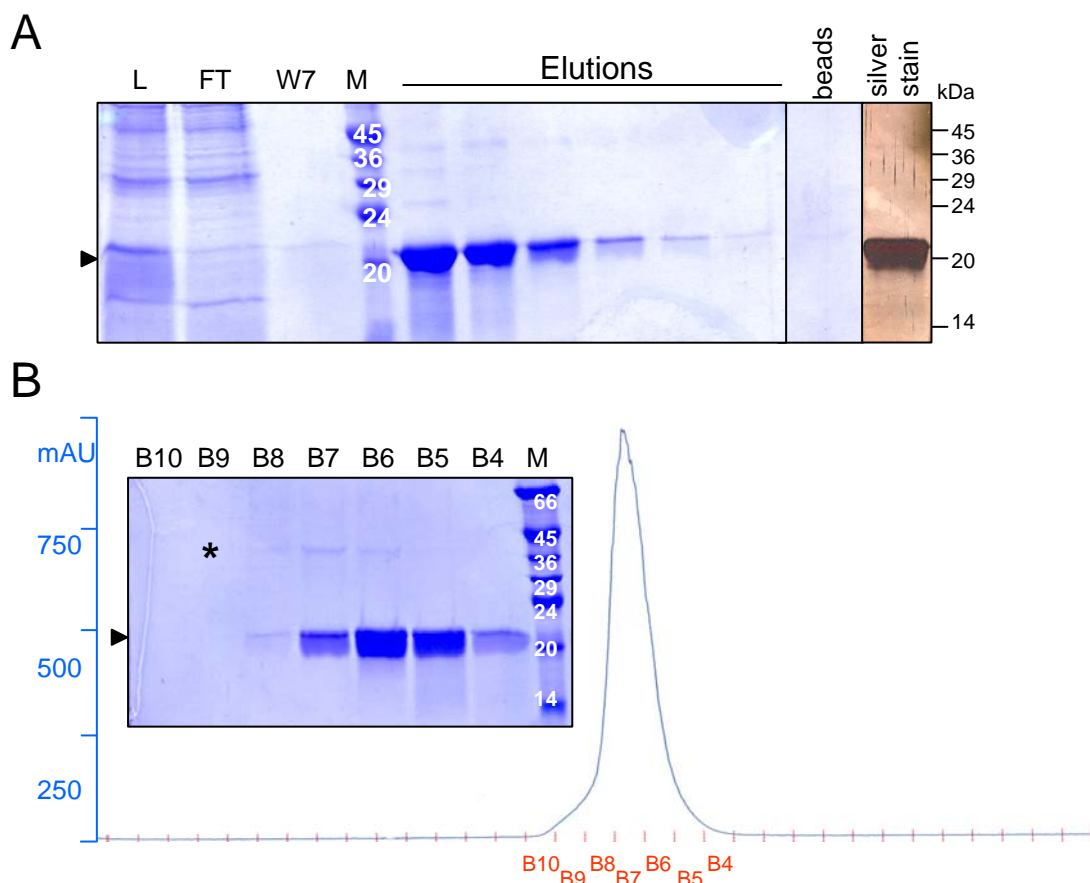
Figure 38: Purification of over-expressed AtmTic20-I. (**A**) AtmTic20-I was first expressed in BL21 (DE3) cells for overnight at 15°C, the bacteria lysed and Tic20 solubilized from the total membrane fraction by incubation with 1% N-LS. Solubilized material was incubated with Ni^{2+}-sepharose. Subsequently, the matrix was washed and bound proteins eluted from the matrix by addition of 100 mM imidazole as described in Methods. Samples from before (L, load) and after (FT, flow-through) incubation with Ni^{2+}-sepharose, the last wash (W7), 1/40 each of six elutions, and an aliquot of the Ni^{2+}-matrix (beads) were applied to SDS-PAGE and stained with Coomassie-blue. Eluted protein was additionally tested for contamination by silver staining (last lane). (**B**) For size-exclusion chromatography of Tic20, the pooled elutions from Ni^{2+}-affinity purification were applied to a Superdex 75 HR 10/30 column. The elution profile is depicted, displaying UV-absorption (mAU) for each sampled elution fraction. Tic20 eluted in a single peak comprising fractions B10 – B4. 1/50 of each fraction was applied to SDS-PAGE and Coomassie-stained. One additional band was visible migrating at the size of a potential Tic20 dimer (*). AtmTic20-I is indicated by an arrowhead. M, marker lane (in kDa).

2.5 Orientation of Tic20 in the inner envelope membrane

As mentioned above, Tic20 belongs to the large family of structurally homologous α-helical bundle proteins with four TM-domains. This can be demonstrated using prediction programs such as TMHMM (Sonnhammer *et al.*, 1998) that display a high probability for four regions in the protein sequence to form a TM-stretch (Figure 39 A). The TMHMM program

furthermore predicts the likeliest orientation of the protein in the membrane, indicating that the N- and C-termini of Tic20 are protruding into the chloroplast stroma (´inside`). With the help of the new antiserum directed against mature Tic20 from pea this prediction was verified using chemical cysteine-modification in IE membranes. PsmTic20 contains four cysteine residues in its primary sequence, which should all be oriented towards the stroma or be buried within the envelope membrane according to the TMHMM prediction (Figure 39 C).
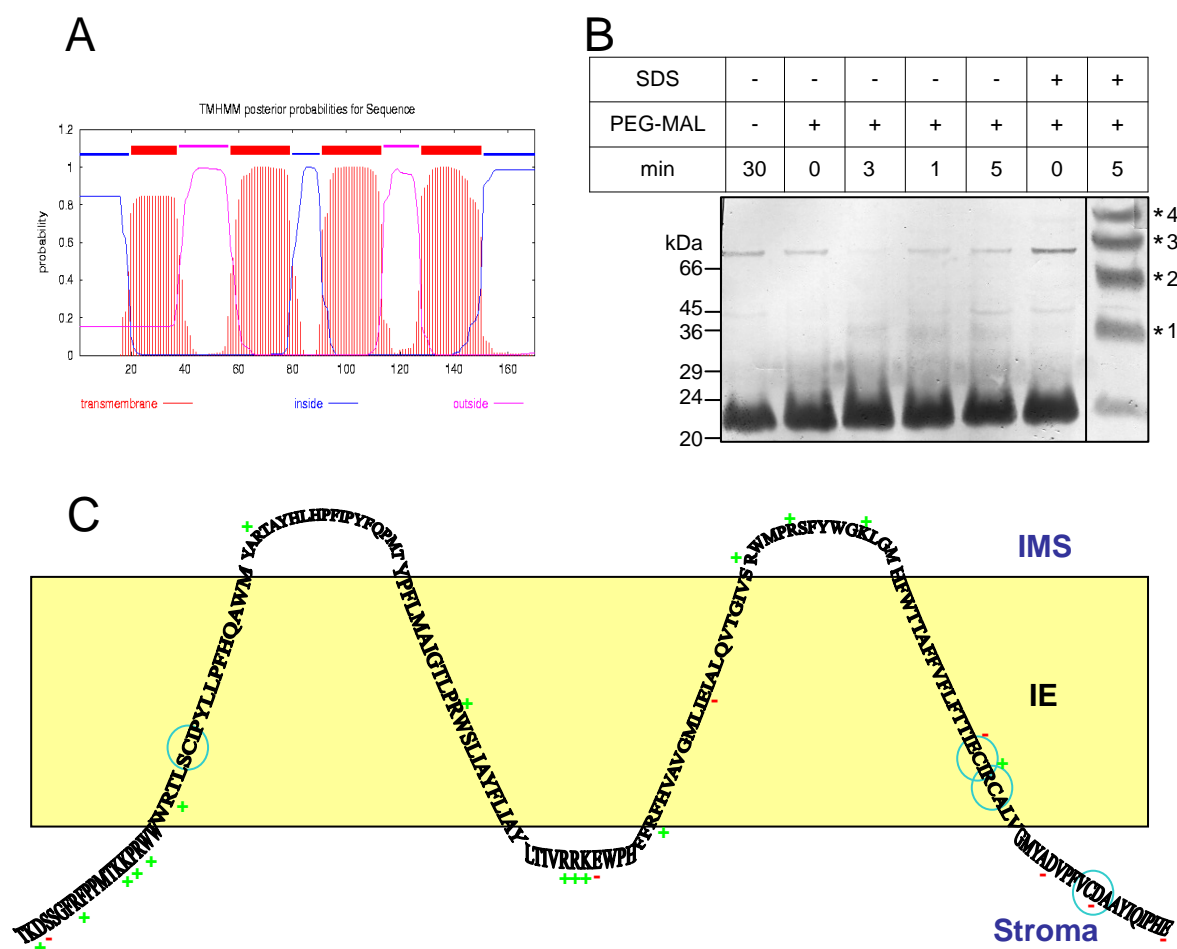
Figure 39: The N- and C-termini of Tic20 are oriented towards the stroma. (**A**) Topology prediction performed for the mature Tic20 from pea with the TMHMM program identifies four regions with high probability to form a TM domain and indicates that both ends of the protein are oriented towards the stroma ("inside"). The graphical output of the prediction is shown. (**B**) Verification of the topology prediction by PEGylation of Tic20 in IE vesicles. IE (20 µg protein) of pea was treated for the indicated time points (min) with 10 mM of PEG-maleimide in presence (+) or absence (-) of 1% SDS or with buffer as control (-/-). The reaction was stopped by addition of 100 mM DTT, applied to SDS-PAGE (Bis-Tris/MES NuPAGE), immunoblotted and Tic20 detected with αPsmTic20 antiserum. PEGylation on one to four Cys residues was detected only in presence of SDS by size-shift of the Tic20 signal (*1C to *4C). (**C**) Topology model of Tic20 in the IE membrane. Based on topology prediction (four TM-regions) and the PEGylation assay (Nt and Ct inside), the primary sequence of PsmTic20 was threaded through the IE membrane. The four Cys residues (C) are marked with a blue ring. Positively (K, Lys and R, Arg) and negatively (D, Asp and E, Glu) charged amino acids are indicated by a green (+) or red (-), respectively.

73

This was tested by incubating IE vesicles with PEG-maleimide (PEG-Mal - M.W. 5,000 Da). Maleimide is spontaneously reactive with free sulfhydryl (–SH) groups of proteins, peptides and other cysteine- as well as thiol-containing molecules. This results in an increase in molecular weight that can be visualized by immunoblotting (Figure 39 B). Since the preparation of IE following the protocols by Keegstra and Youssif (1986) and Waegemann *et al*. (1992) is known to yield vesicles with a right-side-out orientation (Heins *et al*., 2002; Balsera *et al*., 2009), hydrophilic cysteine-modifying agents should not be able to react with Tic20. Indeed, only a very faint additional band became visible in the assay even after 30 min of incubation with PEG-Mal, indicating that the cysteine residues of Tic20 in IE vesicles are not accessible for the reagent. However, in presence of 1% SDS, Tic20 is readily PEGylated, as demonstrated by the presence of four additional bands on the blot after only five minutes of incubation. The observed gain in molecular weight per modification was bigger than expected (~ 15 kD instead of 5 kD each), but this could be attributable to an aberrant mobility of the modified protein in the Bis-Tris/SDS-PAGE used in the assay. The number of four additional bands, on the other hand, corresponds perfectly to the total number of cysteine residues in the molecule, and thus likely represents Tic20 being specifically modified at one to four cysteine residues each. Moreover, the fact that solubilization of the IE vesicles is necessary to achieve efficient PEGylation, strongly supports a topology of Tic20 in the IE membrane as depicted in the model in Figure 39 C.

2.6 *In vivo* comparison of Tic20 and Tic110

It has been hypothesized that Tic20 and Tic110 might function together in the import of preproteins (Inaba *et al*., 2003), but since no conclusive data supporting this notion have been presented so far, the fundamental qualifications for a productive interaction needed to be verified. Firstly, in order for Tic20 and Tic110 to work together, they should be present in the same cells at the same time (co-express). Transcriptional analysis of Tic20 *in silico* however is hampered by the fact that the main isoform of Tic20 in *Arabidopsis*, AtTic20-I (At1g04940), had been wrongly annotated and is not present on the ATH1 Affymetrix chip (see Teng *et al*., 2006). Therefore, data on transcriptional activity are scarce. To be able to compare the expression pattern of AtTic20-I and AtTic110 (At1g06950) nevertheless, GUS-reporter gene constructs for both genes were prepared (pTic20::GUS and pTic110::GUS; Table 1). Seeds of transformed plants were imbibed and the expression of the reporter gene monitored in the days following germination (Figure 40 A). Staining for GUS activity revealed that both constructs are indeed expressed in a roughly similar pattern during early development, even though clear differences became obvious at closer inspection: Tic20 is

obviously present already in the initial stages of development when the embryo is still fully enclosed by the seed coat (see dark blue seed at day one as compared to pTic110::GUS), as well as in both shoots and roots. Transcription of the Tic110 promoter construct, on the other hand, only started between day two and three after germination and was restricted to the above-ground tissues. It can therefore be concluded that Tic20 and Tic110 are both present in green tissue, but nevertheless show clear developmental differences in expression pattern. This makes it highly improbable that they are dependent on each other in their functional properties.
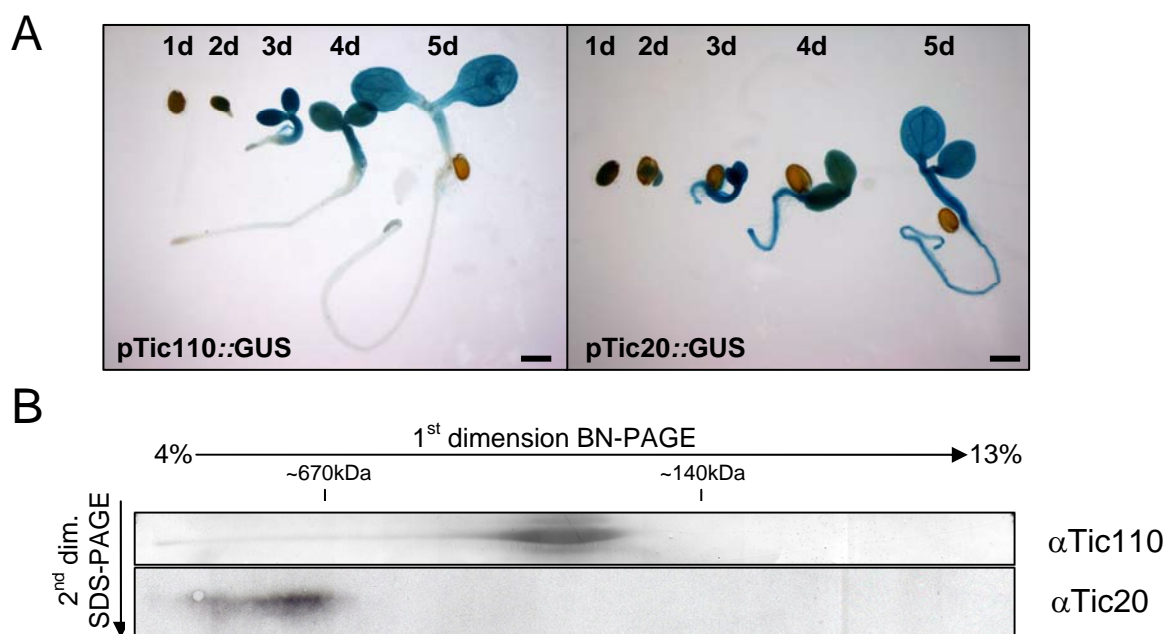
Figure 40: Co-expression and co-migration analyses of Tic20 and Tic110. (**A**) Tic20 and Tic110 are differentially expressed in young seedlings as monitored by GUS-reporter gene analysis. GUS activity in young transgenic *Arabidopsis* seedlings after staining at various time points (one to five days) following germination. To minimize positional effects of the constructs, several independent transgenic insertion lines were analyzed and representative pictures of all of those are presented. The scale bar represents 1 mm. (**B**) Tic20 and Tic110 form separate complexes in the IE membrane. IE from pea was mildly solubilized for 15 min in 5% digitonin and subjected to 2D BN/SDS-PAGE. The proteins were detected by immunoblotting of the 2nd dimension. The acrylamide percentage gradient as well as the approximate position of two marker complexes in the 1D BN-PAGE are indicated.

However, since both proteins are present side-by-side in chloroplasts, it can not be excluded that they interact with each other at certain times in these organelles. A hetero-oligomeric complex comprised of Tic20 and Tic110 (and potentially further Tic components) should be visible by a co-migration behavior in native gels (for further information, see *e.g.* Kugler *et al.*, 1997; Wittig *et al.*, 2006; Krause and Seelert, 2008). Hence, solubilized IE vesicles from pea were subjected to 2D BN/SDS-PAGE and immunodecorated with Tic20 and Tic110 antisera (Figure 40 B). To avoid disintegration of potential complexes, digitonin was used for solubilization, since it is known to be one of the mildest detergents available (Wittig *et al.*,

2006). The immunoblots revealed that Tic20 and Tic110 are both present in distinct HMW complexes in the IE membrane of chloroplasts. However, the main signals for both components did not co-migrate: Tic110 migrated at a size of ~ 200-300 kDa as described before (Küchler *et al*., 2002), whereas Tic20 displayed a much slower mobility in the native PAGE and was present in complexes of >670 kDa. This finding strongly indicates that Tic20 and Tic110 do not associate in a stable joint translocon, but are rather constituents of separate core complexes.

Discussion

1 The Tic62/FNR complex

The regulatory mode by which Tic62 could act as a redox sensor at the Tic translocon has been described to some extend already (Küchler *et al*., 2002; Stengel *et al*., 2008). However, many questions that arose from these observations have not been answered until today. In particular the presence of a second membrane-bound pool of Tic62 at the thylakoids (Peltier *et al*., 2004) as well as the specific association with FNR, an enzyme mainly involved in photosynthetic reactions, remained to be investigated. In the present study a detailed examination was performed to answer these open questions. Evidently, Tic62 is a main FNR interaction partner in the chloroplasts of higher plants. It is particularly involved in the light- and redox-dependent membrane attachment of the flavoprotein and exerts a stabilizing function on the enzyme. Moreover, the Tic62/FNR complexes not only react to the redox conditions, but the obtained results indicate that this dynamic behavior has a function in the regulation of the stromal (thiol) redox poise.

1.1 Tic62 and FNR share a triple localization in the chloroplast

Evaluation of Tic62 co-expression clusters as well as GUS-reporter gene analysis demonstrated a clear link to processes such as protein turnover in the chloroplast and photosynthesis, suggesting a role in the regulation of the fate of chloroplastic proteins involved in general photosynthetic functions (Figure 10). The experimental results fit surprisingly well to these initial *in silico* predictions, since Tic62 is obviously closely connected to the fate of FNR, one of the main photosynthetic proteins present in the chloroplast.

Chloroplast sub-fractionation (Figure 11) as well as the localization of GFP-tagged constructs (Figure 12) *e.g.* demonstrate that Tic62 and FNR display a very similar localization pattern within the chloroplast as they are both found in the same compartments. Notably, the thylakoid pool of Tic62 is obviously present *in addition* to the known pools found at the envelope and in the stroma. However, in contrast to FNR, Tic62 seems to be preferentially (but not exclusively) membrane bound in *Arabidopsis* (Figure 11). It is interesting to note that this feature differs from the situation in pea, where a ~ 50 : 50 distribution between soluble and membrane-bound form was described (Stengel *et al*., 2008). Although the reason for this difference is not clear, it might be based on varying growth conditions of the plants. Since Tic62 seems to react sensibly to changes in the redox status, it is possible that these

differences are reflected by a shift in the balance between membrane-bound and soluble protein.

Thylakoids are complicated sub-organellar structures that are composed of regions with tightly stacked membranes (grana) and rather loosely distributed lamellae (stroma-thylakoids). The presented results indicate a strong preference for Tic62 localization in the stroma lamellae (Figure 18). In addition, localization of GFP-tagged constructs corroborates the hypothesis that the N-terminal half of Tic62 with its hydrophobic patch is responsible for the attachment to membranes (Figure 12; Balsera *et al.*, 2007). The Tic62 Ct, on the other hand, was found to be completely soluble in the chloroplast stroma, although being largely unstructured in solution. The absence of a signal in the stroma or at the envelope is in contrast to the sub-fractionation results and could be due to the artificial overexpression of the constructs in the protoplasts. For FNR, the sub-thylakoidal distribution was less well-defined (Figures 12/18). However, as the FNR-RFP signal was not very strong and found to be dispersed throughout the thylakoid system, the possibility of an unspecific aggregation of the constructs was excluded. Rather, the dot-like pattern represents an accumulation at or around their main site of action, which is clearly located at the thylakoid-stroma border, where FNR mediates the transfer of electrons from PSI/Fd to the reduction equivalents used for the metabolic processes.

It is concluded that Tic62 is almost exclusively present in the stroma thylakoids, similar to PSI, the NDH complex as well as the CF_OCF_1-ATPase. FNR, on the other hand, is not restricted to one location within the thylakoid system. It apparently resides with Tic62 in the stroma lamellae, but seems to be additionally associated to unknown other factors, either at the margins or even in the grana stacks.

1.2 Tic62 acts as a membrane anchor of FNR

In the present work, several lines of evidence were obtained that allow a more detailed understanding of the association of FNR to the thylakoids than before, and clearly exceeding previous reports about potential FNR binding proteins in the thylakoid membrane (*e.g.* Vallejos *et al.*, 1984; Shin *et al.*, 1985; Matthijs *et al.*, 1986; Chan *et al.*, 1987; Soncini and Vallejos, 1989; Guedeney *et al.*, 1996; Zhang *et al.*, 2001). As discussed above, Tic62 and FNR share a very similar distribution among the chloroplast sub-compartments, as they are not only found in the stroma and at the envelope, but also in the stroma lamellae of thylakoids. In *tic62* knockout plants, the amount and distribution of FNR was found to be specifically altered (Figures 16-19). In particular the membrane bound pools of FNR are drastically reduced: roughly 50% of the thylakoid-bound FNR is lost and the envelope

fraction is almost completely depleted (Figure 17). Transcript analysis and *in vitro* import assays indicate that neither expression nor import of the FNR precursors are affected, but that the incorporation into the HMW protein complexes of the thylakoid membrane is defective (Figure 20). By BN-PAGE it was furthermore shown that it is in this HMW range that Tic62 and FNR co-migrate perfectly (Figure 13 A). These results demonstrate that Tic62 acts as a major FNR binding protein at the thylakoids. Moreover, it is most likely the sole FNR binding factor at the IE membrane.

As mentioned above, the presence of a thylakoid-bound form of an otherwise soluble protein like FNR has provoked a number of studies, aimed at the identification of a factor providing a docking station for the protein. Over the course of the last two decades, FNR has thus been described to co-purify or associate with several thylakoidal proteins or protein complexes. Several of these would clearly benefit from the presence of a reductase. Association with FNR was thus suggested to allow the NDH complex the use of NADPH in addition to NADH, but the selectivity of this complex is still unclear (for review see Endo *et al*., 2008). The described interaction with the Cytb$_6$f complex was proposed to provide the membrane protein connection for linear electron flow to Fd-dependent cyclic electron flow (Zhang *et al*., 2001; Okutani *et al*., 2005). And finally, association with PsaE, being located on the stromal side of PSI, was hypothesized to provide a platform bringing Fd (attached to PsaD) and FNR in close physical proximity, thus optimizing the final step of the linear electron transfer chain (Andersen *et al*., 1992; van Thor *et al*., 1999; Scheller *et al*., 2001). However, all these results describing potential FNR binding proteins were to a large extend not followed up, are still disputed, and often the real physiological significance is not well understood. The high number of candidates and some contradictory observations might indicate that FNR is a rather "sticky" protein (Kieselbach *et al*., 1998) that binds with low selectivity to a variety of photosynthetic complexes. To make things even more complicated, another study demonstrated that FNR is able to bind to artificial membranes directly, independent of proteinaceous factors (Grzyb *et al*., 2007), which could provide an explanation for the broad distribution of FNR at the thylakoid surface as seen in the localization experiments (Figure 12). Moreover, the interactions with thylakoidal complexes are likely very short-lived and dynamic. Regarding the linear electron flow, it is also plausible that reduced Fd first detaches from the thylakoids and subsequently interacts with FNR in the stroma. The ability of soluble FNR to sustain the main electron flow is clearly demonstrated by the high viability of *lfnr1* knockout plants, which do not contain any thylakoid-bound FNR (Lintala *et al*., 2007). It is therefore quite reasonable to suggest that the soluble pool of FNR

in the stroma is the most responsible for the photosynthetic electron transport, and that binding to the thylakoids might serve a different purpose – possibly in redox regulation.

In addition to the verification of a third pool of Tic62, the presented results now allow a more detailed understanding of the thylakoid-localized pool of FNR. As indicated by BN-PAGE and thylakoid sub-fractionation, the HMW Tic62/FNR complexes are most likely present in the stroma lamellae. In absence of Tic62, the remaining FNR complexes are small in size and probably located either in the grana or at the margins of thylakoids (Figures 18/19). No indications could be found that Tic62 or FNR associate with any of the mentioned thylakoid protein complexes, since none of those displayed a clear co-migration behavior (Figure 13). In contrast, comparison of the Tic62/FNR complex assembly in *tic62*, *lfnr1* and *lfnr2* plants by BN-PAGE revealed that the HMW complexes depend on the presence of all three components (Figure 21). The amount and migration behavior of FNR, on the other hand, was *e.g.* shown *not* to be affected by absence of a functional NDH complex (Burrows *et al.*, 1998). It is thus proposed that the HMW Tic62/FNR complexes are composed mainly, if not exclusively, of Tic62 and FNR. This would extend the hypothesis of an LFNR1/LFNR2 dimer by Lintala *et al.*, 2007, suggesting that it is actually a hetero-oligomer, composed of both leaf isoforms of FNR together with Tic62, that is required for the attachment of FNR to the envelope and thylakoid membranes.

Another hint for the existence of a hetero-oligomeric complex derives from the binding experiments performed with stromal FNRs and a Tic62 C-terminal affinity matrix (Figure 30). Even though it cannot be ruled out that Tic62 could bind homo-dimers (or homo-oligomers) of both kind, Tic62 obviously does not distinguish between the two FNR isoforms and binds both equally well. A hetero-oligomeric complex therefore seems likely. The observation of several distinct complexes of varying size in the thylakoids would then be due to different oligomerisation states of Tic62 and FNR, although the participation of other proteins cannot be excluded solely based on these facts. Moreover, other proteins might assist in the membrane binding of the smaller FNR complexes that can be found also in absence of Tic62.

1.3 The strong interaction between Tic62 and FNR involves a novel binding mode and has a stabilizing function for the complex

Several lines of evidence suggest that the association between Tic62 and FNR is not only very specific, but also involves a strong binding mode. As shown by high-salt treatment of WT and *tic62* thylakoids, FNR is tightly bound to Tic62 and cannot be washed off easily (Figure 29). High ionic-strength likewise elutes only minor amounts of FNR from the Tic62 Ct affinity

matrix (Figure 30). Incubation with denaturing agents is necessary to achieve higher elution efficiency, and the majority of bound FNR is only eluted upon stripping of the Ni^{2+}-matrix by addition of imidazole. The resistance to high salt concentrations indicates the participation of mainly hydrophobic interactions in the binding of FNR and Tic62 as opposed to extensive hydrogen bonds or ionic interactions, which would be destabilized in the presence of salts.

Further insight into the binding mode of FNR and Tic62 was obtained by NMR spectroscopy and analytical ultracentrifugation (AUC), which was performed in collaboration with Y.-H. Lee and Prof. T. Hase from the University of Osaka, JP (data not shown). A small synthetic peptide, comprising a 30 amino acid repeat motif of the Tic62 Ct, was found to interact with FNR as observed by chemical shift perturbations occurring upon titration of the peptide to the reductase, thereby confirming the interaction between FNR and Tic62 on a molecular basis. NMR spectroscopy furthermore revealed that this peptide (and thus the Tic62 Ct) binds to the back side of FNR, opposite to the known binding sites of Fd and NADP(H). This represents a novel binding mode, because no other flavoprotein is known to use such a binding pattern. Further investigation of the Tic62/FNR interaction might thus lead to the discovery of a new function of flavoproteins.

Association of Tic62 to the back side of FNR should not block the active site, but could be an indication for an allosteric regulation of the enzyme. Whether this assumption is correct or not was tested in enzymatic assays in presence or absence of Tic62 constructs (Figure 27). The Cyt c reduction assay was advantageous for this purpose because it does not involve artificial electron acceptors but mimics the real electron transfer chain by using Fd and NADPH. Surprisingly, addition of Tic62 had absolutely no measurable effect on FNR activity when using freshly purified protein. After an overnight incubation however, FNR retained distinctly more of its initial activity when Tic62 was present than when incubated alone or in presence of control proteins. From this result it was concluded that Tic62 is not acting as a modulator of FNR activity but rather as a stabilizing factor, thereby increasing the half-life of FNR. Instability and subsequent degradation might also be accountable for the observation that FNR, which is not correctly assembled into thylakoid-bound complexes in *tic62* plants and initially accumulates in the stroma after import, is not visible in the steady state situation (*e.g.* Figures 20 B *vs.* 17 A). Interestingly, the same holds true for Tic62 in *lfnr1* plants (Figure 21). Surplus protein that cannot be integrated into the membrane-bound complexes in either mutant thus seems to be prone to proteolytical degradation, further supporting the notion of a reciprocal and interdependent stabilization of the components.

1.4 The basic Tic62/FNR complex adopts a 1 : 3 stoichiometry

In sedimentation equilibrium experiments with FNR and C-terminal Tic62 constructs, Y.-H. Lee and co-workers could determine the molecular mass of the resultant complexes (data not shown). Addition of the small synthetic peptide comprising one Tic62 repeat motif was found to induce dimerization of FNR (one repeat to two FNRs), which probably interact via their back sides, since any additional binding site would have been visible by NMR (see above). Interestingly however, the complete Tic62 Ct from pea (containing three repeats) was found to associate not with six but only with three FNR molecules. Obviously, steric hindrances in the complex formation of FNR with the longer (and more native) polypeptide reduce the number of FNR molecules that are able to bind to Tic62, even though each repeat might have the potential to bind two FNRs at the same time. Another implication that could be derived from this observation is that the Tic62 Ct, that was shown to be unstructured in solution in absence of FNR (Figure 28 B), might become a steric handicap due to structural rearrangements taking place upon FNR binding, as was already suggested by Stengel *et al.*, 2008. This, and in particular the direct possibility of a one FNR per repeat binding mode might not necessarily be the case *in vivo* and will have to be solved by other experimental strategies in the future (as *e.g.* X-ray crystallography).

Further evidence supporting this *in vitro* stoichiometry is derived from a semi-quantitative proteomic analysis of pea IE, in which the ratio of FNR to Tic62 was found to be 3 : 1 (Bräutigam *et al.*, 2008 and personal communication). As mentioned before, FNR is almost completely depleted from the envelopes in *tic62* plants (the residual amount probably representing thylakoid contamination of the envelope preparation), suggesting that all the FNR found at this membrane is complexed by Tic62. Hence, the observed 3 : 1 ratio can be considered a measure of the complex at the envelope *in vivo* and fits surprisingly well to the values derived from the AUC experiments. However, the stoichiometry may vary *in vivo* since the affinity of Tic62 to FNR (and the Tic complex) was demonstrated to be dependent on the redox status of the organelle (Figure 23 and Stengel *et al.*, 2008). This gives room to speculate that the number of FNR molecules per Tic62 Ct can likewise vary dependent on the chloroplast redox conditions, which remains to be tested.

1.5 The thylakoidal Tic62/FNR complexes are integrated into the light-dependent regulation of the stromal redox poise

The presented results allow to draw conclusions about possible functions of the Tic62/FNR complexes. The dissociation of the thylakoidal HMW complexes under light exposure (Figure

24) indicates that those are subject to a light-dependent regulation. This is in accordance with the co-expression data for *AtTIC62*, which demonstrate a close link to photosynthetic processes (Figure 10). Accepting electrons from Fd and using those to produce reduction equivalents, FNR represents the link between photosynthetic electron flow and the reductive metabolism. A decreased amount of FNR could thus lead to a holdup of electrons at some point of the electron transport chain as had been seen by Lintala *et al*. (2007) in *lfnr1* mutants. Interestingly however, no photosynthetic phenotype could be detected in *tic62* plants (Table 7), although about half of the thylakoid-bound FNR is missing in these mutants (Figure 17 A). Since FNR has been discussed to participate in cyclic electron flow around PSI as well as the NDH complex, and as Tic62 was found to be co-expressed with several NDH subunits (Takabayashi *et al*., 2009; this study), cyclic electron flow was also tested in *tic62* plants (Figure 25). However, measurements of the $P700^+$ re-reduction kinetics and the F_0 ´rise` did not result in any apparent difference as compared to the WT, making a direct involvement of the Tic62/FNR complexes in cyclic electron flow unlikely. The analysis of photosynthetic fitness therefore demonstrates that both linear and cyclic electron flow are not inhibited in *tic62* plants, even under high-light. This finding supports the notion that the thylakoidal Tic62/FNR hetero-oligomers are not associated to photosynthetic complexes, and that the stromal pool of FNR is sufficient to sustain the main electron flow away from the thylakoids.

As changes in the availability of pyridine nucleotides were demonstrated to influence the solubilization of Tic62 from the envelope (Stengel *et al*., 2008), it was investigated whether this regulatory mode is also acting on the Tic62/FNR complex at the thylakoids (Figure 22). It was found that the thylakoid-bound pool of Tic62 is indeed affected by the metabolic redox status in a similar fashion to what has been observed at the envelope. FNR was likewise solubilized specifically in the presence of the phosphorylated form of the pyridine nucleotide cofactor, but did not seem to distinguish between the oxidized or reduced form under the conditions applied (pH 7.6). The stromal pH was described to have an influence on FNR structure (Grzyb *et al*., 2007) as well as its affinity for Fd and NADPH (Carrillo *et al*., 1981). It might therefore be possible that FNR is more selective at a different pH. This could be envisioned for instance at night, when the stromal pH can drop to ~ pH 6, conditions in which FNR seems to adopt a more hydrophobic overall conformation. The investigation of how the combination of changes in the pH (a light-dependent effect) and the stromal redox status (a metabolic effect) will act on the Tic62/FNR complex will be interesting for the future.

As mentioned in the introduction, redox maintenance of the $NADP^+/NADPH$ ratio is closely linked to other redox regulatory systems. In particular the Trx network is highly involved in keeping a balance between reductive metabolism and light-driven NADPH generation in the chloroplast at day, an important mechanism stabilizing the overall $NADP^+/NADPH$ ratio. At night, a general switch-off of the main metabolic NADPH consuming pathways helps to prevent a shortage of NADPH, which is also supported by the onset of the oxidative pentose phosphate pathway (OPPP), delivering the reduction equivalents for light-independent processes. Under standard conditions, significant peaks in the NADPH concentration can thus be envisioned only at the beginning of the day (metabolism is still down, but NADPH is produced) and of the night (metabolism is still active, but NADPH regeneration stops). A well-coordinated Trx activity is therefore important to minimize potential concentration peaks. Strikingly, MDH activity was found to be increased both in *tic62* and *lfnr1* plants, indicating an over-reduced Trx-pool in both mutants (Figure 26). This observation might be explicable considering that FNR and FTR are in constant competition for reduced Fd (Figure 4 B). A loss of FNR will thus lead to an augmented electron flow via FTR to the Trx system, particularly in the morning hours. Accordingly, the strongest increase in activity was detectable in the beginning of the day (30 min and 3 h light) as compared to later hours (9 h), when the metabolism was probably fully activated in all plants.

In line with this argumentation, the observed increase in MDH activity for *lfnr1* plants seems reasonable. The mentioned discrepancy to Lintala *et al*. (2007) is not readily explained, but could be due to differences in plant growth: long-day grown plants were used in this study, for which the latest time point (9 h light) was only shortly after their midday. Lintala *et al.* on the other hand tested plants, which had been acclimated to short-day conditions, and thus were already well in their afternoon when harvested. Assuming that the MDH activity in *lfnr1* might decrease even further than observed between the 3 h to 9 h time points, a less than WT activity could be possible in the afternoon, which was however not tested since the present study was focused on the first half of the day.

The observation of a redox phenotype in *tic62* mutants, in which the stromal pool of FNR is unchanged, implies that the thylakoidal Tic62/FNR complexes take part in the distribution of electrons between FNR and FTR. However, since Trx, Fd and FTR are stromal enzymes, a direct involvement of the membrane-bound Tic62/FNR complex is unlikely. Therefore, relocation of FNR between the thylakoids and the stroma seems to be an important regulatory step. In *tic62* mutants, this relocation is greatly disturbed, since the major thylakoid

binding partner is missing and the HMW complexes that were shown to be particularly sensitive to light signals cannot be formed. In summary of the presented data, it can therefore be concluded that Tic62 performs at least two important functions in the chloroplast: (I) stabilizing FNR, probably in form of HMW hetero-trimeric complexes, *e.g.* in phases of prolonged inactivity, and (II) regulating the allocation of FNR between stroma and membranes (thylakoids *and* envelope) by providing a membrane anchor and a platform for efficient redox sensing, which is in line with the proposed function of Tic62 as a redox sensor protein (Küchler *et al.*, 2002; Stengel *et al.*, 2008).

1.6 Working model

Based on the findings of this study, a working model can be presented, describing the proposed functions of Tic62 (Figure 41): At night, Tic62 seems to accumulate FNR at the thylakoid membranes in HMW complexes (Figure 41-1), possibly favored by exposition of hydrophobic structures on the FNR surface due to a decreasing stromal pH (Grzyb *et al.*, 2007). Since FNR stability seems to be lowered at more acidic pH values (Lee *et al.*, 2007), assembly into Tic62 complexes could therefore stabilize the enzyme during the hours of (photosynthetic) inactivity. With the beginning of the day, the Fd pool is reduced by onset of linear electron flow and diffuses into the stroma, where it can reduce either FNR or FTR (Figure 41-2). In case all reduced Fd was used by FNR to produce NADPH, this would lead to a dramatic increase in reduction equivalents, since the Calvin-Benson cycle as well as all other reductive metabolic pathways are not yet active. This activation has to be accomplished by the Trx network, which needs reducing energy in the morning to activate the high amount of metabolic enzymes that are dependent on this regulation, including all Calvin-Benson cycle enzymes, one of them being the vastly abundant RuBisCO, or the enzymes responsible for fatty acid biosynthesis (Soll and Roughan, 1982; Sasaki and Nagano, 2004). Therefore, the Tic62/FNR complex might function in keeping the pool of available FNR in the stroma low and thus increase the electron flow to the FTR in the morning hours. Following this initial activation phase, less and less FTR will be needed to regenerate oxidized Trx and more electrons can be shuttled to FNR for production of NADPH, which can now be efficiently utilized by the activated metabolism (Figure 41-3). Additionally, an alkalized stromal pH due to active thylakoidal electron transport processes and acidification of the lumen might further elevate the stromal pool of FNR by favoring the solubilization from the thylakoids (Grzyb *et al.*, 2007). At the same time, reductase activity and substrate affinity increase (Carrillo *et al.*, 1981). Higher FNR activity as well as increased availability is then beneficial to meet the growing demand of the organelle for reduction equivalents. In the evening when the

photosynthetic electron flow decreases, Tic62 and FNR might assemble in the stroma and return to the membranes due to a slightly oxidized redox environment as well as acidification of the stroma (Figure 41-4). A function in the regulation of the stromal FNR pool could thus explain the observed redox phenotype in the *tic62* mutants. Loss of Tic62, and the concomitant loss of the thylakoid-bound FNR pool and its light-induced solubilization, will interfere with the allocation of electrons between FNR and FTR in the morning hours and increase the reductive flow towards the Trx system. However, loss of this optimization mode is apparently not detrimental enough to produce a severe phenotype – even in the *lfnr* mutants (Lintala *et al.*, 2007; Lintala *et al.*, 2009).
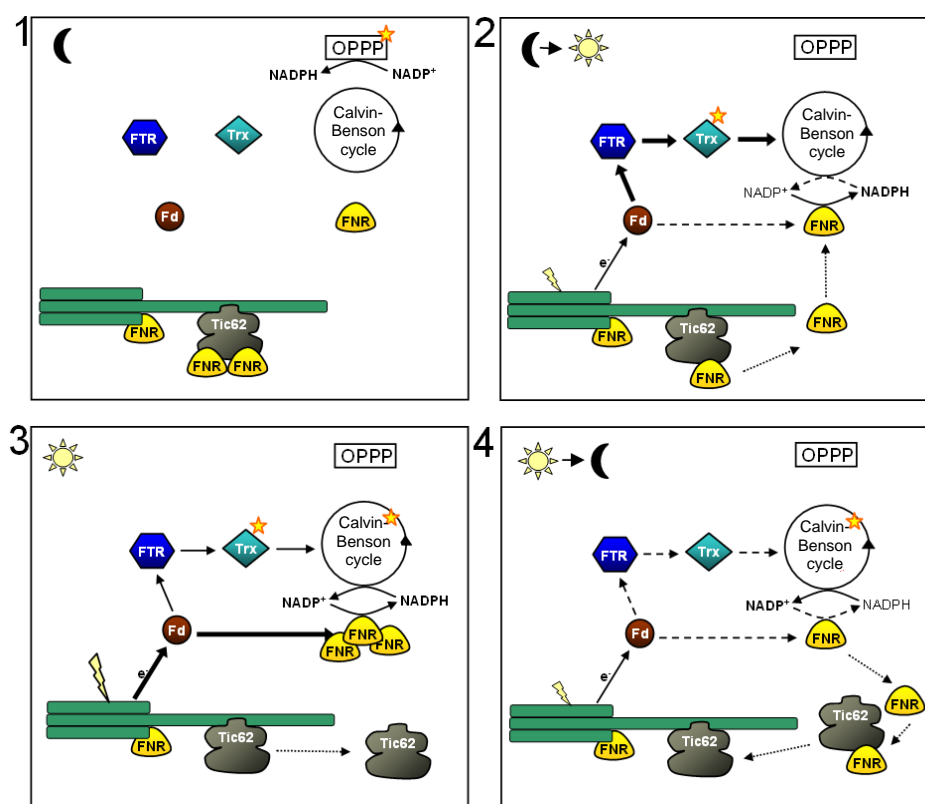
Figure 41: Working model illustrating the role of Tic62 and FNR in the metabolic redox network of the chloroplast. Only few components of the chloroplast redox system are depicted in an exemplary manner. Symbols: moon indicates night and sun day. The lightning bolt indicates irradiation at the thylakoids and a star next to a component or pathway means that it is active/reduced. The flow of electrons (e⁻) is depicted as black arrows (from dashed: minor flow to bold: major flow). Movement of components is indicated by dotted arrows. For further explanation, please refer to the text. OPPP, oxidative pentose phosphate pathway; Fd, ferredoxin; Trx, thioredoxin; FTR, Fd-Trx-oxidoreductase; FNR, Fd-NADP(H)-oxidoreductase

1.7 Concluding remarks

In conclusion, Tic62 seems to be a special protein, being present in three distinct subpools in the chloroplasts. However, since the subpools are probably closely connected by the observed redox-dependent shuttling behavior, a deeper understanding of the Tic62 thylakoid pool will

hopefully allow to draw conclusions about its functions in the context of redox regulation of protein translocation at the envelope in the future. In principle, the transport of electrons from the photosynthetic machinery via the Tic62/FNR complex directly to the Tic translocon should be possible. It is tempting to speculate that this reductive energy could be used in an electron transfer chain, involving also the other redox-active Tic subunits Tic55 and Tic32. The existence of such an electron chain at the IE was demonstrated by at least two independent studies (Jäger-Vottero *et al*., 1997; Murata and Takahashi, 1999) and it will be an interesting and challenging task to address this question in the future.

2 Heterologous expression and initial characterization of Tic20

2.1 Heterologous expression of Tic20 – an example for hydrophobic membrane proteins

In the present work, two heterologous expression systems for Tic20 were successfully established. Previous failure of Tic20 expression could have multiple reasons. Focusing on the *E. coli* system, the high hydrophobicity of the α-helical four TM-domain protein surely leads to the incorporation of Tic20 either into the plasma membrane or to the formation of insoluble aggregates as inclusion bodies (IBs; for review see *e.g.* Wagner *et al.*, 2006). In the first case, a channel-forming protein can affect the integrity of the bacterial membranes, since it might be integrated into the membrane, but correct regulation cannot be achieved by the host cell. This was also likely the case for several tested Tic20 overexpression strains in this study, which were found to hardly grow in culture, maybe due to a leaky promoter (data not shown).

A low protein yield can furthermore be the result of sub-optimal transcription or translation. The genetic code is universal, but since most amino acids are encoded for by several tRNAs (wobbling), evolutionary distinct species developed differing codon preferences (codon bias or codon usage), which is represented in a likewise varying abundance of the corresponding tRNAs in the cells. Wrong codon usage of the GOI in the host organism can therefore be problematic (Farrokhi *et al.*, 2009), since it is used as an important regulatory means in protein biosynthesis. Hence, rare codons inhibit translation, whereas abundant codons can increase translation efficiency. Since this feature can be optimized, this was done in the present work for the mature sequence of the Tic20 gene from pea (Figures 9 and 31). Obviously, however, the toxicity effects of the protein in the *E. coli* host remained, and only the use in a cell-free expression system allowed to circumvent this problem. The optimized sequence was nevertheless also helpful in the *in vitro* expression, since (I) the reaction uses a tRNA mixture from *E. coli*, which thus could be efficiently used, and (II) potential mRNA secondary structures inhibiting translation were less likely with this construct.

Alternatively, in case a particular protein is not efficiently produced in a host organism, it is often advisable to either change the host or use a different homolog of the respective protein. In addition, a major bottleneck for the heterologous production of membrane proteins is thought to be an overburdened translocation and membrane-insertion system of the host cell, since essential components (*e.g.* SRP, Sec or YidC) can be virtually titrated out by overproduction of the recombinant protein (for review see Wagner *et al.*,

2006). One of the possible, though seemingly contradictory, solutions for this problem is to decrease the production speed, either by weaker induction or by an overall decrease of cellular activity *e.g.* due to sub-optimal temperatures. Both lines of argumentation were followed with the generated construct of *Arabidopsis* Tic20 in a cold-induced vector system, which was finally successfully used to express Tic20 also in intact bacteria (Figure 37). However, since reconstitution of the purified proteins (of both sources) into the lipid bilayer seems difficult (data not shown) and has not yielded functional pores yet, no results can be presented from the electrophysiological characterization.

2.2 Initial structural and topological characterization of Tic20

Production of purified full-length protein allowed first experimental assays to verify predicted protein features of Tic20, as *e.g.* secondary structure and topology. It could be confirmed that the protein adopts a mainly α-helical conformation (in a hydrophobic environment due to the presence of detergents; Figure 36), which is in line with a topology of four TM-segments, which would comprise the major part of the mature protein due to its small overall size (Figure 39). PEGylation of Tic20 in the IE membrane solely in presence of SDS furthermore demonstrates that (I) all Cys residues are on one side of the membrane, and (II) strongly suggests an Nt- and Ct-inside topology, as favored by the TMHMM program (Figure 39). A primary sequence alignment of the used Tic20 from pea, PsTic20, with its ortholog from *Arabidopsis*, AtTic20-I, as well as its evolutionary more distant homologs from the moss *Physcomitrella patens*, Phypa_142840 and Phypa_125484, demonstrates a high degree of conservation between the proteins (Figure 42), not only restricted to the predicted TM-domains (indicated by red lines below the alignment), but over the entire mature part of the sequence. Consequently, also the Tic20 homologs in other species are likely to adopt the same conformation and topology in the membrane as shown for PsTic20.

2.3 Experimental data argue against a stable cooperation between Tic20 and Tic110

It has been hypothesized that Tic20 and Tic110 might function together in the import of preproteins (Inaba *et al.*, 2003), but apart from a similarly strong phenotype of the knockout plants (Chen *et al.*, 2002; Inaba *et al.*, 2005; Teng *et al.*, 2006), their co-localization in the IE of chloroplasts and contact to translocated preproteins (Schnell *et al.*, 1994; Kouranov and Schnell, 1997; Inaba *et al.*, 2003), no direct evidence supporting this hypothesis has been presented yet. Indeed, chances are high that they work independently of each other in alternative pathways, as exemplified by the fact that Tic20 is much less abundant in the IE

membrane than Tic110, and thus clearly present in sub-stoichiometric amounts (Gross and Bhattacharya, 2009).
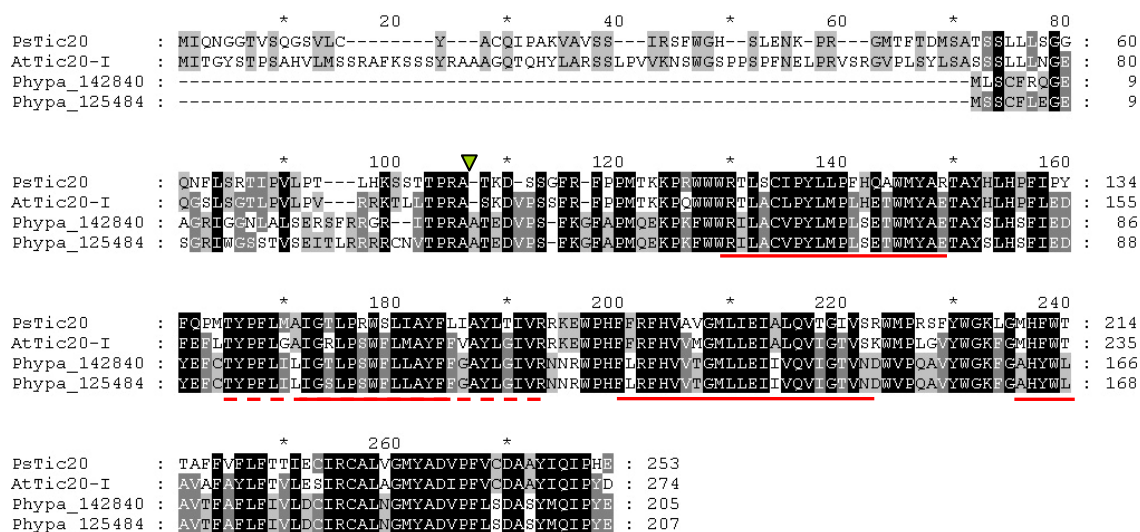
Figure 42: Multiple sequence alignment of Tic20 homologs from *Pisum*, *Arabidopsis* and *Physcomitrella*. Multiple sequence alignment was performed with the full-length sequences of four Tic20 homologs from *Pisum sativum* (PsTic20; AAC64607), *Arabidopsis thaliana* (AtTic20-I; NP_171986) and *Physcomitrella* (Phypa_142840 and Phypa_125484). The *Pisum* and *Arabidopsis* sequences were retrieved from GenBank. The sequences from the *Physcomitrella* Phypas were retrieved from Cosmoss. The representation of the alignment is the "conserved" mode from the Genedoc program. Conserved residues are indicated by shaded boxes. Transmembrane regions are marked by a red line below the sequences. The position of the transit peptide cleavage site of PsTic20 (Chen *et al.*, 2002) is indicated by an arrowhead.

The observations made in the present study likewise argue against a stable interaction of Tic20 and Tic110 even in tissues where they are both expressed at the same time, as demonstrated by the GUS-reporter gene assay and co-migration analysis in BN-PAGE (Figure 40). A clearly different expression pattern already in young seedlings indicates that both proteins not necessarily dependent on each other in their functional properties. Moreover, this finding suggests that Tic20 is functioning in several types of plastids (*e.g.* proplastids of undeveloped tissue, root amyloplasts and chloroplasts), while the function of Tic110 is focused on above-ground organs and thus the presence of chloroplasts. However, due to possible loss of more distant promoter elements and tissue-dependent differences *e.g.* in mRNA stability and translation, the analysis of promoter fragments driving a GUS-reporter gene only gives information on the basic transcriptional potential of a promoter, but does not necessarily correlate perfectly with the protein abundance of Tic20 and Tic110 *in vivo*. For example, Tic110 was demonstrated to be present also in roots, yet being much less abundant than in green parts of the plant (Inaba *et al.*, 2005). Still, the analysis of established GUS-reporter lines provides a simple and fast means to investigate tissues that are difficult to prepare for immunological detection (*e.g.* early developmental stages as used here) with a

possible single-cell resolution, and thus is a powerful genetic tool to complement the more biochemical characterization of a protein.

Dissimilar migration of Tic20 and Tic110 in native PAGE, as shown in Figure 40 (B), further supports the notion of independent functions of both proteins in the IE membrane and was corroborated in the following by similar results of another lab (Dr. M. Nakai, Osaka, JP; unpublished data). In line with this, Tic20 has so far only been described to associate with Tic22 (showing a similarly slow mobility in BN-PAGE as Tic20; data not shown), as opposed to Tic110, that has been conclusively demonstrated to be in contact with the import motor subunits Tic40 and Hsp93 as well as the "redox regulon" comprised of Tic62, Tic55, and Tic32. Moreover, Tic20 is of prokaryotic origin (Reumann and Keegstra, 1999; Reumann *et al.*, 2005), and therefore evolutionary much older than the eukaryotic Tic110. It is therefore reasonable to assume that Tic20 (maybe in combination with the likewise prokaryotic Tic22) is part of an alternative translocase complex, which might be devoted to evolutionary more established functions, that had been important already at the stage of the cyanobacterial ancestor. In contrast to this, the other members of the Tic complex were assembled and partly re-programmed (Gross and Bhattacharya, 2009) to function in the general import pathway, which was only developed after the endosymbiotic engulfment into the eukaryotic host cell. It can therefore be speculated that either various Tic translocons exist, or that Tic20 exhibits a different kind of protein translocation activity – maybe analogous to the inner membrane of mitochondria, where two channels (Tim23/Tim17 and Tim22) exist in parallel, each responsible for translocation of a different subset of precursors (Neupert and Herrmann, 2007).

Reference List

Akita M, Nielsen E, Keegstra K (1997) Identification of protein transport complexes in the chloroplastic envelope membranes via chemical cross-linking. *J Cell Biol* 136: 983-994

Allahverdiyeva Y, Mamedov F, Maenpaa P, Vass I, Aro EM (2005) Modulation of photosynthetic electron transport in the absence of terminal electron acceptors: characterization of the rbcL deletion mutant of tobacco. *Biochim Biophys Acta* 1709: 69-83

Alonso JM, Stepanova AN, Leisse TJ, Kim CJ, Chen HM, Shinn P, Stevenson DK, Zimmerman J, Barajas P, Cheuk R, Gadrinab C, Heller C, Jeske A, Koesema E, Meyers CC, Parker H, Prednis L, Ansari Y, Choy N, Deen H, Geralt M, Hazari N, Hom E, Karnes M, Mulholland C, Ndubaku R, Schmidt I, Guzman P, Aguilar-Henonin L, Schmid M, Weigel D, Carter DE, Marchand T, Risseeuw E, Brogden D, Zeko A, Crosby WL, Berry CC, Ecker JR (2003) Genome-wide Insertional mutagenesis of Arabidopsis thaliana. *Science* 301: 653-657

Altschul SF, Gish W, Miller W, Myers EW, Lipman DJ (1990) Basic local alignment search tool. *J Mol Biol* 215: 403-410

Altschul SF, Madden TL, Schaffer AA, Zhang JH, Zhang Z, Miller W, Lipman DJ (1997) Gapped BLAST and PSI-BLAST: a new generation of protein database search programs. *Nucleic Acids Research* 25: 3389-3402

Andersen B, Scheller HV, Moller BL (1992) The PSI-E subunit of photosystem I binds ferredoxin:NADP+ oxidoreductase. *FEBS Lett* 311: 169-173

Arnon DI (1949) Copper Enzymes in Isolated Chloroplasts - Polyphenoloxidase in Beta-Vulgaris. *Plant Physiology* 24: 1-15

Aro EM, Suorsa M, Rokka A, Allahverdiyeva Y, Paakkarinen V, Saleem A, Battchikova N, Rintamaki E (2005) Dynamics of photosystem II: a proteomic approach to thylakoid protein complexes. *J Exp Bot* 56: 347-356

Aronsson H, Jarvis P (2002) A simple method for isolating import-competent Arabidopsis chloroplasts. *FEBS Lett* 529: 215-220

Balsera M, Goetze TA, Kovacs-Bogdan E, Schürmann P, Wagner R, Buchanan BB, Soll J, Bölter B (2009) Characterization of Tic110, a Channel-forming Protein at the Inner Envelope Membrane of Chloroplasts, Unveils a Response to Ca2+ and a Stromal Regulatory Disulfide Bridge. *Journal of Biological Chemistry* 284: 2603-2616

Balsera M, Stengel A, Soll J, Bölter B (2007) Tic62: a protein family from metabolism to protein translocation. *Bmc Evolutionary Biology* 7:

Bartsch S, Monnet J, Selbach K, Quigley F, Gray J, von Wettstein D, Reinbothe S, Reinbothe C (2008) Three thioredoxin targets in the inner envelope membrane of chloroplasts function in protein import and chlorophyll metabolism. *Proc Natl Acad Sci U S A* 105: 4933-4938

Becker T, Hritz J, Vogel M, Caliebe A, Bukau B, Soll J, Schleiff E (2004) Toc12, a novel subunit of the intermembrane space preprotein translocon of chloroplasts. *Molecular Biology of the Cell* 15: 5130-5144

Benz JP, Soll J, Bölter B (2009) Protein transport in organelles: The composition, function and regulation of the Tic complex in chloroplast protein import. *Febs Journal* 276: 1166-1176

Benz P, Soll J, Bölter B (2007) The Role of the Tic Machinery in Chloroplast Protein Import. In R Dalbey, C Koehler, F Kamanoi, eds, Molecular Machines Involved in Protein Transport across Cellular Membranes, Vol 25. Academic Press/Elsevier, pp 439-462

Biehl A, Richly E, Noutsos C, Salamini F, Leister D (2005) Analysis of 101 nuclear transcriptomes reveals 23 distinct regulons and their relationship to metabolism, chromosomal gene distribution and co-ordination of nuclear and plastid gene expression. *Gene* 344: 33-41

Blum H, Beier H, Gross HJ (1987) Improved Silver Staining of Plant-Proteins, Rna and Dna in Polyacrylamide Gels. *Electrophoresis* 8: 93-99

Bräutigam A, Hofmann-Benning S, Weber APM (2008) Comparative proteomics of chloroplast envelopes from C-3 and C-4 plants reveals specific adaptations of the plastid envelope to C-4 photosynthesis and candidate proteins required for maintaining C-4 metabolite fluxes. *Plant Physiology* 148: 568-579

Breyton C, Nandha B, Johnson GN, Joliot P, Finazzi G (2006) Redox modulation of cyclic electron flow around photosystem I in C3 plants. *Biochemistry* 45: 13465-13475

Buchanan BB, Balmer Y (2005) Redox regulation: a broadening horizon. *Annu Rev Plant Biol* 56: 187-220

Burrows PA, Sazanov LA, Svab Z, Maliga P, Nixon PJ (1998) Identification of a functional respiratory complex in chloroplasts through analysis of tobacco mutants containing disrupted plastid ndh genes. *Embo Journal* 17: 868-876

Caliebe A, Grimm R, Kaiser G, Lübeck J, Soll J, Heins L (1997) The chloroplastic protein import machinery contains a Rieske-type iron-sulfur cluster and a mononuclear iron-binding protein. *Embo Journal* 16: 7342-7350

Carrillo N, Ceccarelli EA (2003) Open questions in ferredoxin-NADP(+) reductase catalytic mechanism. *European Journal of Biochemistry* 270: 1900-1915

Carrillo N, Lucero HA, Vallejos RH (1981) Light-Modulation of Chloroplast Membrane-Bound Ferredoxin-Nadp+ Oxidoreductase. *Journal of Biological Chemistry* 256: 1058-1059

Ceccarelli EA, Arakaki AK, Cortez N, Carrillo N (2004) Functional plasticity and catalytic efficiency in plant and bacterial ferredoxin-NADP(H) reductases. *Biochim Biophys Acta* 1698: 155-165

Chan RL, Ceccarelli EA, Vallejos RH (1987) Immunological studies of the binding protein for chloroplast ferredoxin-NADP+ reductase. *Arch Biochem Biophys* 253: 56-61

Chen X, Smith MD, Fitzpatrick L, Schnell DJ (2002) In vivo analysis of the role of atTic20 in protein import into chloroplasts. *Plant Cell* 14: 641-654

Chigri F, Hörmann F, Stamp A, Stammers DK, Bölter B, Soll J, Vothknecht UC (2006) Calcium regulation of chloroplast protein translocation is mediated by calmodulin binding to Tic32. *Proceedings of the National Academy of Sciences of the United States of America* 103: 16051-16056

Clausen C, Ilkavets I, Thomson R, Philippar K, Vojta A, Mohlmann T, Neuhaus E, Fulgosi H, Soll J (2004) Intracellular localization of VDAC proteins in plants. *Planta* 220: 30-37

Clough SJ, Bent AF (1998) Floral dip: a simplified method for Agrobacterium-mediated transformation of Arabidopsis thaliana. *Plant J* 16: 735-743

Cruz-Ramirez A, Lopez-Bucio J, Ramirez-Pimentel G, Zurita-Silva A, Sanchez-Calderon L, Ramirez-Chavez E, Gonzalez-Ortega E, Herrera-Estrella L (2004) The xipotl mutant of Arabidopsis reveals a critical role for phospholipid metabolism in root system development and epidermal cell integrity. *Plant Cell* 16: 2020-2034

Darie CC, Biniossek ML, Winter V, Mutschler B, Haehnel W (2005) Isolation and structural characterization of the Ndh complex from mesophyll and bundle sheath chloroplasts of Zea mays. *FEBS J* 272: 2705-2716

de Hoon MJ, Imoto S, Nolan J, Miyano S (2004) Open source clustering software. *Bioinformatics* 20: 1453-1454

Dekker JP, Boekema EJ (2005) Supramolecular organization of thylakoid membrane proteins in green plants. *Biochimica et Biophysica Acta-Bioenergetics* 1706: 12-39

Duy D, Wanner G, Meda AR, von Wiren N, Soll J, Philippar K (2007) PIC1, an ancient permease in Arabidopsis chloroplasts, mediates iron transport. *Plant Cell* 19: 986-1006

Eisen MB, Spellman PT, Brown PO, Botstein D (1998) Cluster analysis and display of genome-wide expression patterns. *Proc Natl Acad Sci U S A* 95: 14863-14868

Endo T, Ishida S, Ishikawa N, Sato F (2008) Chloroplastic NAD(P)H dehydrogenase complex and cyclic electron transport around photosystem I. *Mol Cells* 25: 158-162

Farrokhi N, Hrmova M, Burton RA, Fincher GB (2009) Heterologous and cell-free protein expression systems. In DJ Somers, *et al.*, eds, Methods in Molecular Biology, Plant Genomics, Vol 513. Humana Press, pp 175-198

Firlej-Kwoka E, Strittmatter P, Soll J, Bölter B (2008) Import of preproteins into the chloroplast inner envelope membrane. *Plant Molecular Biology* 68: 505-519

Fuhrmann M, Hausherr A, Ferbitz L, Schodl T, Heitzer M, Hegemann P (2004) Monitoring dynamic expression of nuclear genes in Chlamydomonas reinhardtii by using a synthetic luciferase reporter gene. *Plant Molecular Biology* 55: 869-881

Gasteiger E, Gattiker A, Hoogland C, Ivanyi I, Appel RD, Bairoch A (2003) ExPASy: the proteomics server for in-depth protein knowledge and analysis. *Nucleic Acids Research* 31: 3784-3788

Gould SB, Waller RF, McFadden GI (2008) Plastid evolution. *Annu Rev Plant Biol* 59: 491-517

Gross J, Bhattacharya D (2009) Revaluating the evolution of the Toc and Tic protein translocons. *Trends Plant Sci* 14: 13-20

Grzyb J, Gagos M, Gruszecki WI, Bojko M, Strzalka K (2007) Interaction of ferredoxin : NADP(+) oxidoreductase with model membranes. *Biochimica et Biophysica Acta-Biomembranes* 1778: 133-142

Guedeney G, Corneille S, Cuine S, Peltier G (1996) Evidence for an association of ndh B, ndh J gene products and ferredoxin-NADP-reductase as components of a chloroplastic NAD(P)H dehydrogenase complex. *FEBS Lett* 378: 277-280

Hanke GT, Okutani S, Satomi Y, Takao T, Suzuki A, Hase T (2005) Multiple iso-proteins of FNR in Arabidopsis: evidence for different contributions to chloroplast function and nitrogen assimilation. *Plant Cell and Environment* 28: 1146-1157

Heins L, Mehrle A, Hemmler R, Wagner R, Küchler M, Hörmann F, Sveshnikov D, Soll J (2002) The preprotein conducting channel at the inner envelope membrane of plastids. *Embo Journal* 21: 2616-2625

Hilson P, Allemeersch J, Altmann T, Aubourg S, Avon A, Beynon J, Bhalerao RP, Bitton F, Caboche M, Cannoot B, Chardakov V, Cognet-Holliger C, Colot V, Crowe M, Darimont C, Durinck S, Eickhoff H, de Longevialle AF, Farmer EE, Grant M, Kuiper MT, Lehrach H, Leon C, Leyva A, Lundeberg J, Lurin C, Moreau Y, Nietfeld W, Paz-Ares J, Reymond P, Rouze P, Sandberg G, Segura MD, Serizet C, Tabrett A, Taconnat L, Thareau V, Van Hummelen P, Vercruysse S, Vuylsteke M, Weingartner M, Weisbeek PJ, Wirta V, Wittink FR, Zabeau M, Small I (2004) Versatile gene-specific sequence tags for Arabidopsis functional genomics: transcript profiling and reverse genetics applications. *Genome Res* 14: 2176-2189

Hinnah SC, Wagner R, Sveshnikova N, Harrer R, Soll J (2002) The chloroplast protein import channel Toc75: Pore properties and interaction with transit peptides. *Biophysical Journal* 83: 899-911

Hirohashi T, Hase T, Nakai M (2001) Maize non-photosynthetic ferredoxin precursor is mis-sorted to the intermembrane space of chloroplasts in the presence of light. *Plant Physiol* 125: 2154-2163

Hirsch S, Muckel E, Heemeyer F, Vonheijne G, Soll J (1994) A Receptor Component of the Chloroplast Protein Translocation Machinery. *Science* 266: 1989-1992

Hisabori T, Motohashi K, Hosoya-Matsuda N, Ueoka-Nakanishi H, Romano PG (2007) Towards a functional dissection of thioredoxin networks in plant cells. *Photochem Photobiol* 83: 145-151

Hörmann F, Küchler M, Sveshnikov D, Oppermann U, Li Y, Soll J (2004) Tic32, an essential component in chloroplast biogenesis. *Journal of Biological Chemistry* 279: 34756-34762

Inaba T, Alvarez-Huerta M, Li M, Bauer J, Ewers C, Kessler F, Schnell DJ (2005) Arabidopsis tic110 is essential for the assembly and function of the protein import machinery of plastids. *Plant Cell* 17: 1482-1496

Inaba T, Li M, Alvarez-Huerta M, Kessler F, Schnell DJ (2003) atTic110 functions as a scaffold for coordinating the stromal events of protein import into chloroplasts. *J Biol Chem* 278: 38617-38627

Inaba T, Schnell DJ (2008) Protein trafficking to plastids: one theme, many variations. *Biochem J* 413: 15-28

Irizarry RA, Hobbs B, Collin F, Beazer-Barclay YD, Antonellis KJ, Scherf U, Speed TP (2003) Exploration, normalization, and summaries of high density oligonucleotide array probe level data. *Biostatistics* 4: 249-264

Ishihara G, Goto M, Saeki M, Ito K, Hori T, Kigawa T, Shirouzu M, Yokoyama S (2005) Expression of G protein coupled receptors in a cell-free translational system using detergents and thioredoxin-fusion vectors. *Protein Expression and Purification* 41: 27-37

Ishihara S, Takabayashi A, Ido K, Endo T, Ifuku K, Sato F (2007) Distinct functions for the two PsbP-like proteins PPL1 and PPL2 in the chloroplast thylakoid lumen of Arabidopsis. *Plant Physiol* 145: 668-679

Jackson DT, Froehlich JE, Keegstra K (1998) The hydrophilic domain of Tic110, an inner envelope membrane component of the chloroplastic protein translocation apparatus, faces the stromal compartment. *J Biol Chem* 273: 16583-16588

Jäger-Vottero P, Dorne AJ, Jordanov J, Douce R, Joyard J (1997) Redox chains in chloroplast envelope membranes: spectroscopic evidence for the presence of electron carriers, including iron-sulfur centers. *Proc Natl Acad Sci U S A* 94: 1597-1602

Jarvis P (2008) Targeting of nucleus-encoded proteins to chloroplasts in plants. *New Phytol* 179: 257-285

Jensen PE, Bassi R, Boekema EJ, Dekker JP, Jansson S, Leister D, Robinson C, Scheller HV (2007) Structure, function and regulation of plant photosystem I. *Biochimica et Biophysica Acta-Bioenergetics* 1767: 335-352

Keegstra K, Youssif AE (1986) Isolation and characterization of chloroplast envelope membranes. In A Weissbach, H Weissbach, eds, Methods Enzymology - Plant Molecular Biology, Vol 118. Academic Press, USA, pp 316-325

Kelly SM, Jess TJ, Price NC (2005) How to study proteins by circular dichroism. *Biochim Biophys Acta* 1751: 119-139

Kessler F, Blobel G (1996) Interaction of the protein import and folding machineries of the chloroplast. *Proc Natl Acad Sci U S A* 93: 7684-7689

Kessler F, Blobel G, Patel HA, Schnell DJ (1994) Identification of two GTP-binding proteins in the chloroplast protein import machinery. *Science* 266: 1035-1039

Kieselbach T, Hagman, Andersson B, Schroder WP (1998) The thylakoid lumen of chloroplasts. Isolation and characterization. *J Biol Chem* 273: 6710-6716

Kim TW, Keum JW, Oh IS, Choi CY, Park CG, Kim DM (2006) Simple procedures for the construction of a robust and cost-effective cell-free protein synthesis system. *Journal of Biotechnology* 126: 554-561

Klammt C, Schwarz D, Fendler K, Haase W, Dotsch V, Bernhard F (2005) Evaluation of detergents for the soluble expression of alpha-helical and beta-barrel-type integral membrane proteins by a preparative scale individual cell-free expression system. *Febs Journal* 272: 6024-6038

Klammt C, Schwarz D, Lohr F, Schneider B, Dotsch V, Bernhard F (2006) Cell-free expression as an emerging technique for the large scale production of integral membrane protein. *Febs Journal* 273: 4141-4153

Ko K, Bornemisza O, Kourtz L, Ko ZW, Plaxton WC, Cashmore AR (1992) Isolation and characterization of a cDNA clone encoding a cognate 70-kDa heat shock protein of the chloroplast envelope. *J Biol Chem* 267: 2986-2993

Kouranov A, Chen X, Fuks B, Schnell DJ (1998) Tic20 and Tic22 are new components of the protein import apparatus at the chloroplast inner envelope membrane. *J Cell Biol* 143: 991-1002

Kouranov A, Schnell DJ (1997) Analysis of the interactions of preproteins with the import machinery over the course of protein import into chloroplasts. *J Cell Biol* 139: 1677-1685

Krause F, Seelert H (2008) Detection and analysis of protein-protein interactions of organellar and prokaryotic proteomes by blue native and colorless native gel electrophoresis. *Curr Protoc Protein Sci* Chapter 19: Unit

Küchler M, Decker S, Hörmann F, Soll J, Heins L (2002) Protein import into chloroplasts involves redox-regulated proteins. *Embo Journal* 21: 6136-6145

Kugler M, Jansch L, Kruft V, Schmitz UK, Braun HP (1997) Analysis of the chloroplast protein complexes by blue-native polyacrylamide gel electrophoresis (BN-PAGE). *Photosynthesis Research* 53: 35-44

Laemmli UK (1970) Cleavage of Structural Proteins During Assembly of Head of Bacteriophage-T4. *Nature* 227: 680-&

Lee YH, Tamura K, Maeda M, Hoshino M, Sakurai K, Takahashi S, Ikegami T, Hase T, Goto Y (2007) Cores and pH-dependent dynamics of ferredoxin-NADP(+) reductase revealed by hydrogen/deuterium exchange. *Journal of Biological Chemistry* 282: 5959-5967

Li HM, Moore T, Keegstra K (1991) Targeting of proteins to the outer envelope membrane uses a different pathway than transport into chloroplasts. *Plant Cell* 3: 709-717

Lindahl M, Kieselbach T (2009) Disulphide proteomes and interactions with thioredoxin on the track towards understanding redox regulation in chloroplasts and cyanobacteria. *J Proteomics* 72: 416-438

Lintala M, Allahverdiyeva Y, Kangasjarvi S, Lehtimaki N, Keranen M, Rintamaki E, Aro EM, Mulo P (2009) Comparative analysis of leaf-type ferredoxin-NADP oxidoreductase isoforms in Arabidopsis thaliana. *Plant J* 57: 1103-1115

Lintala M, Allahverdiyeva Y, Kidron H, Piippo M, Battchikova N, Suorsa M, Rintamaki E, Salminen TA, Aro EM, Mulo P (2007) Structural and functional characterization of ferredoxin-NADP+-oxidoreductase using knock-out mutants of Arabidopsis. *Plant J* 49: 1041-1052

Lowry OH, Rosebrough NJ, Farr AL, Randall RJ (1951) Protein Measurement with the Folin Phenol Reagent. *Journal of Biological Chemistry* 193: 265-275

Lübeck J, Soll J, Akita M, Nielsen E, Keegstra K (1996) Topology of IEP110, a component of the chloroplastic protein import machinery present in the inner envelope membrane. *Embo Journal* 15: 4230-4238

Ma Y, Kouranov A, LaSala SE, Schnell DJ (1996) Two components of the chloroplast protein import apparatus, IAP86 and IAP75, interact with the transit sequence during the recognition and translocation of precursor proteins at the outer envelope. *J Cell Biol* 134: 315-327

Matthijs HCP, Coughlan SJ, Hind G (1986) Removal of Ferredoxin - Nadp+ Oxidoreductase from Thylakoid Membranes, Rebinding to Depleted Membranes, and Identification of the Binding-Site. *Journal of Biological Chemistry* 261: 2154-2158

May T, Soll J (2000) 14-3-3 proteins form a guidance complex with chloroplast precursor proteins in plants. *Plant Cell* 12: 53-63

Miginiac-Maslow M, Lancelin JM (2002) Intrasteric inhibition in redox signalling: light activation of NADP-malate dehydrogenase. *Photosynth Res* 72: 1-12

Mollier P, Hoffmann B, Debast C, Small I (2002) The gene encoding Arabidopsis thaliana mitochondrial ribosomal protein S13 is a recent duplication of the gene encoding plastid S13. *Curr Genet* 40: 405-409

Montrichard F, Alkhalfioui F, Yano H, Vensel WH, Hurkman WJ, Buchanan BB (2009) Thioredoxin targets in plants: the first 30 years. *J Proteomics* 72: 452-474

Murata Y, Takahashi M (1999) An alternative electron transfer pathway mediated by chloroplast envelope. *Plant and Cell Physiology* 40: 1007-1013

Neupert W, Herrmann JM (2007) Translocation of proteins into mitochondria. *Annu Rev Biochem* 76: 723-749

Nicholas KB, Nicholas HB (1997) GeneDoc: a tool for editing and annotating multiple sequence alignments. *Distributed by the authors*

Nielsen E, Akita M, Davila-Aponte J, Keegstra K (1997) Stable association of chloroplastic precursors with protein translocation complexes that contain proteins from both envelope membranes and a stromal Hsp100 molecular chaperone. *EMBO J* 16: 935-946

Okutani S, Hanke GT, Satomi Y, Takao T, Kurisu G, Suzuki A, Hase T (2005) Three maize leaf ferredoxin:NADPH oxidoreductases vary in subchloroplast location, expression, and interaction with ferredoxin. *Plant Physiol* 139: 1451-1459

Ossenbühl F, Hartmann K, Nickelsen J (2002) A chloroplast RNA binding protein from stromal thylakoid membranes specifically binds to the 5' untranslated region of the psbA mRNA. *Eur J Biochem* 269: 3912-3919

Peltier JB, Ytterberg AJ, Sun Q, van Wijk KJ (2004) New functions of the thylakoid membrane proteome of Arabidopsis thaliana revealed by a simple, fast, and versatile fractionation strategy. *J Biol Chem* 279: 49367-49383

Perry SE, Keegstra K (1994) Envelope membrane proteins that interact with chloroplastic precursor proteins. *Plant Cell* 6: 93-105

Philippar K, Ivashikina N, Ache P, Christian M, Luthen H, Palme K, Hedrich R (2004) Auxin activates KAT1 and KAT2, two K+-channel genes expressed in seedlings of Arabidopsis thaliana. *Plant Journal* 37: 815-827

Pratt JM (1984) Coupled transcription-translation in prokaryotic cell-free systems. In BD Hames, SJ Higgins, eds, Transcription and translation: a practical approach, IRL Press, New York, pp 179-209

Qbadou S, Becker T, Mirus O, Tews I, Soll J, Schleiff E (2006) The molecular chaperone Hsp90 delivers precursor proteins to the chloroplast import receptor Toc64. *Embo Journal* 25: 1836-1847

Quiles MJ, Cuello J (1998) Association of Ferredoxin-NADP oxidoreductase with the chloroplastic pyridine nucleotide dehydrogenase complex in barley leaves. *Plant Physiology* 117: 235-244

Quiles MJ, Garcia A, Cuello J (2000) Separation by blue-native PAGE and identification of the whole NAD(P)H dehydrogenase complex from barley stroma thylakoids. *Plant Physiology and Biochemistry* 38: 225-232

Reumann S, Inoue K, Keegstra K (2005) Evolution of the general protein import pathway of plastids (review). *Mol Membr Biol* 22: 73-86

Reumann S, Keegstra K (1999) The endosymbiotic origin of the protein import machinery of chloroplastic envelope membranes. *Trends Plant Sci* 4: 302-307

Reynolds ES (1963) Use of Lead Citrate at High Ph As An Electron-Opaque Stain in Electron Microscopy. *Journal of Cell Biology* 17: 208-&

Richter ML, Samra HS, He F, Giessel AJ, Kuczera KK (2005) Coupling proton movement to ATP synthesis in the chloroplast ATP synthase. *J Bioenerg Biomembr* 37: 467-473

Richter S, Lamppa GK (1998) A chloroplast processing enzyme functions as the general stromal processing peptidase. *Proc Natl Acad Sci U S A* 95: 7463-7468

Rokka A, Suorsa M, Saleem A, Battchikova N, Aro EM (2005) Synthesis and assembly of thylakoid protein complexes: multiple assembly steps of photosystem II. *Biochem J* 388: 159-168

Romano P, Gray J, Horton P, Luan S (2005) Plant immunophilins: functional versatility beyond protein maturation. *New Phytol* 166: 753-769

Rosso MG, Li Y, Strizhov N, Reiss B, Dekker K, Weisshaar B (2003) An Arabidopsis thaliana T-DNA mutagenized population (GABI-Kat) for flanking sequence tag-based reverse genetics. *Plant Mol Biol* 53: 247-259

Rumeau D, Peltier G, Cournac L (2007) Chlororespiration and cyclic electron flow around PSI during photosynthesis and plant stress response. *Plant Cell Environ* 30: 1041-1051

Saldanha AJ (2004) Java Treeview--extensible visualization of microarray data. *Bioinformatics* 20: 3246-3248

Sambrook J, Fritsch EF, Maniatis T. (1989) Molecular Cloning - A Laboratory Manual. Cold Spring Harbour Laboratory Press, New York,

Sasaki Y, Nagano Y (2004) Plant acetyl-CoA carboxylase: Structure, biosynthesis, regulation, and gene manipulation for plant breeding. *Bioscience Biotechnology and Biochemistry* 68: 1175-1184

Schagger H, von Jagow G (1991) Blue native electrophoresis for isolation of membrane protein complexes in enzymatically active form. *Anal Biochem* 199: 223-231

Scheibe R, Stitt M (1988) Comparison of Nadp-Malate Dehydrogenase Activation, Qa Reduction and O-2 Evolution in Spinach Leaves. *Plant Physiology and Biochemistry* 26: 473-481

Scheller HV, Jensen PE, Haldrup A, Lunde C, Knoetzel J (2001) Role of subunits in eukaryotic Photosystem I. *Biochimica et Biophysica Acta-Bioenergetics* 1507: 41-60

Schmid M, Davison TS, Henz SR, Pape UJ, Demar M, Vingron M, Scholkopf B, Weigel D, Lohmann JU (2005) A gene expression map of Arabidopsis thaliana development. *Nat Genet* 37: 501-506

Schnell DJ, Blobel G (1993) Identification of intermediates in the pathway of protein import into chloroplasts and their localization to envelope contact sites. *J Cell Biol* 120: 103-115

Schnell DJ, Blobel G, Pain D (1990) The chloroplast import receptor is an integral membrane protein of chloroplast envelope contact sites. *J Cell Biol* 111: 1825-1838

Schnell DJ, Kessler F, Blobel G (1994) Isolation of components of the chloroplast protein import machinery. *Science* 266: 1007-1012

Schürmann P, Buchanan BB (2008) The ferredoxin/thioredoxin system of oxygenic photosynthesis. *Antioxid Redox Signal* 10: 1235-1274

Schwacke R, Schneider A, van der Graaff E, Fischer K, Catoni E, Desimone M, Frommer WB, Flugge UI, Kunze R (2003) ARAMEMNON, a novel database for Arabidopsis integral membrane proteins. *Plant Physiology* 131: 16-26

Seedorf M, Waegemann K, Soll J (1995) A Constituent of the Chloroplast Import Complex Represents A New-Type of Gtp-Binding Protein. *Plant Journal* 7: 401-411

Seigneurin-Berny D, Salvi D, Dorne AJ, Joyard J, Rolland N (2008) Percoll-purified and photosynthetically active chloroplasts from Arabidopsis thaliana leaves. *Plant Physiology and Biochemistry* 46: 951-955

Shikanai T, Endo T, Hashimoto T, Yamada Y, Asada K, Yokota A (1998) Directed disruption of the tobacco ndhB gene impairs cyclic electron flow around photosystem I. *Proc Natl Acad Sci U S A* 95: 9705-9709

Shin M, Ishida H, Nozaki Y (1985) A New Protein Factor, Connectein, As A Constituent of the Large Form of Ferredoxin-Nadp Reductase. *Plant and Cell Physiology* 26: 559-563

Sirpiö S, Allahverdiyeva Y, Suorsa M, Paakkarinen V, Vainonen J, Battchikova N, Aro EM (2007) TLP18.3, a novel thylakoid lumen protein regulating photosystem II repair cycle. *Biochem J* 406: 415-425

Soll J, Roughan G (1982) Acyl Acyl Carrier Protein Pool Sizes During Steady-State Fatty-Acid Synthesis by Isolated Spinach-Chloroplasts. *Febs Letters* 146: 189-192

Soncini FC, Vallejos RH (1989) The chloroplast reductase-binding protein is identical to the 16.5-kDa polypeptide described as a component of the oxygen-evolving complex. *J Biol Chem* 264: 21112-21115

Sonnhammer EL, von Heijne G, Krogh A (1998) A hidden Markov model for predicting transmembrane helices in protein sequences. *Proc Int Conf Intell Syst Mol Biol* 6: 175-182

Spurr AR (1969) A low-viscosity epoxy resin embedding medium for electron microscopy. *J Ultrastruct Res* 26: 31-43

Steinhauser D, Usadel B, Luedemann A, Thimm O, Kopka J (2004) CSB.DB: a comprehensive systems-biology database. *Bioinformatics* 20: 3647-3651

Stengel A, Benz P, Balsera M, Soll J, Bölter B (2008) TIC62 redox-regulated translocon composition and dynamics. *J Biol Chem* 283: 6656-6667

Takabayashi A, Ishikawa N, Obayashi T, Ishida S, Obokata J, Endo T, Sato F (2009) Three novel subunits of Arabidopsis chloroplastic NAD(P)H dehydrogenase identified by bioinformatic and reverse genetic approaches. *Plant J* 57: 207-219

Teng YS, Su YS, Chen LJ, Lee YJ, Hwang I, Li HM (2006) Tic21 is an essential translocon component for protein translocation across the chloroplast inner envelope membrane. *Plant Cell* 18: 2247-2257

Thimm O, Blasing O, Gibon Y, Nagel A, Meyer S, Kruger P, Selbig J, Muller LA, Rhee SY, Stitt M (2004) MAPMAN: a user-driven tool to display genomics data sets onto diagrams of metabolic pathways and other biological processes. *Plant J* 37: 914-939

Tusher VG, Tibshirani R, Chu G (2001) Significance analysis of microarrays applied to the ionizing radiation response (vol 98, pg 5116, 2001). *Proceedings of the National Academy of Sciences of the United States of America* 98: 10515

Vallejos RH, Ceccarelli E, Chan R (1984) Evidence for the existence of a thylakoid intrinsic protein that binds ferredoxin-NADP+ oxidoreductase. *J Biol Chem* 259: 8048-8051

van Dooren GG, Tomova C, Agrawal S, Humbel BM, Striepen B (2008) Toxoplasma gondii Tic20 is essential for apicoplast protein import. *Proceedings of the National Academy of Sciences of the United States of America* 105: 13574-13579

van Thor JJ, Geerlings TH, Matthijs HCP, Hellingwerf KJ (1999) Kinetic evidence for the PsaE-dependent transient ternary complex photosystem I/ferredoxin/ferredoxin : NADP(+) reductase in a cyanobacterium. *Biochemistry* 38: 12735-12746

Waegemann K, Eichacker S, Soll J (1992) Outer Envelope Membranes from Chloroplasts Are Isolated As Right-Side-Out Vesicles. *Planta* 187: 89-94

Waegemann K, Soll J (1995) Characterization and isolation of the chloroplast protein import machinery. *Methods in Cell Biology, Vol 50* 50: 255-267

Wagner S, Bader ML, Drew D, de Gier JW (2006) Rationalizing membrane protein overexpression. *Trends in Biotechnology* 24: 364-371

Whitmore L, Wallace BA (2004) DICHROWEB, an online server for protein secondary structure analyses from circular dichroism spectroscopic data. *Nucleic Acids Res* 32: W668-W673

Whitmore L, Wallace BA (2008) Protein secondary structure analyses from circular dichroism spectroscopy: methods and reference databases. *Biopolymers* 89: 392-400

Wittig I, Braun HP, Schagger H (2006) Blue native PAGE. *Nat Protoc* 1: 418-428

Zhang H, Whitelegge JP, Cramer WA (2001) Ferredoxin:NADP+ oxidoreductase is a subunit of the chloroplast cytochrome b6f complex. *J Biol Chem* 276: 38159-38165

Supplementary data

Tic62 co-expression analysis results

Table S1: Result of combined Tic62 co-expression analysis.
List of the 142 genes that were found to be specifically ($\rho \geq 0.9$) co-regulated with Tic62 in the *A. thaliana* Co-Response Database (http://csbdb.mpimp-golm.mpg.de/csbdb/dbcor/ath.html) as well as in the hierarchical clustering analysis. The AGI gene code as well as a short description of the encoded protein (annotation according to TAIR8 (http://www.arabidopsis.org/index.jsp) are given. Genes that were annotated to belong to bin 1 (photosynthesis) are indicated by white letters on black background, and to bin 29 (protein) with black letters on grey background. White letters on grey background (#113) indicates that this gene belongs to both bins.

	AGI code	Encoded protein or gene model description (condensed, acc. to TAIR)
1	AT1G01790	Potassium efflux antiporter (KEA1)
2	AT1G03630	Protochlorophyllide oxidoreductase (Por C)
3	AT1G04420	aldo/keto reductase family protein; similar to KAB1 (potassium channel beta subunit)
4	AT1G04640	Lipoyltransferase 2 (Lip2)
5	AT1G08540	RNA polymerase sigma subunit 2 (Sig2)
6	AT1G08550	Non-photochemical quenching 1 (NPQ1)
7	AT1G09340	Chloroplast RNA binding (CRB)
8	AT1G11860	Aminomethyltransferase, mitochondrial precursor (GDCST)
9	AT1G12410	Clp protease proteolytic subunit 2 (Clp2)
10	AT1G12900	Glyceraldehyde 3-P dehydrogenase A subunit 2 (GapA-2)
11	AT1G14150	oxygen evolving enhancer 3 (PsbQ) family protein
12	AT1G14270	CAAX amino terminal protease family protein
13	AT1G14345	oxidoreductase; similar to hypothetical protein; thylakoid membrane
14	AT1G15140	similar to AtLFNR2
15	AT1G15980	NDH-dependent cyclic electron flow 1 (Ndf1)
16	AT1G16080	unknown protein
17	AT1G17220	fu-gaeri1 (Fug1)
18	AT1G18730	NDH-dependent cyclic electron flow 6 (Ndf6)
19	AT1G20340	recombination and DNA-damage resistance protein (DRT112, Pete2 or Plastocyanin 2)
20	AT1G20810	immunophilin / FKBP-type peptidyl-prolyl cis-trans isomerase 1, chloroplast precursor
21	AT1G22700	TPR protein with homology to Ycf37 from Synechocystis; thylakoid membrane; involved in photosystem I biogenesis.
22	AT1G23400	AtCAF2 (Promotes the splicing of chloroplast group II introns)
23	AT1G26230	chaperonin, putative; similar to Cpn60B (Chaperonin 60 beta)
24	AT1G31800	Cyt P450-type monooxygenase 97A3 (Cyp97A3)
25	AT1G32470	glycine cleavage system H protein, mitochondrial, putative
26	AT1G32500	Non-intrinsic ABC protein 6 (AtNap6)
27	AT1G35340	ATP-dependent protease La (LON) domain-containing protein
28	AT1G43560	Arabidopsis thioredoxin y2 (Aty2)
29	AT1G44575	Non-photochemical quenching 4 (NPQ4)
30	AT1G44920	unknown protein
31	AT1G45474	Lhca5
32	AT1G49380	cytochrome c biogenesis protein family
33	AT1G50450	binding / catalytic; similar to unknown
34	AT1G51110	plastid-lipid-associated protein 12, chloroplast precursor (PAP12)
35	AT1G54500	rubredoxin family protein

36	AT1G60990	similar to aminomethyltransferase
37	AT1G62750	Snowy cotyledon 1 (Sco1)
38	AT1G62780	unknown protein
39	AT1G64150	unknown protein
40	AT1G67700	contains oligopeptidase domain and protease M3 thimet oligopeptidase-related domain
41	AT1G70760	NDH-L; also: chlororespiratory reduction 23 (Crr23)
42	AT1G71500	Rieske (2Fe-2S) domain-containing protein
43	AT1G72610	Germin-like protein 1 (Ger1)
44	AT1G73060	unknown protein
45	AT1G73655	immunophilin / FKBP-type peptidyl-prolyl cis-trans isomerase family protein
46	AT1G74730	unknown protein
47	AT1G76450	oxygen-evolving complex-related
48	AT1G77490	Thylakoidal ascorbate peroxidase (TApx)
49	AT1G79790	haloacid dehalogenase-like hydrolase family protein
50	AT1G80030	DNAJ heat shock protein, putative
51	AT1G80480	Plastid transcriptionally active 17 (PtaC17)
52	AT2G01590	Chlororespiratory reduction 3 (Crr3)
53	AT2G01870	unknown protein
54	AT2G17033	pentatricopeptide (PPR) repeat-containing protein
55	AT2G20270	Monothiol glutaredoxin-S12, chloroplast precursor (GrxS12)
56	AT2G20690	putative riboflavin synthase
57	AT2G21170	Triosephosphate isomerase (TIM)
58	AT2G21860	violaxanthin de-epoxidase-related; similar to NPQ1 (Non-photochemical quenching 1)
59	AT2G25830	YebC-related
60	AT2G27680	aldo/keto reductase family protein
61	AT2G28605	PsbP domain-OEC23 like protein localized in thylakoid (peripheral-lumenal side)
62	AT2G30390	Ferrochelatase 2 (FC2)
63	AT2G32500	unknown protein
64	AT2G34860	embryo sac development arrest 3 (EDA3)
65	AT2G35370	GDCH (glycine decarboxylase complex H protein; involved in photorespiration)
66	AT2G35410	33 kDa ribonucleoprotein, chloroplast, putative; RNA-binding protein cp33
67	AT2G39470	PsbP-like protein 2 (PPL2)
68	AT2G43560	immunophilin; identical to FKBP-type peptidyl-prolyl cis-trans isomerase 2, chloroplast
69	AT2G44920	thylakoid lumenal 15 kDa protein 1, chloroplast precursor
70	AT2G47450	CHAOS (CAO)
71	AT3G01440	oxygen evolving enhancer 3 (PsbQ) family protein
72	AT3G01480	cyclophilin 38 (Cyp38)
73	AT3G04550	unknown protein
74	AT3G04790	ribose 5-phosphate isomerase-related
75	AT3G05350	aminopeptidase; similar to ATAPP1 (aminopeptidase P1)
76	AT3G07670	SET domain-containing protein
77	AT3G09050	unknown protein
78	AT3G11950	prenyltransferase (At3g11945)
79	AT3G20930	RNA recognition motif (RRM)-containing protein
80	AT3G22210	unknown protein
81	AT3G23700	S1 RNA-binding domain-containing protein; similar to RPS1 (ribosomal protein S1)
82	AT3G24430	High-chlorophyll-fluorescence 101 (HCF101)

83	AT3G26650	Glyceraldehyde 3-P dehydrogenase A subunit (GapA)
84	AT3G26710	Cofactor assembly of complex c (CCB1)
85	AT3G26900	shikimate kinase family protein
86	AT3G43540	unknown protein
87	AT3G54050	Fructose-1,6-bisphosphatase, chloroplast precursor (FBP)
88	AT3G55250	similar to calcium homeostasis regulator CHoR1
89	AT3G55330	PsbP-like protein 1 (PPL1)
90	AT3G56650	thylakoid lumenal 20 kDa protein
91	AT3G58140	phenylalanyl-tRNA synthetase class IIc family protein
92	AT3G60750	transketolase, putative
93	AT3G63140	Chloroplast stem-loop binding protein of 41 kDa (Csp41A)
94	AT4G01150	unknown protein, chloroplast precursor
95	AT4G01800	Protein translocase subunit secA, chloroplast precursor (secA)
96	AT4G02530	Thylakoid lumenal 16.5 kDa protein, chloroplast precursor
97	AT4G12060	Clp amino terminal domain-containing protein
98	AT4G13670	Plastid transcriptionally active 5 (PtaC5)
99	AT4G14870	P-P-bond-hydrolysis-driven protein transmembrane transporter; contains SecE domain; chloroplast thylakoids
100	AT4G14890	ferredoxin family protein; similar to AtFd3 (Fd 3)
101	AT4G18370	DegP protease 5 (Deg5)
102	AT4G21280	PsbQ
103	AT4G24930	thylakoid lumenal 17.9 kDa protein, chloroplast
104	AT4G33470	histone deacetylase 14 (Hda14)
105	AT4G33500	protein phosphatase 2C-related
106	AT4G33520	P-type ATP-ase 1 (PAA1)
107	AT4G34190	Stress enhanced protein 1 (Sep1)
108	AT4G34820	expressed protein
109	AT4G35450	Ankyrin repeat-containing protein 2 (AKR2)
110	AT4G36390	radical SAM domain- and TRAM domain-containing protein; CDK5RAP1-like
111	AT4G37040	Methionine aminopeptidase 1D (Map1D)
112	AT4G39970	haloacid dehalogenase-like hydrolase family protein
113	AT5G01920	Chloroplast thylakoid protein kinase STN8
114	AT5G02120	One helix protein (OHP)
115	AT5G07020	proline-rich family protein
116	AT5G08050	unknown protein
117	AT5G12860	dicarboxylate transporter 1 (DiT1)
118	AT5G13410	immunophilin / FKBP-type peptidyl-prolyl cis-trans isomerase family protein
119	AT5G16710	dehydroascorbate reductase 1 (DHAR3)
120	AT5G19220	ADP glucose pyrophosphorylase (AGPase) large su 1 (APL1)
121	AT5G22620	phosphoglycerate/bisphosphoglycerate mutase family protein
122	AT5G22830	Mg transporter 10 (AtMgt10)
123	AT5G27290	unknown protein
124	AT5G27560	unknown protein
125	AT5G28750	thylakoid assembly protein, putative; similar to HCF106
126	AT5G35630	Glutamine synthetase 2 (GS2)
127	AT5G36170	High chlorophyll fluorescence 109 (HCF109)
128	AT5G36700	2-P glycolate phosphatase 1 (PGLP1)
129	AT5G39830	DEG protease 8 (DegP8)

130 | AT5G42070 | unknown protein
131 | AT5G42310 | pentatricopeptide (PPR) repeat-containing protein; similar to chloroplast RNA processing1
132 | AT5G43750 | unknown protein
133 | AT5G45680 | FK506-binding protein 1 (FKBP13), chloroplast precursor
134 | AT5G46800 | A Bout De Souffle (BOU)
135 | AT5G47840 | Adenosine monophosphate kinase (AMK2)
136 | AT5G51110 | similar to dehydratase family
137 | AT5G53490 | thylakoid lumenal 17.4 kDa protein, chloroplast precursor (P17.4)
138 | AT5G55710 | AtTic20-V
139 | AT5G57930 | Accumulation of PSI 2 (APO2)
140 | AT5G58260 | NDH-N
141 | AT5G59250 | sugar transporter family protein; identical to D-xylose-proton symporter-like 3
142 | AT5G64290 | Dicarboxylate transporter 2.1 (DiT2.1)

Acknowledgements

First of all, I would like to thank Prof. Dr. Soll for giving me the possibility to perform my PhD work in his lab, and for his continuous support.

I would also like to thank my supervisor Bettina for her constant readiness to help and answer all my stupid questions that came up in the lab over the years.

A special thanks, of course, to Anna, for being my second self in the project, for numerous and fruitful discussions and for bringing me back on the track when I was lost in details again.

I cannot thank Yvonne and Eike enough for all the help with the experiments, for keeping the lab up and going, and for being real good friends next to being colleagues.

Thanks also for the technical help by Anna, Linda, Sarah and Sebastian.

I am grateful to all the people who contributed with experiments, samples and discussions to this project: first of all Minna and Paula (Turku) for the nicest collaboration ever, Mónica for the introduction into CD spectroscopy, Tom Alexander (Osnabrück) for the Tic20 electrophysiology trials, Prof. Andreas Weber (Düsseldorf) for the co-expression data, Christoph Schwartz & Hüseyin Besir (MPI, Martinsried) for their help with the cell-free *E. coli* lysate, Young-Ho Lee (Osaka) for NMR and AUC data on the Tic62/FNR complex, Ute (AG Leister) for help with the PSII PAM measurements, Katrin, Daniela and Ulrike for the Affymetrix analysis of *tic62* mutants, Irene for electron microscopy, Serena and Jörg Meurer for providing antibodies, and Cordelia Bolle for the Agrobacterium strain UIA.

Thanks to the post-docs and PDs (and by now Profs.) Ute, Enrico, Katrin, Mónica, and Manu for a lot of advice and good ideas.

Thanks to the Soll-lab-alumni Friede, Lars, and Thomas, who probably helped most in the beginning of my PhD to get me started.

Many thanks to my lab colleagues (mostly female), who brought fun into the lab day and were nice to me (most of the time) even when I was the only guy around – and also for (almost never) making me realize it ;-)
But, honestly, I have found friends, and you cannot want more from colleagues!

Special thanks to those people who helped me to write this thesis, who read it and gave me lots of advice (how to make it better next time…).

Last but not least, my greatest thanks is dedicated to my parents and my family for their life-long support and much, much more!

Curriculum vitae

Personal Details:

Birth Date: September 2nd, 1977

Birth Place: Bremen, Germany

Marital Status: engaged

Citizenship: German

Education and Research Experience:

School (1983-1997)

08.1994 – 07.1997:   *´Gymnasium an der Hermann-Böse-Straße`* (German secondary school) in Bremen

04.07.1997:   Graduation: Abitur (grade: 1.2)

Civil Service

07.1997 - 07.1998:   *´Montessori Kinderhaus Oberneuland`* (Kindergarten) in Bremen

University

10.1998 – 09.2000:   Undergraduate studies of Biology at the *´Technische Universität Carolo-Wilhelmina zu Braunschweig`*

29.09.2000:   Prediploma in the subjects Zoology, Genetics, Microbiology, Botany, Mathematics and Organic Chemistry (grade: 1.0)

09.2000 – 08.2003:   Graduate studies of Biology: Botany (main subject), Genetics, Cell Biology (subsidiary subjects)

10.2002 – 08.2003:   Preparation of the Diploma thesis in the lab of Prof. Dr. Nigel M. Crawford at the *´University of California at San Diego`* (UCSD), USA

                     Title: „Analysis of the Transcriptional Regulation of the Dual-Affinity Nitrate Transporter Gene *AtNRT1.1* (*CHL1*) from *Arabidopsis thaliana*"

18.08.2003:   Academic degree: Diplom-Biologe (grade: „passed with distinction")

11.2003 – 08.2004:   Continued work in the lab of Prof. Dr. Nigel M. Crawford (at UCSD) in the position of a full scientific lab assistant

10.2004 – today: PhD graduate student in the lab of Prof. Dr. J. Soll at the *'Ludwig-Maximilians-Universität München'* (LMU München), Munich, Germany

                     Thesis Topic: „Molecular Characterization of two Subunits of the Translocon at the Inner Envelope of Chloroplasts"

Scholarships, Memberships and Awards:

2001-2003:	Scholarship by the *´Studienstiftung des deutschen Volkes`* (*German National Academic Foundation*). Admission on the basis of the prediploma grade average including a graduate student scholarship
02.2003:	Award of a short-term grant for research abroad by the *´Deutscher Akademischer Austausch Dienst e.V.`* (DAAD; *German Academic Exchange Service*)
2005 - today:	Member of the *´Gesellschaft für Biochemie und Molekularbiologie e.V.`* (GBM; the German constituent society of FEBS and IUBMB)
11.2005:	Admission to the International Graduate Program '*Protein Dynamics in Health and Disease*' as part of the ENB initiative (Elite Network of Bavaria) funded by the Government of the State of Bavaria, Germany
08.2008:	Best student poster award at the XVI Congress of the Federation of European Societies of Plant Biology (FESPB); 17.08.-22.08.2008; Tampere, FIN

List of publications

Publications:

Stengel A[*], <u>Benz P</u>[*], Balsera M, Soll J, Bölter B. (2008) Tic62 - redox-regulated translocon composition and dynamics. *J Biol Chem.*, **283** (11): 6656-67   [*](contributed equally)

Stengel A, <u>Benz JP</u>, Buchanan B, Soll J, Bölter B. (2009) Preprotein import into chloroplasts via the Toc and Tic complexes is regulated by redox signals in *Pisum sativum. Molecular Plant*, in revision

<u>Benz JP</u>, Stengel A, Lintala M, Lee YH, Weber A, Philippar K, Guegel IL, Kaieda S, Ikegami T, Mulo P, Soll J, Bölter B. (2009) Tic62 and FNR form light-regulated complexes that are integrated into the chloroplast redox poise, in preparation

Reviews:

<u>Benz P</u>, Soll J, Bölter B. (2007) The Role of the Tic Machinery in Chloroplast Protein Import. in *The Enzymes*, **Vol. 25**; *Molecular Machines Involved in Protein Transport across Cellular Membranes* (Dalbey R, Koehler C & Kamanoi F, eds.), Academic Press/Elsevier: 439-62

<u>Benz JP</u>, Soll J, Bölter B. (2009) Protein transport in organelles: The composition, function and regulation of the Tic complex in chloroplast protein import. *FEBS J*., **276** (5): 1166-76

Posters:

<u>Benz JP</u>, Soll J, Bölter B. Characterization of the Chloroplast TIC Complex. FEBS-EMBO Advanced Lecture Course: Cellular and molecular biology of membranes; 20.06.-01.07.2005; Cargèse, Corse, F

<u>Benz JP</u>, Soll J, Bölter B. Purification and Characterization of the Translocon of the Inner Chloroplast Envelope. EMBO Conference: Protein transport systems: Protein targeting and translocation; 30.09-05.10.2006; Gdansk, PL

Stengel A, <u>Benz JP</u>, Soll J, Bölter B. Tic62 - New Insights Into Redox-regulated TIC Function and Composition. Gordon Research Conference: Protein transport across cell membranes; 10.6.-15.6.2007; Il Ciocco, IT

<u>Benz JP</u>, Stengel A, Soll J, Bölter B. Characterization of Tic62: a possible link between chloroplast preprotein import and photosynthesis? XVI Congress of the Federation of European Societies of Plant Biology (FESPB); 17.08.-22.08.2008; Tampere, FIN

Talks:

Tic62 - a link from photosynthetic e[-] transport to preprotein import?
Intl. Photosynthesis Workshop; 01.10.´08; Bichl, Germany

Ehrenwörtliche Versicherung

Ich versichere hiermit ehrenwörtlich, dass die vorgelegte Dissertation von mir selbständig und nur unter Verwendung der angegebenen Hilfsmittel und Quellen angefertigt wurde.

München, den

Philipp Benz

Erklärung

Hiermit erkläre ich, dass ich zuvor nicht versucht habe, anderweitig eine Dissertation einzureichen oder mich einer Doktorprüfung zu unterziehen. Die vorliegende Dissertation wurde keiner weiteren Prüfungskommission weder in Teilen noch als Ganzes vorgelegt.

München, den

Philipp Benz

Versicherung der Co-Autoren

Hiermit wird im Namen aller Co-Autoren versichert, dass sämtliche Passagen dieser Arbeit, die wörtlich oder nahezu wörtlich aus den unten aufgeführten Veröffentlichungen entnommen wurden, vom Autor dieser Dissertation selbst stammen.

München, den

Prof. Dr. J. Soll

Benz P, Soll J, Bölter B. (2007) The Role of the Tic Machinery in Chloroplast Protein Import. in *The Enzymes*, **Vol. 25**; *Molecular Machines Involved in Protein Transport across Cellular Membranes* (Dalbey R, Koehler C & Kamanoi F, eds.), Academic Press/Elsevier: 439-62

Stengel A, Benz P, Balsera M, Soll J, Bölter B. (2008) Tic62 - redox-regulated translocon composition and dynamics. *J Biol Chem.*, **283** (11): 6656-67

Benz JP, Soll J, Bölter B. (2009) Protein transport in organelles: The composition, function and regulation of the Tic complex in chloroplast protein import. *FEBS J.*, **276** (5): 1166-76